



Interrogating T cells specific to mutated and shared tumor epitopes in mouse and man

Petersen, Nadia Viborg

Publication date:
2019

Document Version
Publisher's PDF, also known as Version of record

[Link back to DTU Orbit](#)

Citation (APA):
Petersen, N. V. (2019). *Interrogating T cells specific to mutated and shared tumor epitopes in mouse and man*. DTU Health Technology.

General rights

Copyright and moral rights for the publications made accessible in the public portal are retained by the authors and/or other copyright owners and it is a condition of accessing publications that users recognise and abide by the legal requirements associated with these rights.

- Users may download and print one copy of any publication from the public portal for the purpose of private study or research.
- You may not further distribute the material or use it for any profit-making activity or commercial gain
- You may freely distribute the URL identifying the publication in the public portal

If you believe that this document breaches copyright please contact us providing details, and we will remove access to the work immediately and investigate your claim.

Interrogating T cells specific to mutated and shared tumor epitopes in mouse and man

PhD thesis

Nadia Viborg Petersen
December 2019



Department of Health Technology
Technical University of Denmark

Kemitorvet
Building 202
2800 Kgs. Lyngby

PREFACE

The following PhD thesis has been submitted to the Technical University of Denmark, Department of Health Technology, as part of the requirements for obtaining a PhD degree. The presented research was carried out from January 2017 to December 2019 as a collaboration between the Technical University of Denmark (first the Veterinary Institute, then Department of Micro- and Nanotechnology, and lastly at the Department of Health Technology) and Evaxion Biotech. The project was supervised by Sine Reker Hadrup (Professor, Section for Experimental and Translational Immunology, Department of Health Technology, Technical University of Denmark) and Birgitte Rønø (PhD, Senior Director of Cancer Immunotherapy, Evaxion Biotech). The research was in part funded by the Danish Innovation Fund via their Industrial PhD programme.

The thesis is comprised of a common introduction followed by relevant research papers, each introduced by a short preface, and finally an epilogue discussing the major findings and perspectives of the work.

Copenhagen, December 2019



Nadia Viborg Petersen

ABSTRACT

It is by now acknowledged that immunological recognition of cancer is a many-sided interplay, able to both promote and reject tumor growth. With cancer immunotherapy, the ambition is to harness immunity towards long lasting tumor elimination, for which T cells are important mediators. Tumor cells differ genetically from healthy tissue, which will be visible to surveilling T cells via aberrant peptide-MHC presentation. Hence, a large effort is being put into understanding T cells and their epitope targets in cancer, via techniques to monitor and augment tumor specific T cells. Little is known about the characteristics that govern immunogenicity of T cell epitopes, and current strategies depend on *in silico* prediction of peptide-MHC binding affinity. The outlined thesis contains three research papers that investigate T cells and their associated epitopes in mice and humans, with emphasis on cancer.

In the first study, we developed novel conditional ligands for murine H-2 alleles H-2D^d and H-2K^d, that enable rapid generation of multiple pH-2 multimers via UV-mediated peptide exchange, without the need for individual peptide-H-2 refolding. pH-2^d multimers were successfully used for fluorescent tetramer staining and large-scale DNA barcode labelled multimer libraries. This provides the first description of H-2D^d and H-2K^d conditional ligands, and proof-of-concept of DNA barcode labelled multimers for murine H-2^d haplotype screening. This technology will enable epitope mapping in a wide variety of disease models on e.g. BALB/c background, including syngeneic models of cancer.

The second study investigated neo-epitope vaccination in the murine CT26 syngeneic tumor model. We explored DNA and peptide-based delivery of neo-epitopes and found only DNA vaccination to induce protective tumor immunity. Correspondingly, DNA based vaccination preferentially induced neo-epitope specific CD8⁺ T cells, whereas peptide vaccination induced neo-epitope specific CD4⁺ T cells. Our DNA based vaccination strategy thus represents an interesting framework for future neo-epitope discovery, from which putative epitope libraries are often large and will benefit from the technology outlined in the first study.

In the third study we show T cell recognition of epitopes from previously undescribed shared tumor associated antigens in breast cancer patients. Similar to the first study, this study employs high-throughput DNA barcode labelled pHLA multimers, and the investigated T cell epitopes do not give rise to recognition in HLA-matched healthy donors. Breast cancer remains a major cause of female mortality worldwide and is not thoroughly researched in the field of immunotherapy. Breast cancer harbors low mutational burden compared to other cancer types, thus investigations on shared tumor epitopes are of importance compared to mutation-derived neo-epitopes. As such, our findings represent novel T cell targets in breast cancer, that might be of relevance in patient immune monitoring.

Collectively, these studies represent tools for, and investigations of, T cell epitopes in cancer. With an increased understanding of what the T cells “see” and how to enhance them, we can better steer them towards tumor eradication via immunotherapy.

DANSK RESUMÉ

Det er anerkendt, at immunologisk genkendelse af cancer udgør et mangesidet sammenspil, der kan både fremme og hæmme tumorvækst. Ambitionen med cancer immunterapi er at dirigere immunsystemet for at opnå langvarig tumor eliminering, og her er T celler betydningsfulde. Tumorceller er genetisk forskellige fra raskt væv, hvilket vil være synligt for overvågende T celler via afvigende peptid-MHC-præsentation. Der bliver derfor ydet en stor indsats for at forstå T celler og deres epitoper i kræft, via teknikker til at monitorere og forøge tumor-specifikke T celler. Der findes begrænset viden om de karakteristika der afgør immunogenicitet af T celle epitoper, og nuværende strategier afhænger af *in silico* prædiction af peptid-MHC bindingsaffinitet. Den her beskrevne afhandling indeholder tre studier, der undersøger T celler og deres associerede epitoper i mus og mennesker, med fokus på cancer. I det første studie udviklede vi nye betingede ligander for murine H-2 alleler; H-2D^d og H-2K^d, der muliggør sideløbende generering af adskillige pH-2 multimerer via UV-medieret peptidudveksling, uden behov for individuel peptid-H-2 refoldning. pH-2^d multimerer blev med succes anvendt til fluorescerende tetramer-farvninger og stor-skala DNA mærkede multimer biblioteker. Dette udgør den første beskrivelse af betingede ligander for H-2D^d og H-2K^d, samt belæg for at kunne benytte DNA mærkede multimer til murin H-2^d vævstype screening. Denne teknologi vil facilitere kortlægning af epitoper i mange sygdomsmodeller på BALB/c baggrund, inklusive syngene cancer modeller.

Det andet studie undersøgte neo-epitoper in den murine syngene CT26 tumor model. Vi udforskede DNA og peptid-baseret levering af neo-epitoper, og fandt, at kun DNA-vaccinering inducerede beskyttende tumorimmunitet. Tilsvarende inducerede DNA-baseret vaccinering præferentielt neo-epitop specifikke CD8⁺ T celler, hvorimod peptid-baseret vaccinering inducerede neo-epitop specifikke CD4⁺ T celler. Vores DNA-baserede vaccinationsstrategi repræsenterer derfor en interessant ramme til fremtidig kortlægning af neo-epitoper, hvor de undersøgte epitop-biblioteker ofte er omfattende og vil drage fordel af teknologien beskrevet i det første studie.

I det tredje studie observerer vi T celle genkendelse af nogle hidtil ubeskrevne epitoper fra tumor associerede antigener in brystkræftpatienter. Ligesom i det første studie, benytter vi

her DNA mærkede pHLA multimerer, og de undersøgte T celle epitoper giver ikke anledning til genkendelse i vævstype-matchede raske donorer. Brystkræft er fortsat en væsentlig dødsårsag på verdensplan, og er ikke videre undersøgt indenfor cancer immunterapi. Brystkræft har generelt en lav mutationsbyrde sammenlignet med andre typer af cancer, og derfor er undersøgelser af ikke-muterede epitoper af høj relevans, sammenlignet med mutationsderiverede neo-epitoper. Samlet set præsenterer vores forskning nye T celle epitoper i brystkræft, som kan blive relevante indenfor immunmonitorering af patienter. Tilsammen repræsenterer disse studier værktøjer til, og undersøgelser af, T celle epitoper i cancer. Med en øget forståelse for hvad det er, T cellerne ”ser”, og hvordan vi kan styrke dem, kan vi i højere grad benytte dem til tumor destruktion via immunterapi.

ACKNOWLEDGEMENTS

After more than eight years at DTU as a BSc and MSc student, an employee and latest an aspiring PhD graduate I am now handing in my PhD thesis. This is an emotional and grand milestone for me.

First, the biggest of thank you goes to the power-women who supervised me during my PhD project: Sine Reker Hadrup and Birgitte Rønø. Sine for including me in your wonderful research group in early 2014, which led me to BSc, MSc and now a PhD project under your supervision. I am grateful for everything you have taught me, and before my projects with you, I did not even consider pursuing a PhD. You continuously challenge and inspire me in my scientific ventures, which is why I have become quite the MHC multimer nerd. Birgitte for your patience, trust, inclusion and your never-ending encouragement of my work. For going with me to the lab on a Christmas holiday, staining cells and sharing pizza in the FACS room. Both of you, for hours of sparring, optimism and confidence boosts. Thank you.

Many appreciations go out to everyone in the SRH research group at DTU for great collaborations, countless hours of science, laughter, FACS sorting, dancing, travels, coffees and group meetings. My years spent at DTU will be truly unforgettable thanks to all of you. To Amalie, Natasja and Sofie, for following me since my early steps as a scientist (in the lab and on the dancefloor...). Sofie, O.G. grandma, for feedback on my first thesis draft. Trine and Sara for fruitful and fun collaborations in the mouse team and long hours spent processing mouse organs. Trine, for many long talks and your last-minute comments and corrections that I am immensely grateful for. To Agnes, Ulla, Jeppe, Simone, Rasmus, Keith, Matilda, and Emma, for sharing the ups and downs of the PhD journey with me.

To everyone in the Evaxi-family for inclusion and encouragement. For listening to all my talk about multimers, T cells and whatnot. You all contributed to making me feel right at home, especially in the Friday bar. Brilliant PioNerds for sharing my neo-epitope enthusiasm. Marina for numerous hours spent immunizing mice and a growing friendship, always there to help me get my mind off things when I need it (and when I don't know that I need it). To Stine, Bettina and the IO EXP team for making experiments feasible and fun. I look forward to getting to know you all even better in the time to come.

Lastly, to my family and friends for your understanding, enthusiasm and curiosity of my work, always believing in me even when I do not.

Nadia Viborg Petersen (Doctor of Philosophy *in spe*)

PUBLICATIONS

The following research is included in this thesis:

Manuscript I:

Nadia Viborg, Trine Sundebo Meldgaard, Tripti Tamhane, Sara Suarez Hernandez, Christian Garde, Thomas Trolle, Dario Vazquez Albacete, Sine Reker Hadrup. "H-2 multimers for high-throughput T cell interrogation and description of novel conditional ligands for H-2D^d and H-2K^{dβ}"

(manuscript formatted for submission to Journal of Immunology)

Manuscript II:

Nadia Viborg, Marina Barrio Calvo, Stine Friis, Thomas Trolle, Christian Skjødt Hansen, Jens Kringelum, Sine Reker Hadrup and Birgitte Rønø. "DNA based neo-epitope vaccination induces tumor control in the CT26 syngeneic mouse model"

(manuscript in preparation)

Paper III:

Nadia Viborg, Sofie Ramskov, Rikke Sick Andersen, Theo Sturm, Tim Fugmann, Amalie Kai Bentzen, Vibeke Mindahl Rafa, Per thor Straten, Inge Marie Svane, Özcan Met, Sine Reker Hadrup (2019). "T cell recognition of novel shared breast cancer antigens is frequently observed in peripheral blood of breast cancer patients"

Oncoimmunology, 8:12, DOI: 10.1080/2162402X.2019.1663107

CONTENTS

1.	Introduction	1
	From innate to adaptive immunity	1
	T cells.....	3
	Immunological recognition by pMHC-TCR interactions	3
	Tumor immunology	5
	Immunoediting.....	6
	T cells and their targets in cancer.....	7
	Monitoring of antigen specific T cells.....	12
	Cancer immunotherapy	14
	Clinical advances and considerations.....	14
	Lessons from preclinical mouse models	18
2.	Manuscript I	21
3.	Manuscript II	47
4.	Paper III	79
5.	Epilogue	109
6.	Bibliography	115

1. INTRODUCTION

From innate to adaptive immunity

The human immune system is complex and comprises numerous components able to sense, respond and defend us against threats of different nature, such as pathogens or malignantly transformed cells. Immediate sensing is facilitated by components of the innate immune system which discriminates non-self from self via interactions between host pattern recognition receptors (PRRs) and conserved pathogen associated molecular patterns (PAMPs) and cellular stress related damage associated molecular patterns (DAMPs). Several families of PRRs have been described, e.g. Toll-like receptors (TLRs) that have different cellular distribution, enabling recognition of distinct invariant molecular patterns or threats in intra- and extracellular compartments. Downstream of PRR-PAMP interactions innate immune responses recruit relevant cells and produces effector molecules in the form of cytokines and chemokines [1]. Innate immune responses are rapid and generic and do not induce memory for future re-encounters. However, the type of innate immune response that is mounted fundamentally shapes the adaptive immune response that will follow, as this depends profoundly on the signature of cytokines produced by the initial innate phase [2], an attribute utilized actively in vaccination, schematically illustrated in Figure 1.

Antigen presenting cells (APCs), particularly dendritic cells (DCs), are essential in bridging innate and adaptive immunity. DCs recognize, take up and degrade pathogens and their antigens at the site of recognition. Antigen loaded DCs move via lymphatics to lymph nodes, where they present antigens on the major histocompatibility complex (MHC) to naïve lymphocytes; the key effectors of adaptive immunity [1], [3]. Upon antigen presentation and co-stimulatory signals from DCs (“priming”), lymphocytes will mature and proliferate, giving rise to antigen specific immune responses. The cytokine milieu surrounding DCs during antigen uptake shapes the induction of adaptive immunity that follows [4], [5]. Adaptive immunity is developed throughout life and responds slower than innate immunity. Due to selective induction of specific and persisting memory cells, responses occur rapidly and effectively upon re-exposure [3]. B lymphocytes (B cells) and T lymphocytes (T cells) embody

adaptive humoral and cellular immune responses respectively via their antigen specific receptors. T cells are key components of adaptive immunity responsible for the direct killing of infected or transformed cells (i.e. CD8+ T cells) and orchestrating the immune response in several ways (CD4+ T cells) and will be the focus for the remainder of this thesis.

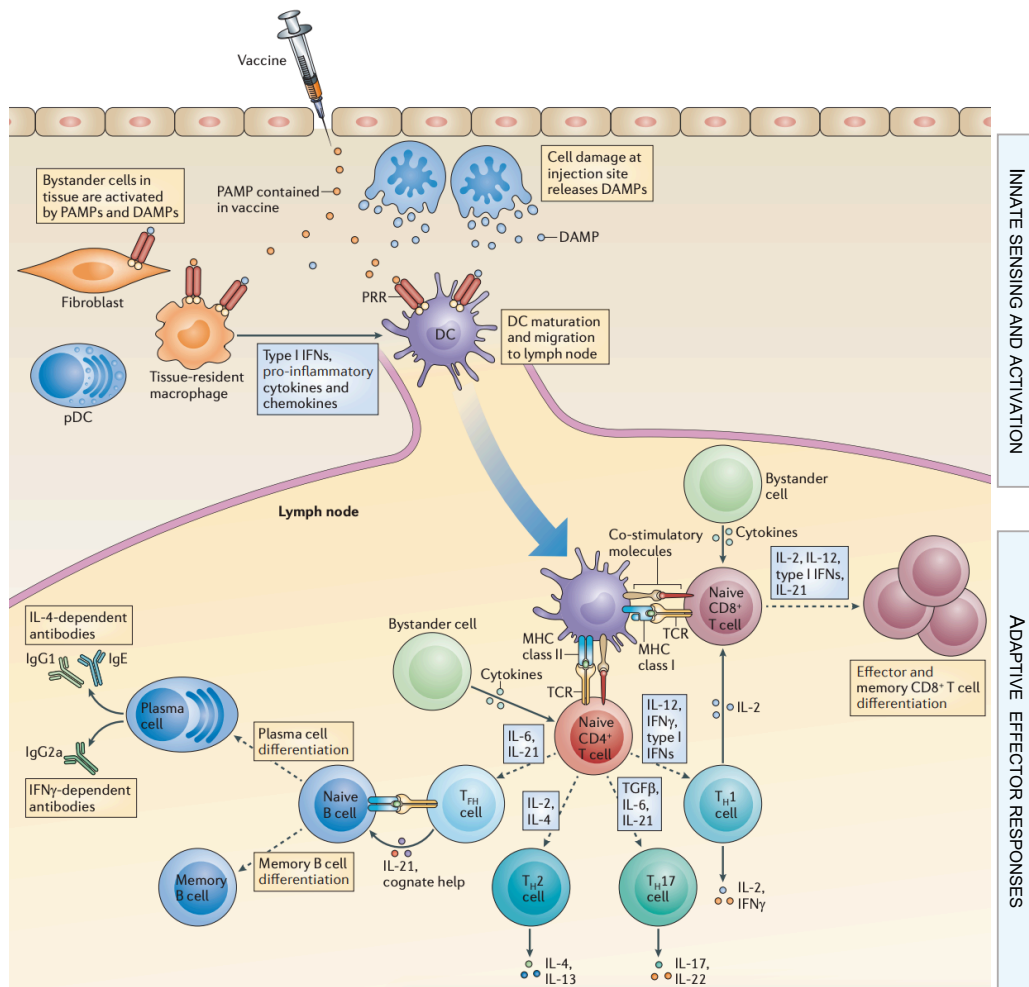


Figure 1 - From innate to adaptive immunity via vaccination. The immune response obtained via vaccination starts already at the injection site where PAMPs and DAMPs are sensed by local cells and APCs via PRRs. Antigen loaded DCs travel to lymph nodes, capable of antigen presentation and priming of lymphocytes. Here, adaptive immunity starts, which is composed of various types of effector B and T cells. The type of lymphocytes that are activated depends on cytokines present in the milieu and signals from the DC. Proper co-stimulation from DC to T cells is also driven by innate sensing via PRRs. Abbreviations: PAMP; pathogen-associated molecular pattern, DAMP; damage-associated molecular pattern, PRR; pathogen recognition receptor, pDC; plasmacytoid dendritic cell, DC; dendritic cell, T_{H1}; T follicular helper cell, IL; interleukin, IFN; interferon, IgG; immunoglobulin. Figure adapted from [6]

T cells

T cells originate from hematopoietic progenitors in the bone marrow and mature in the thymus, where they undergo extensive selection processes. T cells express a T cell receptor (TCR) for antigen recognition associated with co-receptor CD3 [7]. Two subtypes of T cells are relevant for this thesis, distinguished by expression of surface co-receptors CD4 or CD8. CD4+ T cells or T helper cells (T_H) instruct and influence adaptive immunity and comprise multiple functionally distinct subtypes (Figure 1) under the control of separate transcription factors, induced as a consequence of signaling patterns from APCs. Most important for the scope of this thesis are T_H1 cells, which are characterized by interleukin-2 (IL-2) and interferon- γ (IFN γ) cytokine production, controlled by transcription factor T-bet, and support responses to intracellular threats such as viral infections and malignant transformations. CD8+ T cells or cytotoxic T lymphocytes (CTLs) are supported by T_H1 cytokines (as visible on Figure 1) and respond to changes of intracellular origin. The CD8+ T cell respond by selectively killing target cells via release of cytolytic effector molecules upon recognition of aberrant cells.

Immunological recognition by pMHC-TCR interactions

MHC presentation

T cells depend on self MHC display of peptides to exert effector functions via TCR interactions. The MHC locus is polygenic and constitutes the most polymorphic region within the human genome, of which each allele has distinct amino acid binding preferences. This makes for a comprehensive repertoire of peptide-MHC (pMHC) presentations to the immune system, a benefit in the continuous battle against pathogens. In humans the MHC is referred to as human leukocyte antigen (HLA) and in mice H-2, and across species two MHC regions facilitate antigen presentation to T cells: MHC class I and class II molecules. MHC class I is expressed on all nucleated cells and presents peptides of intracellular origin to CD8+ T cells, as outlined in detail in Figure 2A. MHC class I typically binds and presents peptides of 9-11 amino acid length [8]. MHC class II is restrictively expressed by APCs and presents peptides of exogenous (vesicular and extracellular) origin for interaction with CD4+ T cells, as outlined in detail in Figure 2B. MHC class II has an open peptide binding groove, allowing longer peptides to be presented, typically 13-25 amino acid length [9]. Also noteworthy is cross presentation, in which peptides of extracellular origin are presented by

MHC class I on a subset of DCs, which gives rise to effective CD8⁺ T cell responses [10]. Cross presentation is mainly facilitated by immunoproteasomal degradation of peptides and driven by the presence of interferons in the milieu as an effect of PRR signaling in the innate immune phase [11], [12].

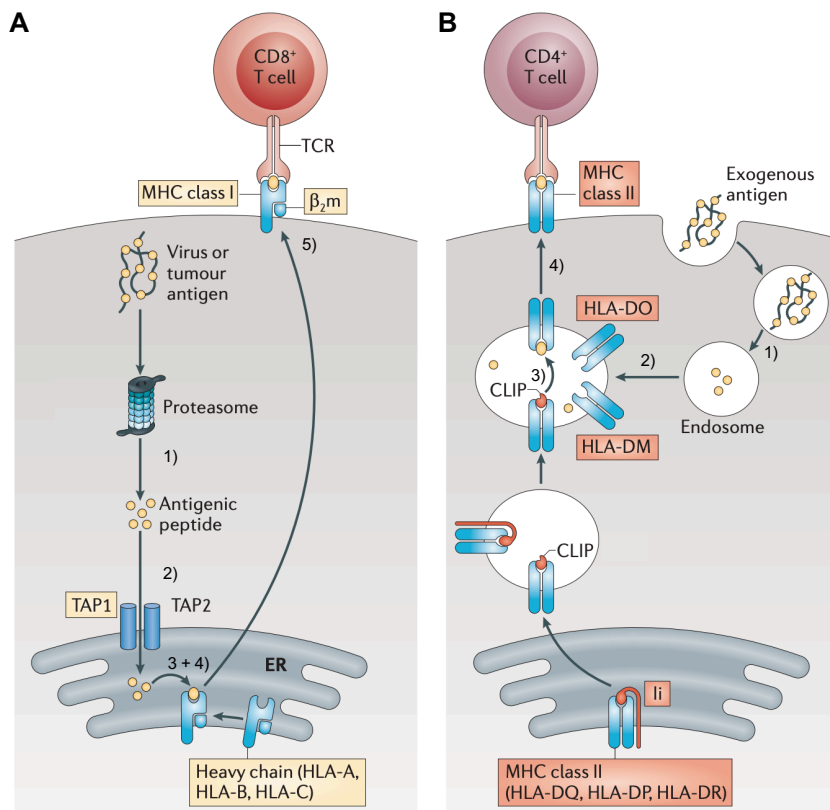


Figure 2 – peptide processing and presentation by MHC molecules. (A) Proteins of intracellular origin are degraded and presented by MHC class I in the form of peptides by the following steps: 1) proteasomal degradation, 2) transport to endoplasmic reticulum (ER) by transporter associated with antigen processing (TAP), 3) ER trimming by aminopeptidases to a length of 9-11 amino acids, 4) loading onto newly synthesized MHC class I molecules in the ER, and 5) the stable pMHC complex departs for cell surface presentation to cognate CD8⁺ T cells. **(B)** Proteins of exogenous origin are taken up, degraded and presented by MHC class II molecules and comprises: 1) uptake and endolysosomal degradation, 2) fusing with MHC class II containing endosomes, produced in ER loaded with invariant chain (Ii) and later class II-associated invariant chain peptide (CLIP), 3) displacement CLIP from class II binding groove with exogenous peptide, 4) the stable pMHC complex departs for cell surface presentation to cognate CD4⁺ T cells. Abbreviations: TCR; T cell receptor, MHC; major histocompatibility complex, HLA; human leukocyte antigen, β₂m; beta-2-microglobulin. Figure adapted from [13]

TCR recognition

The majority of T cells in humans and mice bear a heterodimeric αβ-TCR with a constant and a variable region, of which the variable region is the antigen-binding site. Genetic loci

for TCR α and β chains produce an immensely diverse TCR repertoire via somatic recombination for comprehensive antigen recognition. Hypervariable loops in TCRs interact with cognate pMHCs to form highly specific TCR-pMHC interactions. During priming of naïve T cells by professional APCs, TCR-pMHC interaction delivers signal 1, which is strengthened by interaction of T cell co-receptors (CD4 or CD8) with invariant sites of the MHC. Signal 2 is provided by APCs expressing co-stimulatory ligands (B7.1 and B7.2, expression driven by PAMP-PRR interactions during the innate phase) that bind to T cell surface protein CD28. Lastly, T cell stimulatory cytokines such as IL-2 provide signal 3 for activation and are essential for T cells to proliferate and differentiate into effector cells. Clonal expansion of antigen specific T cell clones follows, and mature, antigen experienced T cells will reach the periphery, with the ability to exert effector functions upon interaction with cells that present their cognate pMHC [14]. If T cells are primed only with signal 1, they become hyporeactive or anergic with inhibited effector functions. The upregulation of co-stimulatory elements on APC cell surface is driven innate PRR signaling, again, an example of the importance of inducing the right innate response to achieve functional adaptive T cells [4].

Interactions between mature T cells and target cells confer very specific and potent cytotoxic responses. Therefore, T cells are under strict regulation during thymic development, to avoid T cells with the potential to destroy self-tissue. In brief, thymic epithelial cells present self-peptide-MHC to developing T cells in a process of central tolerance. During positive selection only T cells that can interact with peptides presented by self MHC will survive. Concurrently, T cells with very high affinity to the self-peptides presented will be deleted by negative selection. These processes ensure that the T cells of an individual will see peptides presented by self MHCs and to a large extent avoid destruction of healthy tissue. A process that is somehow incomplete, as evident by the fact that we observe multiple autoimmune diseases mediated by T cells [15], [16]. The T cells that escape negative selection are however kept in check by peripheral tolerance, in part mediated by T regulatory (Treg) helper cells.

Tumor immunology

Cancer is a group of diseases characterized by malignant transformations of self-cells resulting in abilities of unlimited proliferation and tissue invasion [17]. Transformation of cells is a complex genetic process leading to most cancers sharing several traits of broken

homeostasis, commonly referred to as Hallmarks of Cancer [18]. Despite major medical advancements, cancer remains a leading cause of mortality worldwide. Following decades of research and debate, it is now well established and described that the immune system plays an important, yet dichotomous, role in tumor establishment, progression and eradication. Acknowledged through descriptions such as the cancer immunity cycle [19] and the addition of immunological enabling in the updated Hallmarks of Cancer [20], the concept of tumor immunology is today textbook material that describe both the pro- and anti-tumor effects of the immune system. Additionally, the Immunoscore concept described by Galon et al. [21], [22] provide a clinical correlate between intratumoral presence of T cells and disease improved prognosis, and could be used to stratify patients to a suitable therapy [23].

Immunoediting

Cancer cells can be perceived as non-self by a competent immune system resulting in immune mediated tumor regression. However, this process adds selective pressure on tumor cells, favoring persistence of cell variants that are less immunogenic and less visible to the immune system. This concept has been described as the immunoediting theory [24], [25], consisting of three phases, as outlined in **Fejl! Et bogmærke kan ikke henvise til sig selv.:** elimination (A), equilibrium (B), and escape (C). In the elimination phase, mediators of innate and adaptive immunity recognize and respond to altered cells, destroying variants that display aberrant transformation. At this stage the immune system holds the emerging tumor in check. But few less immunogenic tumor cell variants (present in the heterogenic cell pool of the original tumor) might evade immune destruction. Thus, an equilibrium phase can commence, where immunological sculpting continuously decreases immunogenicity of tumor cells. The surviving tumor cell variants are insensitive to immune destruction and can consequentially grow uncontrolled and become clinically visible, thus reaching the escape phase. Several tumor intrinsic and extrinsic mechanisms support immune escape, such as tumor cell loss of MHC class I expression, defective antigen processing, display and secretion of immune inhibitory molecules and the recruitment and presence of immunosuppressive cells in the tumor microenvironment (TME). Notably, the phases of immunoediting are plastic and interconnected processes, so that a tumor in the immunoediting phase can turn towards both escape and elimination. Meanwhile, some tumors are eradicated completely in early elimination phases, whereas other more aggressive tumors reach escape phase rapidly.

With cancer immunotherapy the aim is to harness immunity in favor of elimination processes.

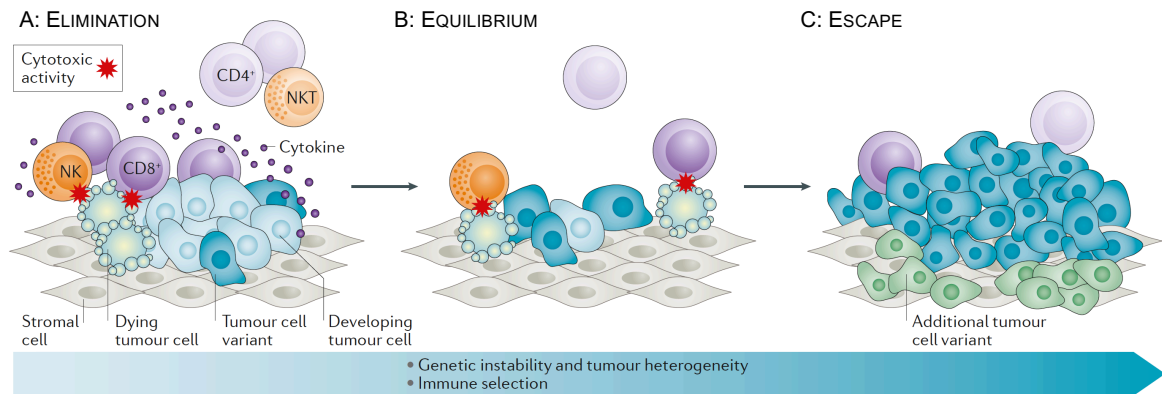


Figure 3 - The process of immunoediting. (A) Elimination phase: due to foreignness of tumor cells they are recognized and attacked by cells of the immune system. (B) Equilibrium phase: constant pressure from immune system favors the survival of less immunogenic tumor cell variants, the immune system is thus less capable of ‘seeing’ tumor cells. (C) Escape: outgrowth of tumor cell variants with very low immunogenicity. Tumor cells evade immune destruction and are able to grow more or less uncontrollably. Abbreviations: NK; natural killer, NKT; natural killer T cell. Figure adapted from [25]

T cells and their targets in cancer

T cells constitute a major part of immune elimination and resultant immunoediting of tumors as they are potent killers of aberrant looking cells [26]–[28]. Genetic instability of cancer is mirrored by differential peptide expression by MHC on the surface of tumor cells which will be visible to surveilling T cells. If a displayed peptide is recognized by a specific TCR, it is referred to as a T cell epitope or antigen [29]. Major efforts have been put into research of T cell epitopes with potential use in immune monitoring and therapy. T cell epitopes in cancer are conventionally assigned into classes, as illustrated in Figure 4, where it is outlined how T cell epitopes moreover differ with regard to their unique or shared expression profile. For the scope of this thesis, focus will be on endogenously derived peptides described in more detail in sections below. An additional noteworthy category constitutes tumor antigens originating from virally induced cancers, such as E6 and E7 oncogene expression by human papilloma virus (HPV) induced cervical cancers [30]. Moreover, recent reports describe T cell epitopes resulting from non-canonical or out-of-frame genetic regions expressed as a result of tumor genetic instability, which present interesting putative new T cell epitopes, not affected by central tolerance [31]–[33].

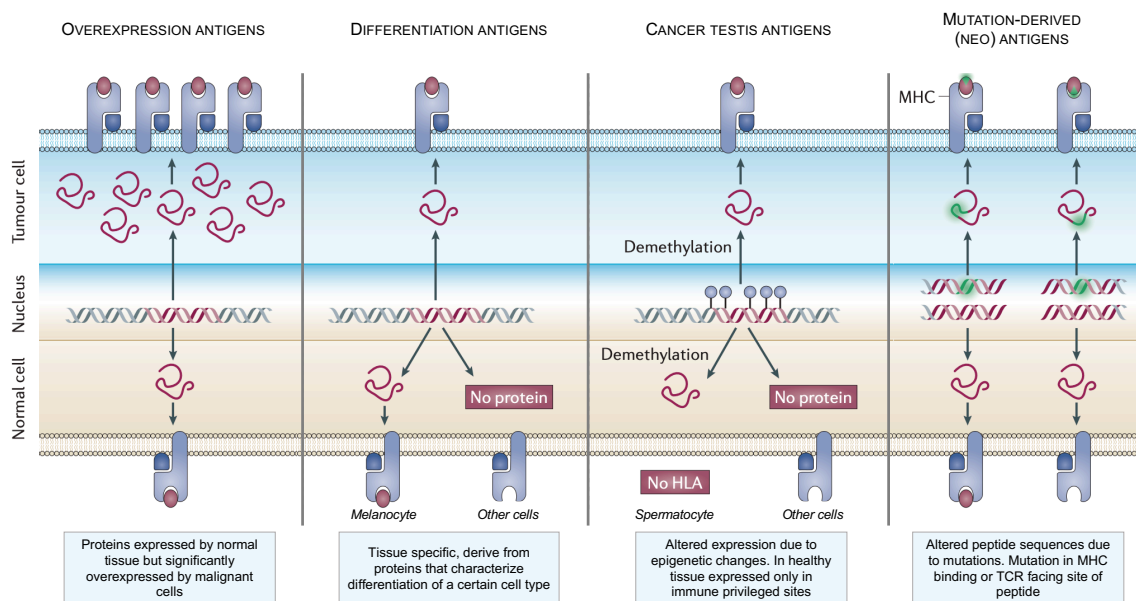


Figure 4 – categories of endogenously derived T cell antigens. Aberrant expression of antigens by MHC class I on the surface of tumor cells (top), due to genetic alterations (middle). Antigen expression on normal/healthy tissue (bottom). From left to right, increasing degree of tumor restricted expression. Figure adapted from [29]

Shared T cell epitopes

T cell epitopes expressed by both tumor and healthy tissue are commonly referred to as shared, self- or tumor associated antigens and include overexpression, differentiation and cancer testis antigens. Overexpression antigens are profoundly expressed by tumor cells compared to corresponding healthy tissue, but expression in healthy tissue is often below a threshold for T cells to recognize. An example is the expression of survivin in several cancers and HER2 in certain breast cancers [34], [35]. Expression of differentiation antigens is normally limited to distinct differentiated cell types, such as melanocytes of the skin, and tumor cells originating from that tissue. An example is tyrosinase in melanomas, where specific T cells are observed in circulation of cancer patients and healthy donors alike, suggestive of incomplete thymic negative selection [36]. Cancer testis antigens constitute a group of proteins that are normally only expressed in immune privileged sites of the body, such as placenta and male germ cells that lack HLA expression. Tumor epigenetic changes lead to expression of these proteins in some tumors, resulting in tumors appearing non-self to T cells, such as New York esophageal squamous cell carcinoma 1 (NY-ESO-1) in multiple cancers [37]. Shared T cell epitopes have been explored for therapeutic applicability in different cancers, but past attempts have not been clinically successful [38], [39]. In part, this

is attributed by the fact that stimulating T cells to target self-epitopes confers a risk of autoimmune destruction of healthy tissues [40], [41]. Furthermore, T cells to these self-targets are likely hampered by mechanisms central and peripheral tolerance.

However, shared T cell antigens are still of clinical relevance due to their advantageous potentially wide applicability across cohorts of patients and cancers. As such, cancer immunotherapy company BioNTech are currently exploring RNA vaccines containing overexpression, cancer testis, and differentiation T cell antigens in melanoma and prostate cancer in clinical phase I/II trials with promising preliminary results, as presented by Dr. Özlem Tureci at the 5th CRI-CIMT-EATI-AACR International Cancer Immunotherapy Conference in September 2019. The clinical potential of shared tumor antigens is therefore not exhausted, and novel delivery modalities and adjuvant systems might facilitate exploiting said antigens in off-the-shelf therapeutics to benefit many patients.

Neo-epitopes

In contrast to shared T cell epitopes stand T cell neo-epitopes; the products of genetic alterations such as somatic mutations or in tumor cells. From the overall limited successes of exploiting shared T cell epitopes for cancer therapy, there is now an increasing interest in neo-epitopes, whose expression is restricted to tumor cells. In theory, if we are able to harness immune cells to target neo-epitopes, we can achieve tumor elimination while avoiding destruction of healthy tissue. Neo-epitopes have been described as the “Achille’s heel” of cancer, owing to the fact that mutations are what defines a tumor and enables malignant behavior, but at the same time mutations flag tumors as aberrant and non-self to cells of the immune system. There are several reports on patient tumor mutational burden (TMB) and putative neo-epitope load correlating with intratumoral T cell activity and disease prognosis [42]–[44]. Combined with observations that beneficial clinical responses from checkpoint inhibitor (CPI) therapy [24]-[25] and adoptive cell transfer (ACT) [47], [48] have been associated with neo-epitope reactive T cells, tumor neo-epitopes are now a major focus in the field of cancer immunotherapy. Interestingly, harnessing the immune system to target neo-epitopes has been suggested to make up a “final common pathway of cancer” [49], based on the positive associations described above. Ironically, this would mean that mutations, the very enablers of malignant transformation, will also provide the ideal targets for immunotherapy in a variety of cancers.

Subtypes of neo-epitopes have been defined, based on the position or effect of the somatic mutation. This classically includes non-synonymous single nucleotide variants, also referred to as point mutations, and insertions/deletions leading to frameshift mutations. A T cell neo-epitope can arise in two ways. First, by mutations in residues that affect binding to MHC, so called peptide anchor positions, whereby a prior non-binding peptide becomes an MHC binder (Figure 5A). Second, by mutations in residues that interacts with the TCR, but anchor positions are retained (Figure 5B)[50]. Importantly, neo-epitopes that arise as a result from anchor position mutations will display improved MHC binding (IB) and since the corresponding wild type (WT) peptides were not MHC ligands, IB neo-epitope recognizing T cells were not eliminated by central tolerance. Therefore, presented IB neo-epitopes will inherently be perceived as non-self to T cells. In the second case, where neo-epitopes arise due to TCR facing residue mutations, MHC binding is conserved (CB), and an important determinant for CB neo-epitope immunogenicity has been shown to be low degree of self-similarity of the resulting peptide, as outlined by Bjerregaard et al. [51]. This is due to the WT peptide being displayed by MHC during thymic development and high affinity T cells specific to WT peptide deleted by negative selection. Thus, tolerance mechanisms differentially affect putative neo-epitopes, depending on the position of the mutations, and for CB neo-epitopes the TCR facing mutation must make the neo-epitope look more different from self to overcome this, as is not the case with IB neo-peptides.

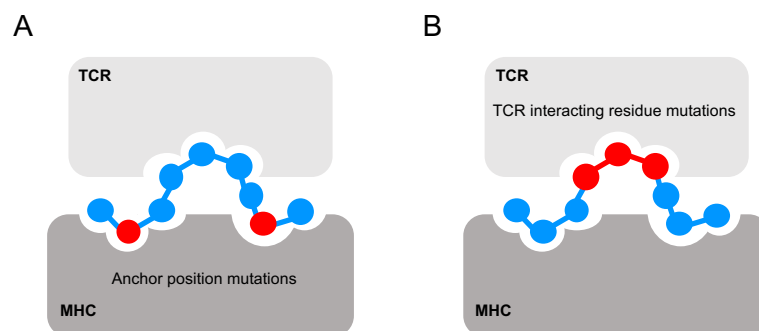


Figure 5 – Position of mutated amino acid residue(s) as a determinant for how neo-epitopes becomes visible to T cells. Mutations arise in amino acid residues that make a prior MHC non-binder into a binder (**A**). Mutations arise in TCR facing residues which facilitates different recognition by T cells (**B**).

Additional considerations on tumor mutations include the driver and passenger mutation concept and the heterogeneity of mutation expression by tumor cells. Driver mutations provide tumor cells selective growth advantages and directly promote tumor development, e.g. loss-of-function mutations of tumor suppressor genes and gain-of-function mutations

of oncogenes [52]. Passenger mutations have seemingly no role in tumorigenesis but are products of tumor genetic instability that are carried along by driver mutations. Some mutations are proposedly categorized in-between, as “mini-drivers” [53] or essential passengers [54], and harboring multiple of these might provide tumorigenic effects as a driver mutation. Mutations in tumors happen at random, why the resulting neo-epitopes are strictly patient unique, with very few exceptions of described “public” or recurrent neo-epitopes [55]. The concept of tumor heterogeneity can be analyzed bioinformatically and exists on different levels: from patient to patient, between two different tumor lesions (metastases) in the same patient (intra-patient), and within a single tumor lesion of one patient (intra-tumoral). The intra-patient/intra-tumor framework encompasses mutations taking place at different stages of tumor evolution, and mutations are described as clonal when present in all tumor cells or subclonal when only present in a subset of cells [56]. Our understanding of tumor heterogeneity is still developing, and reports suggest that targeting clonal mutations over subclonal confers clinical benefit [57].

Neo-epitope prediction framework

Bioinformaticians can now map a patient’s tumor mutations with high confidence owing to advances and lower costs of next generation sequencing (NGS), the overall process is outlined in Figure 6. Tumor specific mutations are called by sequencing of tumor DNA via whole exome sequencing (WES/WXS) or whole genome sequencing (WGS) from a tumor fragment or cell line, comparing it to corresponding normal tissue [58]. The mutated or variant allele frequency in the tumor sample compared to normal provides information on clonal abundance of tumor cells that carry the given somatic mutation. Furthermore, tumor expression of mutated gene product is confirmed by RNA sequencing platforms or mass spectrometry (MS) [59]–[62]. Most pipelines moreover prioritize putative neo-epitopes based on *in silico* predicted peptide-MHC binding, e.g. via NetMHCpan [63], [64]. Selected neo-epitopes can be used to screen patient samples for spontaneously occurring or therapy induced neo-epitope specific T cells and/or be included in personalized vaccination strategies.

The number of somatic mutations and neo-epitope load varies greatly between cancers of different origin [65]. With melanoma and lung cancers in top of the range due to correlation of cancer incidence and carcinogen exposure of ultra-violet light and tobacco smoke,

respectively. Far from all predicted neo-epitopes are immunogenic [51]. To date, little is known about the rules that govern immunogenic neo-epitopes, but the consensus is that predicted peptide-MHC binding affinity and stability are robust correlates of neo-epitope immunogenicity [66]. Studies further propose the importance of prioritizing neo-epitopes based on low self-similarity [51], and amount of mutated peptide that reaches the ER and MHC loading machinery [67].

In summary, the amount of putative neo-epitopes to screen is vast and patient specific, imposing technical challenges for T cell detection methods.

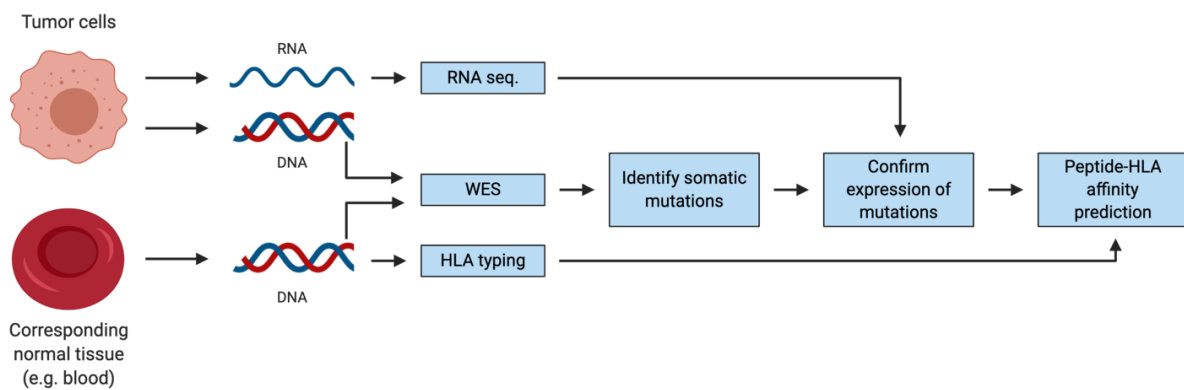


Figure 6 – Neo-epitope prediction based comparative sequencing between tumor and healthy tissue. Framework for neo-epitope prediction and selection strategies on a personalized basis. Somatic mutations are discovered in tumor tissue by whole exome sequencing (WES), compared to corresponding normal tissue, which is often a blood sample. RNA sequencing is often employed to confirm expression of mutated genes. Patient HLA type is determined from normal tissue DNA, where after mutated peptides able to be presented by patient HLAs can be affinity predicted by *in silico* methods. Figure made by the author, inspired by [68]

Monitoring of antigen specific T cells

Characterization of interactions between T cells and their cognate epitopes presented by MHCs holds implications for diagnostic and therapeutic approaches in a variety of diseases, particularly cancer. Immunological methods have been established to dissect specificity of T cells, with novel single cell sequencing based options allowing high dimensional profiling of relevant T cells, which reflects the growing understanding that not all cells are identical. Classical immune assays can be employed to measure the functionality of T cells, such as enzyme-linked immune absorbent spot (ELISPOT), intracellular cytokine staining (ICS), and cytotoxicity assays. These functional assays commonly involve stimulating T cells with antigens (peptide or protein), target cells (tumor cells or antigen pulsed DCs), or stimulatory

molecules (IL-2, anti-CD3/anti-CD28 beads) before measuring cytokine production in bulk culture, sorted cell fractions, or individual cells. Advantageous to functional assays is that peptide antigens of varying amino acid length can be used in the T cell stimulation, accommodating both MHC class I and II presentation to CD4⁺ and CD8⁺ T cells respectively. As an alternative or add-on to further dissect the specific peptide recognition of T cells, MHC multimer analyses can be applied. The affinity of a single TCR-pMHC interaction is very low, which originally hindered direct *ex vivo* detection of antigen specific T cells via pMHC molecules [69]. Altman and colleagues uncovered a solution by multimerization of recombinant biotinylated pMHCs with streptavidin, to form tetramer pMHC complexes that hold sufficient avidity to monitor specific T cells via fluorescent labeling and flow cytometry analysis [70]. A breakthrough that has significantly advanced epitope discovery in multiple disease settings. Later, the introduction of effective peptide-MHC exchange technologies, particularly UV-mediated peptide exchange by Toebes and colleagues, allowed production of larger pMHC multimer libraries in parallel, thus circumventing the prior tedious individual refolding of MHC with each putative T cell epitope [71]. There are now multiple descriptions of HLA and H-2 allele restricted ligands (i.e. conditional ligands) for UV-mediated peptide exchange, why this technology is broadly used for pMHC multimer screening purposes [71]–[75].

Newer developments in the MHC multimer field include: 1) applying backbones for higher order multimerizations, potentially increasing sensitivity to detect lower affinity pMHC-TCR interactions [76], 2) fluorescent combinatorial encoding or metal tags for higher complexity screening of multiple T cell specificities via flow or mass cytometry [77], [78], 3) DNA barcodes as multimer tags allowing high throughput screening for >1000 pMHC specific T cells in parallel in a single sample [79], 4) applying stable empty loadable MHC molecules to form multimers [80]. MHC multimer based T cell detection methods are, for now, mostly applicable for CD8⁺ T cells. This is in part due to the fact that MHC class II multimers have proved difficult to produce, requiring mammalian or insect cell expression systems [81]. Furthermore, *in silico* MHC class II affinity predictions are less developed than the MHC class I counterparts and CD4⁺ T cells often display low TCR-pMHC affinity, as reviewed by Hadrup and Newell [82]. Monitoring of antigen specific CD4⁺ T cells therefore often relies on functional readouts such as ELISPOT and ICS, where the measured cytokine production will uncover presence, frequency, type and functionality of CD4⁺ T cells in a given sample.

The number of potential T cell epitopes in human diseases is immense and will to a large extent be patient specific due to HLA diversity and, for cancer, unique neo-epitope landscapes resulting from somatic mutations. As such, the described advances in T cell detection technologies are imperative to explore the large candidate neo-epitope outputs from NGS pipelines.

The above described methods are often combined with further T cell characterization via cell surface markers and transcription factors, to determine e.g. exhaustion, tissue residency and memory status of T cells. As outlined, several T cell detection assays are flow cytometry based and the advent of ever developing polychromatic flow cytometry with novel fluorescent markers and increased capacities of flow cytometers has paved the way for in-depth T cell interrogation. In cancer, these advances have proved valuable for diagnosis and immune monitoring and potential stratification of patients to certain immunotherapies based on their T cell signatures.

Cancer immunotherapy

Clinical advances and considerations

The ability of the immune system to specifically recognize and eliminate cancer cells is exploited through cancer immunotherapy. Though intrinsic interactions between a developing tumor and the immune system are, as outlined previously in this text, multifaceted and often lead to tumor outgrowth, immunotherapy offers ways to shift that balance towards tumor elimination. As such, advances in immunotherapy have revolutionized cancer treatment through the last decades, and immune mediated interventions have become mainstream clinical therapy for several cancer indications [83]. Cancer immunotherapy has thus joined surgery, radiation, and chemotherapy as a pillar of cancer therapy.

Successful immunotherapies harbor approaches of ‘off-the-shelf’ or more personalized character. The advent of monoclonal antibodies for immune checkpoint inhibition such as anti-cytotoxic T lymphocyte associated protein 4 (CTLA-4) and anti-programmed death 1 or anti-programmed death ligand 1 (PD-1/PD-L1) have provided remarkable results in the clinic and now benefit patients with multiple cancer types [84]. Discoveries that were awarded with the Nobel Prize in Physiology and Medicine in 2018. Checkpoint inhibitor (CPI) therapy releases the brakes imposed on T cells in the often suppressive TME, thus reinvigorating their effector functions from an otherwise dysfunctional state. The mechanisms behind

beneficial CPI therapy are not completely understood, but for anti-CTLA-4 the mechanism is thought to be in part by depletion of regulatory T cells from the TME [85], [86]. Anti-PD-1 is recognized to induce expansion of exhausted-like, tumor recognizing PD-1+ CD8+ T cells [87]–[89] and response to therapy has recently been associated with a clonal replacement of intratumoral CD8+ T cells that were not present in the tumor prior to treatment [90]. Response to anti-PD-1 therapy and overall improved prognosis for cancer patients has been associated with TIL presence of CD8+ T cells that express CD39 and CD103 [91], [92]. CD8+ T cells in tumors with these markers are considered tumor specific or tumor reactive, distinguishing them from bystander T cells that are also present in the tumor infiltrate. CPI therapy is termed as somewhat unspecific, since it confers potential unleashing of all systemic T cells, which can lead to severe autoimmune adverse events [93].

Adoptive cell transfer (ACT) is another and more personalized approach that relies on *ex vivo* expansion of autologous TILs, genetically engineered Chimeric Antigen Receptor (CAR) T cells or otherwise TCR transduced T cells for cancer therapy [94]. These cellular therapies have been successful across multiple cancer types, with particularly CAR T cells making a recent breakthrough in treatments of hematological B cell malignancies [95].

However, for reasons that are not fully understood, only a fraction of patients respond to current cancer immunotherapy, and some even relapse after initially responding [96]. There is a growing interest in trying to define and stratify which patients will respond, and which will not. The field is therefore investigating new approaches in the form of combination therapies and novel treatment modalities.

Therapeutic cancer vaccines

Cancer vaccines are considered to work synergistically with CPI therapy in cancer, since vaccination can ideally both boost existing T cell responses and induce them *de novo*, as outlined in Figure 7. Several considerations go into rational cancer vaccine design, including choice of antigen(s), antigen format, and adjuvants [97]. Regarding antigen selection, there are options of more or less personalized character, of which neo-epitopes are proposedly ideal tumor targets since they are truly tumor specific [49], [98]. With neo-epitopes as targets, vaccines are selected and produced individually for each patient, leading to higher cost and time consumption than off-the-shelf therapeutics. Epitopes of shared origin are in this sense advantageous since they are broadly expressed between different cancer types and patients, however they bring risks of autoimmunity if targeted and are highly affected by central

tolerance. Furthermore, since not all cancers are equally burdened by somatic mutations, different cancer types call for different antigen selection strategies. Leading companies in the field of personalized vaccinations BioNTech and Neon Therapeutics are both currently pursuing therapeutic combinations of neo- and off-the-shelf targeted antigens [97]. Whatever the approach, it is sensible to include multiple tumor epitopes in a cancer vaccine to increase the breadth of the anti-tumor response and overcome challenges of tumor heterogeneity and loss of tumor cell variants as an escape mechanism.

Fundamental to inducing potent anti-tumor responses is the activation and priming of T cells by APCs. As outlined previously, this process starts with innate sensing of danger signals, which shapes the adaptive immune responses that follows. A process, that can be controlled by both the format of the antigen, administration route and choice of adjuvant. A plethora of adjuvants have been developed, and these can overall be divided in two categories: depot-effect delivery systems and immunostimulants, or combinations thereof [99], [100]. In general, adjuvants contribute to upregulate co-stimulatory molecules, MHC presentation and cytokines by DCs. A frequently used depot-effect delivery is aluminum salts (mostly aluminum hydroxide/alum), used in common pathogen vaccines, but a robust inducer of T_H2-like immunity when delivered alone and thus not considered suitable for cancer vaccines [101]. Another option is water-in-oil emulsions such as Montanide, that ensures slow release of e.g. peptide antigens which induce prolonged immune responses and has been investigated in clinical cancer vaccine trials without observation of toxicities [102]. Polymer and liposome-based delivery technologies are also being investigated for capability to deliver cancer antigens and cytotoxic drugs, offering biocompatible cargo protection and possibilities of specific delivery to e.g. DCs via coupling to antibodies [103], [104]. Cationic liposomes have been reported to improve cross-presentation by DCs in murine models, allowing priming of CD8⁺ T cells [105], [106].

The immunostimulants are primarily PRR agonists that trigger innate immune sensing. An example relevant for the scope of this thesis, is the different TLR ligands of which some are being investigated in cancer vaccines. Clinical trials have used TLR3 ligand polyinosinic-polycytidylic acid with poly-L-lysine (poly-ICLC) together with synthetic neo-peptides in melanoma and glioblastoma [68], [107] or NY-ESO-1 derived peptides in ovarian cancer [108]. TLR3 ligands such as poly-ICLC are synthetic double-stranded RNA and thus mimic viral infection, giving rise to solid T_H1-like immune responses [109], [110]. Antigens delivered in the format of synthetic peptides or whole protein are poorly immunogenic on their own

and require adjuvants and/or carrier system for efficient delivery and immunogenicity [101]. Antigen in the form of DNA and RNA harbor self-adjuvating effects that mimic viral infections but might need delivery by carrier systems to provide protection from systemic clearance. Antigens encoded by plasmid DNA will be detected by intracellular components of the innate DNA sensing machinery, particularly stimulator of interferon genes (STING) and TANK binding kinase 1 (TBK1) pathways [111]–[113]. CpG rich DNA will mimic intracellular bacterial infection via TLR9 sensing [114]. Antigen encoded by RNA will be sensed primarily by TLR7 [115], which has been exploited with success in recent clinical trials of personalized neo-epitope vaccination [116], [117]. The recent clinical trials mentioned in this paragraph all reported that their vaccines induced more neo-epitope specific CD4+ than CD8+ T cells, albeit including antigens with minimal epitope determinants for patients’ HLA class I and II. Though CD8+ T cells are the main mediators of tumor destruction, CD4+ T cell help is indeed essential to induce effective CD8+ T cell responses [118].

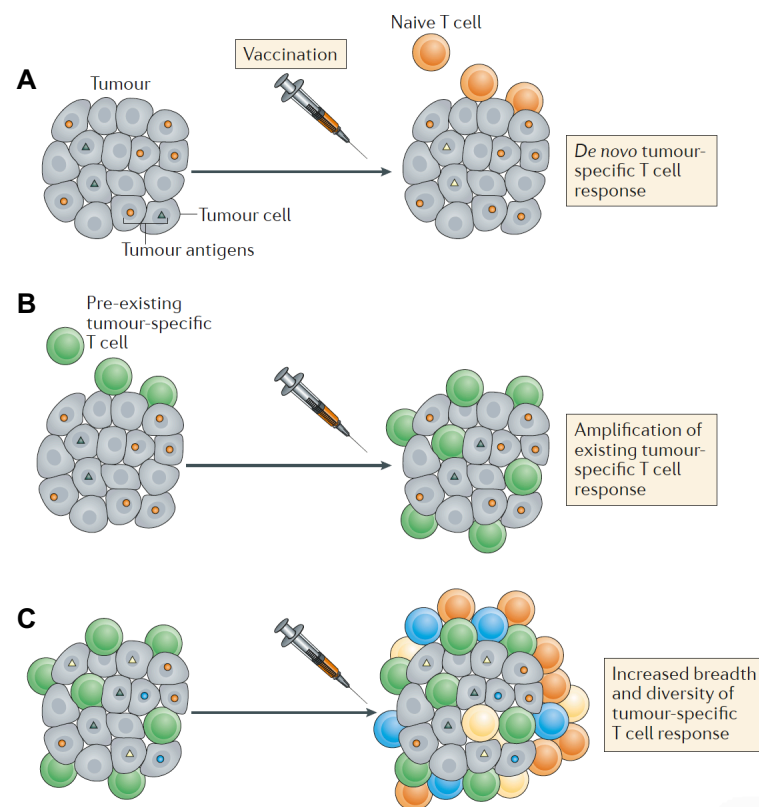


Figure 7 – Vaccination to induce increased anti-tumor immune responses. Vaccination can be used to increase (A) *de novo* T cell responses that were not present before vaccination, (B) amplify or boost T cells that were present in lower numbers before vaccination, and (C) a combination of A and B, where diverse populations of T cells are induced, conferring potentially broad tumor recognition of multiple antigens. Figure adapted from [68]

In conclusion, after years of limited clinical success [38], [119] cancer vaccines are revisited and show promising preliminary results particularly in the neo-epitope space. Vaccine combinations with CPI therapy confers the potential to unleash the brakes imposed on immune cells and specifically steer the immune system towards relevant tumor targets. The field is increasingly moving towards tailored, personalized vaccination strategies, which imposes increased demands for neo-epitope prediction and prioritization based on bioinformatic approaches as well as individual vaccine manufacturing [120].

Lessons from preclinical mouse models

Mice have for decades been the most commonly used animal model for immunology and cancer research. Importantly, mouse models have provided important insights into the dynamic interplay between cancer and the immune system, reviewed in detail by Dunn et al. [121]. Initially, mouse models demonstrated the role of immune surveillance and immunologic recognition of tumors by showing how mice that lack central components of innate and adaptive immunity have enhanced susceptibility to chemically induced and spontaneously developed tumors. Next, mouse models provided the basis for the immunoeediting theory, showing how tumor immunogenicity is shaped by the immune system. This was apparent by several studies, where tumors grown on immunocompromised mice were immunogenic and rapidly rejected when transplanted to immunocompetent mice. Conversely, tumors grown on immunocompetent mice were not immunogenic and were not rejected when transplanted to other immunocompetent mice.

The most commonly used mouse models in cancer are the syngeneic models. Here, immunocompetent host mice, often of inbred C57BL/6 and BALB/c background, are transplanted with histocompatible tumor cell lines. Many syngeneic models have been developed, representing diverse tissue origins with differential levels of immunogenicity, TME compositions, and varying sensitivity to immunotherapy [122]. These inbred mice offer reproducible tumor growth experiments, in which tumor cells are often inoculated subcutaneously and easily measurable. However, inbred mice inherently have a limited MHC class I and II repertoire and syngeneic models neither recapitulate interpatient or intratumor heterogeneity. Alternatively, patient-derived xenograft (PDX) models can be used. PDX models entail immunodeficient mice that allow inoculation of patient derived tumor cell lines for evaluation of personalized, clinically relevant therapies. However, in conventional PDX

models that lack a competent immune system, the tumor is not subjected to immune surveillance and immunoediting. To mitigate this, humanized mice have been developed, such as the human IL-2 expressing PDX model that facilitates assessment of a patient's autologous *ex vivo* expanded TILs towards patient's tumor cell line [123] and also mice that have further humanized immune systems after transfer of hematopoietic stem cells [124], for testing of immunotherapies.

For several well characterized syngeneic tumor models there are descriptions of therapeutically relevant neo-epitopes, such as: CT26 [125], [126], MC38 [127], [128], and B16-F10 [129]. Murine neo-epitope vaccination studies, either alone or in combination with CPI therapy, have contributed to our understanding of tumor neo-epitopes and the framework we use to predict them [129], [130]. These models have uncovered that CPI therapy-mediated rejection of established tumors is mainly driven by neo-epitope specific T cell responses [131]. Further, that CPI therapy modulates neo-epitope specific T cells and myeloid cells inside the tumor and not to the same extent those that are present in periphery [132], [133]. Moreover, we have recently seen evidence from syngeneic models that vaccination and CPI therapy can induce CD4+ and CD8+ neo-epitope specific T cells important for tumor rejection [126], [134], even when tumor does not express MHC class II [135]. Thus, both clinical and preclinical observations underline an important role of cytotoxic and helper T cells in the anti-tumor response [136].

Neo-epitope discovery studies in murine models will, together with clinical studies, contribute to interrogate the rules that define ideal neo-epitopes. However, the aforementioned narrow MHC repertoire of these mouse models naturally limits the epitopes that can be displayed, compared to humans. Similarly, majority of tumor antigens, let alone neo-epitopes, will not be shared between mice and humans, why therapies to target them are difficult to translate. Furthermore, many common syngeneic tumors grow rapidly upon transplantation on the mice, why there is a narrow therapeutic window and a short time to mount anti-tumor immunity via e.g. vaccination [122], [137]. Since the syngeneic tumor is transplanted, there is no extensive phase of co-development between mouse and tumor as there is in patients, where a tumor can develop over several years. Though some lessons from mouse models might be 'lost in translation' [138], they remain applicable for examining the effects of different vaccination approaches such as dosing, vaccination schedules, antigen formats and adjuvants [97]. Mouse models provide mechanistic insights of relevance to the clinical realm.

2. MANUSCRIPT I

H-2 multimers for high-throughput T cell interrogation and description of novel conditional ligands for H-2D^d and H-2K^d

MHC multimer technologies have for long been instrumental in the monitoring of antigen specific T cells and epitope discovery in a wide range of diseases. Here, we designed and validated murine H-2D^d and H-2K^d conditional ligands for UV-mediated peptide exchange. Furthermore, we used H-2D^d, H-2K^d and H-2L^d molecules for H-2 tetramer stainings and provided proof-of-concept for their use in DNA barcode-labeled H-2 multimers for large-scale CD8⁺ T cell interrogation. We expect these new conditional ligands and the high throughput screening methodology to improve epitope mapping in various diseases in H-2^d models, including cancer and autoimmunity.

This manuscript has been written and formatted for submission to Journal of Immunology, specifically their subsection on 'Novel Immunological Methods'.

H-2 multimers for high-throughput T cell interrogation and description of novel conditional ligands for H-2D^d and H-2K^d

Authors: Nadia Viborg^{1*}, Trine Sundebo Meldgaard^{1*}, Tripti Tamhane¹, Sara Suarez Hernandez¹, Christian Garde², Thomas Trolle², Dario Vazquez Albacete^{1#}, and Sine Reker Hadrup¹

Affiliations: ¹Department of Health Technology, Technical University of Denmark, Lyngby, Denmark, ²Evaxion Biotech, Copenhagen, Denmark, *These authors contributed equally, #Current affiliation: Department of Biotechnology and Biomedicine, DTU Bioengineering, Technical University of Denmark, Lyngby, Denmark

Corresponding author: Sine Reker Hadrup, Section for Experimental and Translational Immunology, Department of Health Technology, Technical University of Denmark, Kemitorvet Building 204, 2800 Kgs. Lyngby, Denmark. Phone: +45 35886290. E-mail: sirha@dtu.dk.

Financial support: This research was funded in part The Danish Innovation Fund (project XVAC and NeoPepVac) and The European Research Council, ERC StG nextDART.

Number of figures: 4

Number of tables: 1

Number of supplementary figures: 2

Number of supplementary tables: 1

Abstract

MHC multimer technologies have facilitated flow cytometric tracking of antigen specific T cells since the first description of the concept in 1996. With implementation of UV-mediated peptide exchange one decade later, Toebes and colleagues portrayed a technique enabling the generation of multiple different MHC multimer specificities in parallel, surpassing tedious individual refolding of MHC molecules with peptide ligands. Murine models are acknowledged as an effective tool for pre-clinical research to advance our understanding of immunological mechanisms, with potential translatability of key learnings from mouse models to the clinic. The common inbred mouse strain BALB/c is frequently used in immunological research. However, for BALB/c haplotype H-2 alleles only one conditional UV ligand has been described thus far, restricted to H-2Ld. To overcome this challenge, we designed and experimentally validated conditional ligands restricted to murine MHC alleles H-2Dd and H-2Kd. We demonstrated the ability of the three H-2d molecules folded in-house with conditional ligands to generate fluorescently labeled peptide-H-2 tetramers that could stain antigen specific CD8⁺ T cells in splenocyte samples. Finally, we generated peptide-H-2 multimer libraries with a DNA-barcode labeling system for high-throughput interrogation of CD8⁺ T cell specificity in murine samples. In summary, the described techniques will contribute to our understanding of the antigen specific CD8⁺ T cell repertoire in murine pre-clinical models of various diseases.

Introduction

Major histocompatibility complex (MHC) class I molecules display endogenous peptide products of proteasomal degradation on the surface of all nucleated cells. T cell based immune surveillance relies on this presentation and the specific interaction between peptide-MHC (pMHC) and the T cell receptor (TCR), enabling cytotoxic T cells to identify and eliminate aberrant cells. Two decades of research have provided tools to identify, characterize and isolate antigen specific T cells. In particular, multimerization and fluoro-chrome labeling of MHC I molecules have accelerated the understanding of pMHC-TCR interactions within infections, autoimmune diseases and cancer, where CD8⁺ T cells play a pivotal role [1]. pMHC tetramers are commonly used in the field and can facilitate the detection of multiple different antigen specific CD8⁺ T cells in parallel, when e.g. combinatorial fluorescent labeling is used [2].

An innovative contribution to the pMHC multimer space occurred when MHC protein was produced and refolded with a so-called conditional ligand. A technique first described by Toebe et al. [3], where an amino acid moiety in the T cell receptor-exposed site of a known MHC ligand is replaced with a non-natural amino acid (2-nitrophenylglycine or 3-amino-3-(2-nitrophenyl)-propionic acid) that is cleavable upon exposure to 366 nm UV light (denoted “J”). Upon UV light mediated cleavage of the conditional ligand, the MHC binding groove is left empty and receptive of another ligand of choice. This UV-mediated exchange allows for the rapid and high-throughput generation of large panels of distinct pMHC specificities.

Since the development of pMHC tetramers and the introduction of the UV exchange technology, higher order pMHC multimerizations and high-throughput labeling systems have been developed. Recently, DNA barcode labeled pMHC multimers were proven to allow large-scale detection of antigen specific CD8⁺ T cells, with the possibility to screen samples for recognition of >1000 different pMHC multimers simultaneously [4]. A technology that can contribute to uncover new T cell epitopes and understand pMHC-TCR interactions in a wide variety of diseases.

Preclinical models have proven important for acquiring mechanistic understanding of immunological diseases and supporting the development and evaluation of new therapeutic interventions. Mouse models are frequently used in cancer research, where especially the tumor neoepitope field is being extensively studied [5]–[8]. A number syngeneic murine tumors have been

developed based on the inbred strains C57BL/6 and BALB/c. These syngenic tumor models represent a range of different tissue origins, and show different levels of immunogenicity and treatment sensitivity [9]. There is a great need to enable the screening of murine samples in a high-throughput manner to identify CD8⁺ T cells responsive to e.g. tumor neo-epitopes predicted via mutational mapping and following *in silico*-based prediction of the MHC I binding characteristics. Such predictive strategies lead to the identification of large peptide libraries, for which limited knowledge is currently available governing the rules that determine T cell immunity. For the generation of large libraries of pMHC complexes, conditional ligands are a prerequisite. There are several published descriptions of murine conditional ligands, but for the BALB/c haplotype only one has been presented, namely H-2L^d [10]–[12].

In this study we design and validate conditional ligands for murine MHC I alleles H-2D^d and H-2K^d. We use these together with H-2L^d to setup up a DNA barcode labeled peptide-H-2 (pH-2) multimer library, with 72 different pH-2 specificities and use this to screen murine splenocyte samples in a high-throughput manner for antigen specific CD8⁺ T cells.

Results

Design of conditional ligands for murine MHC alleles H-2D^d and H-2K^d

We designed and tested conditional ligands for H-2D^d and H-2K^d in house, based on well described, high affinity ligands; RGPGRAFVTI from HIV Env gp160 antigen and IYSTVASSL from influenza HA antigen. For both H-2D^d and H-2K^d we introduced the a UV-labile amino acid modification, 3-amino-3-(2-nitrophenyl)-propionic acid (“J”), in the TCR-facing part of the peptide sequence, to avoid the anchor residues and thus retain binding between peptide and MHC molecule. For H-2D^d the characteristics of a good binder, that we sought to preserve, includes: glycine (G) at P2, proline (P) at P3, and i leucine (L), isoleucine (I), or phenylalanine (F) at P9 or P10 along with a positive charge (e.g. R) at P5 [13]. Hence, we introduced the “J” modification at P7 (Table I). For H-2K^d the characteristics of a good binder comprises: tyrosine (Y) at P2, leucine (L) at P9 or P10 along with an uncharged residue at P5 (e.g. V) [14], [15]. Therefore, we introduced the “J” modification by substitution at position 6 (Table I). H-2D^d and H-2K^d peptide binding motifs are visualized in supplementary figure 1, generated based on ligand data from [16]–[19].

Mouse strain	Murine H-2 allele	Conditional UV ligand	Specific/immunization epitopes (%rank score) ^a
BALB/c	H-2D ^d	RGPGRA-J-FVT	RGPGRAFVTI (HIV Env gp160 ₃₁₁₋₃₂₀) [20] (0.0081)
	H-2K ^d	IYSTV-J-SSL	IYSTVASSL (Influenza HA ₅₁₈₋₅₂₆) [21] (0.0077)
	H-2L ^d	YPNVNIH-J-F [12]	RPQASGVYM (LCMV NP ₁₁₈₋₁₂₆) [22] (0.0586)

Table I. Overview of investigated MHC class I molecules and relevant epitopes.

For H-2D^d and H-2K^d no conditional UV ligands have been described in the literature thus far. Therefore, these have been designed for this study. ^a Italic values in parenthesis represent predicted NetH2pan %rank score of peptides to their corresponding MHC allele. “J” denotes the position of a UV labile residue within conditional ligands.

UV exchangeable H-2 monomers were produced for H-2^d alleles

Murine H-2 molecules were produced in house and folded with an allele-specific UV cleavable conditional ligand (called p*H-2 going forward) (Table I). A UV light induced degradation of the conditional ligand in the presence of a peptide of interest facilitates peptide exchange. Thus, we measured the stability of these monomers by exposing them to 366 nm UV light for one hour and analyzed them on an analytical HPLC column. A complete degradation of all five investigated H-2

molecules was observed as compared to samples not exposed to UV light (Figure 1). This suggests that the UV light induced cleavage of the conditional ligand and dissociation from the binding groove results in MHC disintegration, which can be stabilized by adding an MHC-binding peptide of interest during the UV light exposure. Thus, in conclusion the p*H-2^d possess the properties required for UV-mediated peptide exchange and large library pH-2 generation.

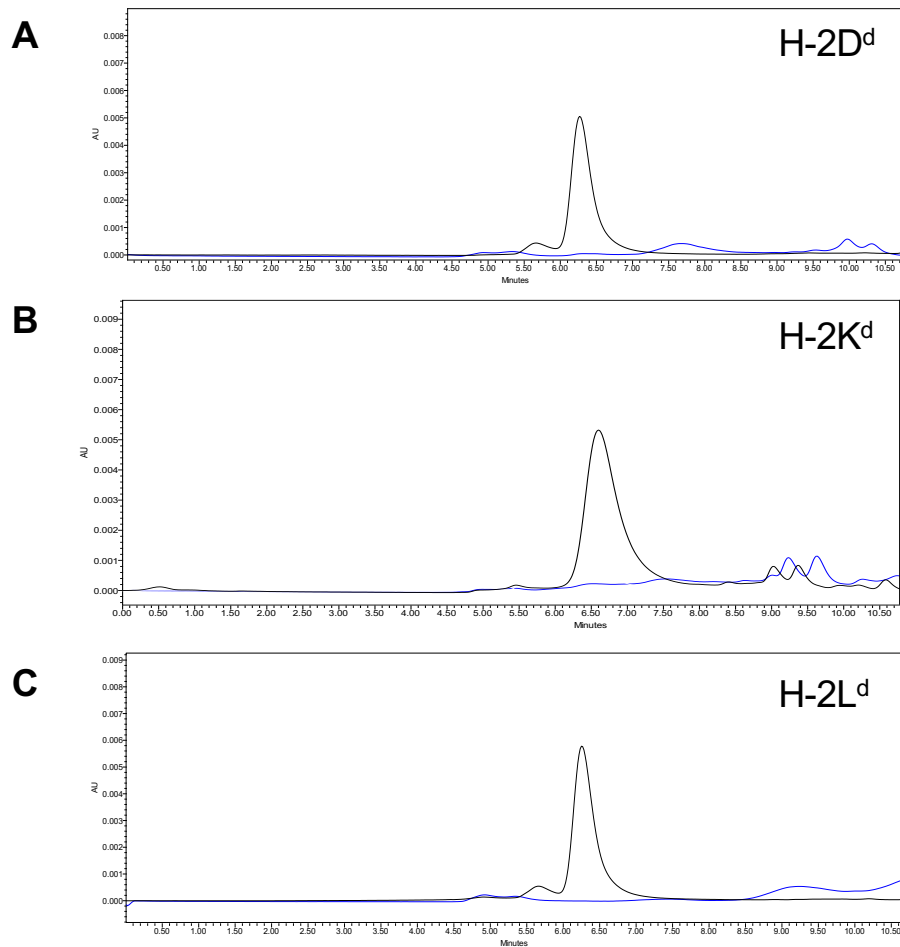


Figure 1. Conditional UV-ligands were successfully used to fold H-2 monomers.

HPLC chromatograms showing MHC monomers purified after folding with a photocleavable-peptide (black) and comparing with monomers incubating under UV-light for one hour (blue) for H-2D^d (A), H-2K^d (B), and H-2L^d (C). Peak height corresponds to the amount of stable protein normalized for comparative runs on each plot.

Detection of antigen specific CD8⁺ T cells in murine splenocyte samples via pH-2 tetramer staining

To confirm the presence of antigen specific CD8⁺ T cells in our murine splenocyte samples and validate the potential use of the newly designed UV ligand p*H-2 monomers, we generated pH-2 tetramers by UV exchange and coupling of exchanged biotinylated pH-2 products to PE-conjugated streptavidin. Splenocyte samples from immunized or transgenic mice (from here on: antigen specific mice) were stained with either 1) pH-2 tetramers exchanged with the specific peptides corresponding to specificity induced by immunization or transgenic TCR clone specificity (Table I), and 2) pH-2 tetramers exchanged with an irrelevant peptide (predicted H-2^d ligand neo-peptides from murine syngenic tumor cell line CT26 – supplementary table 1). As controls, splenocyte samples from naïve BALB/c mice were stained with the same specific peptide tetramers as the antigen specific mice.

By flow cytometry, we confirmed pH-2 tetramer specific CD8⁺ T cells present in all antigen specific mouse samples (Figure 2). Observed frequencies of antigen specific CD8⁺ T cells varied, with the TCR transgenic mouse sample (IYSTVASSL/H-2K^d) having >90% tetramer specific cells, and the immunized mice ranging from 2.7% (RGPGRAFVTI/H-2D^d) to 10% (RPQASGVYM/H-2L^d). The different antigen specific CD8⁺ T cell populations also displayed varying binding for their cognate epitope as apparent by the difference in separation of the tetramer positive from the tetramer negative CD8⁺ T cells. Control staining of antigen specific samples with irrelevant pH-2 tetramers and staining of naïve splenocyte samples with specific pH-2 tetramers revealed that the H-2 tetramers generate limited background, and display a pH-2-TCR restricted T cell interaction. FACS gating strategy for pH-2 tetramer stainings is shown in supplementary figure 2A. Thus, we have successfully generated pH-2^d tetramers after UV mediated peptide-exchange, and demonstrated successful staining of antigen specific CD8⁺ T cells in relevant mouse splenocytes.

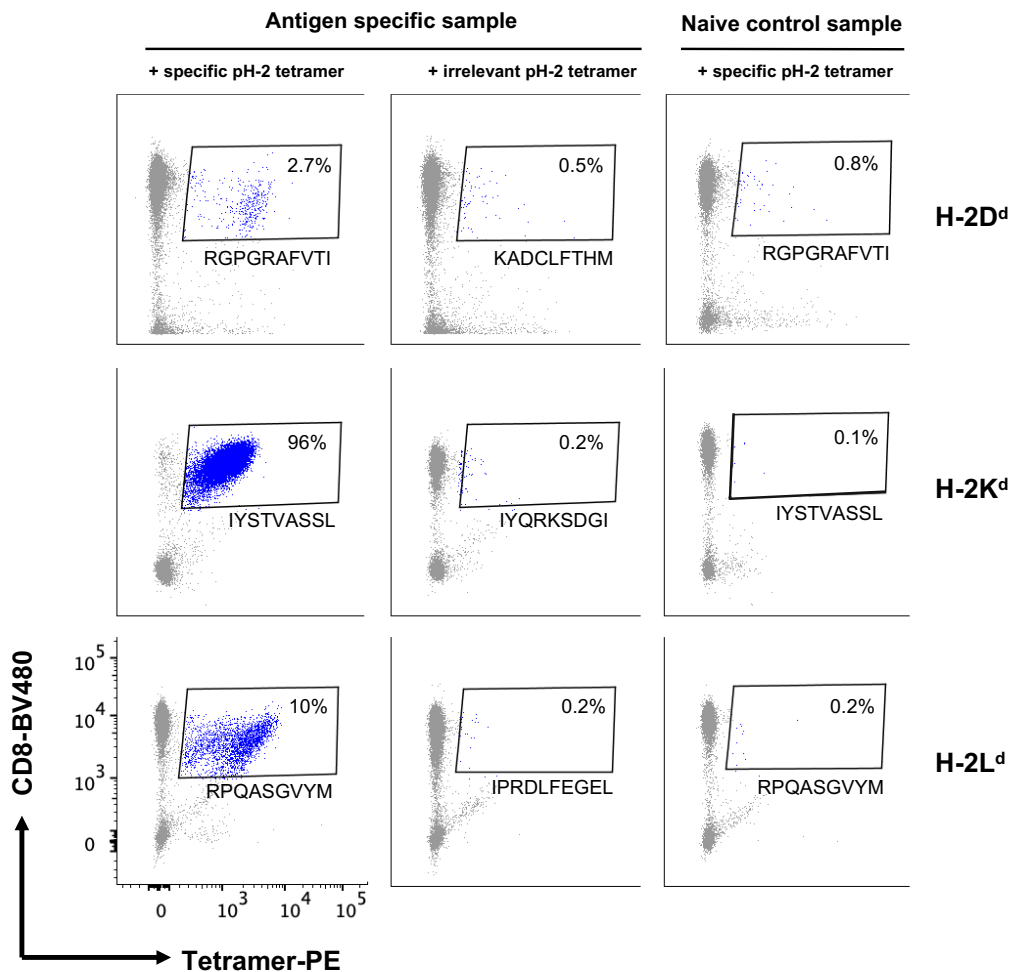


Figure 2. Detection of antigen specific CD8+ T cells via PE-labeled pH-2 tetramers

Successful UV-mediated peptide exchange and pH-2 tetramer assembly was validated for all H-2 alleles by tetramer staining (PE fluorophore label). Antigen specific splenocytes were stained with specific peptide tetramers and tetramers exchanged with irrelevant peptides to examine unspecific background staining from the tetramer reagents. Naïve control splenocytes from BALB/c mice were stained with specific peptide tetramers as a negative control. The frequency of pH-2 multimer specific T cells out of total CD8+ T cells is noted on each plot.

Large-scale interrogation of CD8+ T cell specificity using DNA barcode-labeled pH-2 multimer libraries

To evaluate the use of pH-2^d for large-scale interrogation of CD8+ T cell specificity, we generated a DNA barcode-labeled pH-2 multimer panel as previously described [4]. In brief, we performed UV mediated peptide exchange, followed by multimerization of the peptide-exchanged products onto a PE-labeled polysaccharide backbone individually coupled to DNA barcodes, forming a unique label

for each pH-2 specificity. We included three peptides corresponding to the T cell reactivities induced by immunization or transgenic TCR clone specificity (RGPGRAFVTI/H-2D^d, IYSTVASSL/H-2K^d and RPQASGVYM/H-2L^d). For each H-2^d allele, we furthermore included 22 irrelevant control peptides (predicted H-2^d ligand neo-peptides from murine syngeneic tumor cell line CT26). As an additional control, we included a multimerized form of the MHC without UV-mediated exchange, thus allowing the pH-2 multimer to contain the conditional UV ligand. This yielded 24 different specificities for each allele, adding up to a total pH-2 library of 72 different specificities, (see supplementary table 1 for full list of peptides).

Antigen specific and naïve control splenocyte samples were stained with the entire 72 pH-2 multimer library. Splenocytes from transgenic CL-4 mice were spiked into naïve BALB/c samples to reduce frequency of specific CD8⁺ T cells to approximately 20%. DNA barcode-labeled pH-2 multimers were used to individually stain and detect single populations of antigen specific CD8⁺ T cells in relevant samples (Figure 3). All samples were acquired by flow cytometry and CD8⁺ T cells bound to pH-2 multimers were sorted (all PE⁺ cells, see supplementary figure 2B for FACS gating strategy), where after the associated DNA barcodes were amplified by PCR and the specificity of the CD8⁺ T cells found by sequencing of the DNA barcodes. T cell responses were identified based on the enrichment of a given pH-2 complex in the sorted T cell fraction.

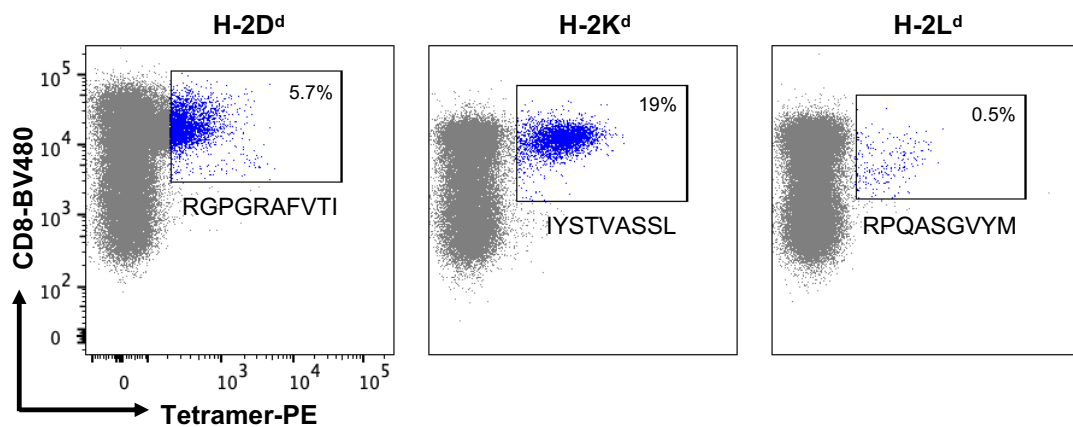


Figure 3. Single of antigen specific CD8⁺ T cells via DNA barcode labeled pH-2 multimers

DNA barcode labeled pH-2 multimers were validated via single staining of antigen specific samples. The frequency of pH-2 multimer specific T cells out of total CD8⁺ T cells is noted on each plot. Different mice were used for this staining than for figure 2, hence the differences in % antigen specific CD8⁺ T cells between the two figures.

With this large-scale technology, we were able to detect the specific CD8⁺ T cells in the antigen specific samples, corresponding to the observations with single pH-2 multimer stainings, i.e. in the RGPGRFVTI /H-2D^d immunized mouse, a RGPGRFVTI /H-2D^d CD8⁺ T cell response was detected, out of the total pool of 72 specificities, and so forth (Figure 4). In naïve control splenocytes (BALB/c) no antigen specific CD8⁺ T cell responses were detected. These findings were consistent across two replicate experiments.

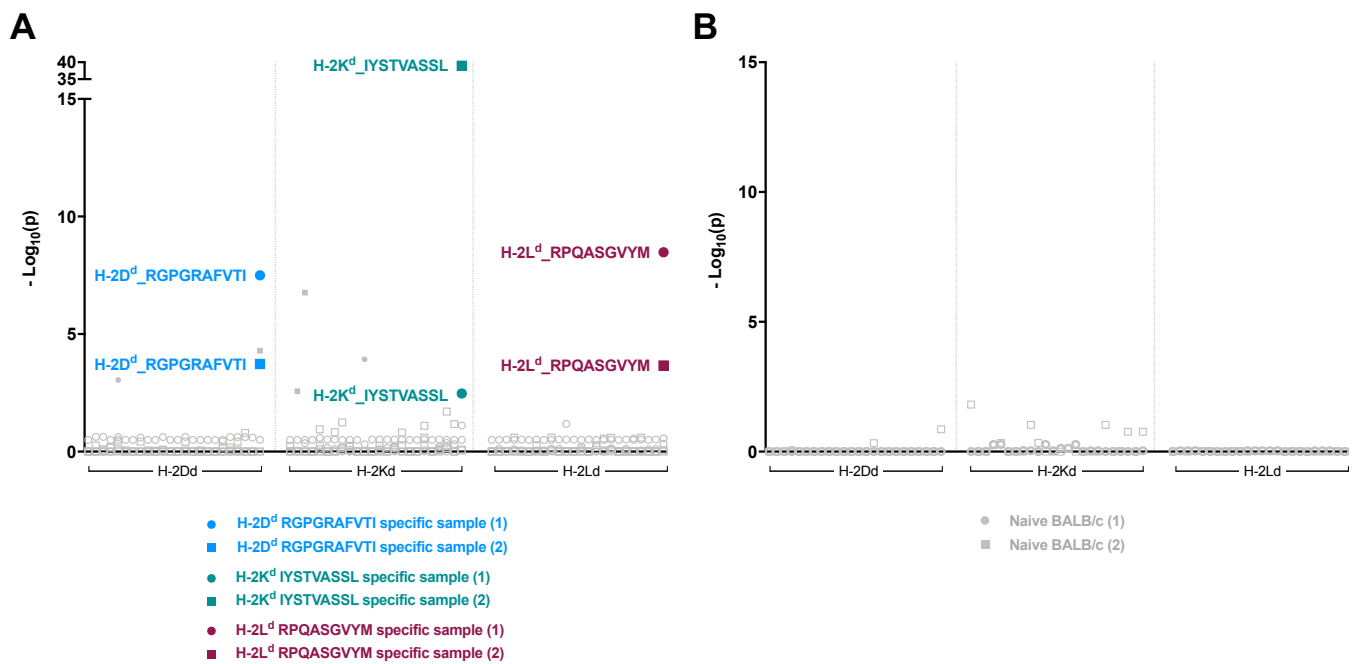


Figure 4. Detection of H-2 antigen specific CD8⁺ T cell responses via DNA barcode labeled pH-2 multimer screening

Screening for T cell recognition by DNA barcode-labeled pH-2 multimers in splenocytes from antigen specific mice (A) and naïve control mice (B), with a library of 72 different pH-2 specificities (24 specificities per allele). Filled symbols represent CD8⁺ T cell responses detected in H-2D^d RGPGRFVTI specific sample (blue), H-2K^d IYSTVASSL specific sample (green), or H-2L^d RPQASGVYM specific sample (dark red) samples. Data has been plotted on the y-axis as $-\text{Log}_{10}(p)$ of the relevant pH-2 associated DNA barcode. The values represent replicates from two different screenings (1, circles) and (2, squares).

Discussion

The data presented here display, for the first time, the design and use of conditional ligands for murine MHC class I alleles H-2D^d and H-2K^d. These novel conditional ligands facilitated the generation of specific pH-2 multimers via UV-mediated peptide exchange, alongside p*H-2L^d for which a conditional ligands has previously been described. UV-mediated peptide exchange technology enabled the production of several pH-2 multimers in parallel, overcoming the challenges and need for tedious individual folding of H-2 molecule with specific peptides. First, we were able to generate fluorescently labeled H-2 tetramers to stain murine pH-2^d haplotype samples for single antigen specific CD8⁺ T cell populations, obtained via peptide immunization or from transgenic T cells. Flow cytometric analysis confirmed presence of specific CD8⁺ T cells in relevant splenocyte samples and limited background signal in irrelevant samples. Second, we used the UV-mediated peptide exchange to generate a DNA barcode-labeled pH-2 multimer library containing 72 different pH-2 specificities. Flow cytometric sorting of multimer positive populations and recovery of DNA barcodes by sequencing corresponded to our findings from the tetramer stainings, i.e. antigen specific CD8⁺ T cells were observed in specific splenocyte samples.

The high-throughput DNA barcode labeled pMHC multimer methodology has recently been used to describe human autoreactive CD8⁺ T cells in narcolepsy [23] and CD8⁺ T cells specific to novel overexpression antigens in breast cancer [24]. This technology enables the interrogation of samples for hundreds of pMHC specificities in parallel, which is particularly advantageous when sample material is sparse, as described previously [4]. Importantly, platforms like the one described here allow extensive screening for pMHC-TCR interactions that will contribute to characterize what makes for a CD8⁺ T cell epitope, and not merely a good MHC binder, as is the output from current *in silico* prediction platforms. As an additional layer to these analyses, a recent publication reported the use of barcode labeled pMHC multimers to interrogate the motifs or “fingerprints” that govern TCR recognition of pMHC [25].

In cancer research preclinical mouse models have provided lessons that were translatable to clinical settings. Syngeneic tumor models based on inbred strains C57BL/6 and BALB/c are being extensively studied in immunotherapeutic settings, where particularly tumor neo-epitopes are considered therapeutically relevant. The *in silico* platforms that map tumor mutations and predict MHC binding peptides from the tumor peptidome generate large output libraries of putative neo-

epitope. Use of p*H-2 molecules with high-throughput multimer screening via the methodology described here, provides a tool to address the neo-epitope specific T cell repertoire across tumor models and therapies. It has been established, that different syngeneic tumor models are not equally sensitive to immunotherapies [9], [26]. Large-scale multimer analyses of the T cell repertoire will contribute to investigate the signatures of neo-epitope reactive T cells that favor immunotherapy responses.

We therefore argue that our description of novel conditional ligands for p*H-2D^d and p*H-2K^d adds to the value of previously described ligands and the proof of concept of p*H-2^d multimers for large-scale detection of antigen specific CD8⁺ T cells in murine samples will be of useful in the field of epitope discovery and immune monitoring going forward.

Materials and Methods

UV ligand design

To produce stable murine H-2 class I monomers, the molecules were loaded with a conditional photocleavable peptide for UV exchange. For three of the conditional UV ligands the amino acid sequence was described in the literature, the other two were designed for the purpose of this study (Table 1). The conditional UV ligands were designed with anchor residues in mind that differ between different MHC alleles, based on their structure and different binding motifs. The photolabile “J” amino acid was placed in the TCR-facing part of the peptide sequence, and was either replacing one of the amino acids of the original peptide, or was positioned between two amino acids in the sequence. The predicted rank score for each UV ligand was predicted using NetH2pan [27] and reported in this study as %rank score (Table 1). As per recommendations, strong H-2 binders are generally considered to have a %rank score <0.5, weak MHC binders have a %rank score <2. Peptides to be used as conditional UV ligands were purchased and synthesized from Leiden University Medical Center peptide synthesis unit (LUMC).

Expression and purification of murine MHC class I heavy chains and β 2 microglobulin

Bacterial expression system was used to produce murine H-2 class I heavy chains (H-2D^d, H-2K^d, and H-2L^d), and human β 2m macroglobulin as described previously [28]. Briefly, proteins were produced in *Escherichia coli* B121(DE3) pLysS strain using pET series plasmids. Protein expression was induced by 0.5 mM isopropyl-beta-D-thiogalactopyranoside for 4 h. Inclusion bodies containing expressed proteins were lysed in lysis buffer (50 mM Tris·HCl (pH 8.0), 25% sucrose, 1 mM EDTA, and Lysozyme). Inclusion bodies were harvested by washing in detergent buffer (20 mM Tris-HCl, (pH 7.5), 200 mM NaCl, 1% NP40, and 1% Deoxycholic acid) followed by wash buffer (1 mM EDTA, 5% Triton X-100, 1 mM DTT). Next, inclusion bodies were dissolved in 8M Urea buffer (8M Urea, 50 mM K·HEPES pH 6.5 and 100 μ M β -mercaptoethanol) and insoluble impurities were removed by centrifugation at 40,000 x g for 20 minutes. The soluble fraction containing proteins was stored at -80 °C until used for *in vitro* folding.

In vitro folding and purification of murine MHC class I monomers

The *in vitro* folding of murine H-2 class I molecules were performed using photocleavable ligand as described above and previous [3]. To setup the refolding reaction, heavy chains (1 μ M) and β 2m

(2 μ M) were diluted in a folding buffer composed of 0.1M Tris pH 8.0, 500 mM L-Arginine-HCl, 2 mM EDTA, 0.5 mM oxidized glutathione and 5 mM reduced glutathione with 60 μ M respective photocleavable peptide (p*H-2D^d: RGPGRA-J-FVT, p*H-2K^d: IYSTV-J-SSL, p*H-2L^d: YPNVNIH-J-F) (Table 1). After folding for 3-5 days at 4 °C, folded protein was upconcentrated with a 10 kDa cut off membrane filters (Vivaflow-200; Sartorius) and biotinylated using BirA biotin-protein ligase standard reaction kit (Avidity, LLC- Aurora, Colorado). Finally, folded biotinylated monomer complexes were purified with size exclusion chromatography using HPLC (Waters Corporation, USA), and aliquots were stored at -80 °C until further use.

In vivo studies and splenocyte preparation

BALB/cJRj mice were acquired from Janvier Labs and housed at the Department of Health Technology, Technical University of Denmark. CL-4-TCR transgenic mice were a kind gift from Dr. Ana Misslitz, Hannover Medical School and Torsten Joeris from Lund University, respectively. To assess the binding of murine H-2 class I monomers, the following in vivo studies were performed to induce reactive CD8⁺ T cells:

H-2D^d antigen specific T cells: BALB/cJRj mice were injected with 80 μ g HIV Env gp160 peptide (RGPGRAFVTI) adjuvanted by 30 μ g poly-ICLC (Hiltonol®, from Oncovir). The mice were immunized four times i.p. with a weekly interval, spleens were harvested 7 days post last immunization. **H-2K^d** antigen specific T cells: splenocytes from transgenic CL-4 mice were harvested and 1-10% specific cells spiked into splenocytes from naïve BALB/cJRj mice. **H-2L^d** antigen specific T cells: BALB/cJRj mice were injected with 80 μ g LCMV NP (RPQASGVYM) adjuvanted by 30 μ g poly-ICLC. The mice were immunized four times i.p. with a weekly interval, spleens were harvested 7 days post last immunization.

Mice were euthanized by cervical dislocation and spleens were harvested and kept on 4°C in cRPMI (RPMI (Gibco RPMI 1640) and 10% FCS (Gibco)). Spleens were placed in a GentleMACS C-tube (Miltenyi, #130-093-237) with 3 mL cRPMI. The tubes were loaded onto GentleMACS dissociator and run with the appointed program. The dissociated splenocytes were placed on top of a 70 μ m cell strainers (Corning, # 43175) and 50mL Falcon tube and filtered through. Cells were washed twice by resuspension in cRPMI and centrifugation at 1500 rpm for 5 minutes at 4°C. The cells were finally dissolved in pure FCS and 10% DMSO (dimethyl sulfoxide, Sigma-Aldrich, Cat#C6164) and

1 mL was aliquoted into cryo tubes and stored at (-80 in a Mr. Frosty for 24 hours before moved to) a -180 tank for precevation.

Generation of specific pH-2 multimers

All peptides for pH-2 multimer libraries were purchased from Pepscan (Pepscan Presto BV, Lelystad, Netherlands) or TAG Copenhagen (Frederiksberg, Denmark) and dissolved to 10 mM in 100% DMSO. A full list of peptides used in the study can be found in Supplementary Table 1. Specific peptide binding to H-2 class I monomers was in silico predicted via NetH2pan [1], as described in above section on UV ligand design. The five different murine H-2 class I monomers and their corresponding peptides were diluted in PBS. Monomers (50-100 $\mu\text{g/mL}$ final concentration) were added to the corresponding peptide (100-200 μM final concentration) and placed under a 366 nm UV light for 1 hour at room temperature, to remove the UV ligand and replace with peptide of interest. A corresponding UV ligand control for each H-2 allele was in parallel incubated at RT on the bench.

Generation of PE-conjugated pH-2 tetramers and detection of pH-2-specific T cells

Tetramers were used to screen for T cell recognition against the specific peptide or irrelevant peptides in immunized or naïve mice. PE labeled streptavidin (phycoerythrin, Biolegend, Cat#405203, 0.2 mg/mL/100 μl pH-2) was loaded with exchanged pH-2 (100 $\mu\text{g/mL}$ monomer and 200 μM peptide) for 30 minutes on ice. 500 μM D-biotin was added 0.05x and incubated 20 minutes on ice, and the final product was stabilized using a 10x freezing media (0.5% BSA and 5% glycerol) and stored at -20°C .

Splenocytes from immunized and naïve mice were thawed and washed twice in cRPMI. $3-4 \times 10^6$ cells were plated into individual wells in a V-bottom 96 well plate and washed with FACS buffer (PBS and 2% FCS). Cells were treated with 0.5 μl Fc receptor block (Biolegend #101301) for 15 minutes to block unspecific binding. Tetramers were centrifuged prior to use. 1 μl of each pH-2 tetramer specificity was added to the corresponding sample with 49 μl BV buffer (BD) and 0.5nM Dasatinib and incubated for 15 minutes at 37°C . Cells were stained with an antibody mix (CD3-FITC: Biolegend #100306, CD8-BV480: BD ##566096 and the dead cell marker LIVE/DEAD Fixable Near-IR: ThermoFischer L10119) for 30 minutes at 4°C . After two washes in FACS buffer

the cells were either filtered using blue cap FACS tubes (Falcon # 352235) and acquired directly on the flow cytometer or fixed using 1% filtered paraformaldehyde for 1 – 24 hours previous acquisition.

Generation of large pH-2 multimer library and detection of pH-2-specific T cells

A DNA barcode-labeled pH-2 library was used to screen for T cell recognition against the five specific pH-2 or 115 irrelevant pH-2 specificities in immunized or naïve mice. The technique is as described earlier [4]. Briefly, 72 different pH-2 complexes (50 µg/mL monomer and 100 µM peptide) were prepared (Supplementary Table 1) and coupled to PE-labeled dextran backbones loaded with a unique DNA barcode (2.17×10^{-6} M). Splenocytes from immunized and naïve mice were thawed and washed twice in cRPMI. $3-4 \times 10^6$ cells were plated into individual wells in a 96 well plate and washed with BCB. 1.5 µl of each specificity was pooled and filtered through a 10 kDa cut off membrane filters (Vivaflow-200; Sartorius). Cells were stained with the pool of the 72 pH-2-multimers and with an antibody mix (CD3-FITC, CD8-BV480 and the dead cell marker LIVE/DEAD Fixable Near-IR). pH-2 multimer-specific T cells were sorted based on single, live CD3+ CD8+ PE+ cells. The sorted cells with DNA barcodes were centrifuged and pellet stored at -20°C. The DNA barcodes that were present in the samples at sorting were amplified along with triplicate full library baseline samples for comparison (aliquot of pH-2 multimer reagent pool). The amplified product was purified using QIAquick PCR Purification kit (Qiagen, Cat#28104), sequenced (IonTorrent, Primbio) using a 314 or 316 chip (Life Technologies) and data was processed by the online publically assessible software Barracoda, developed at DTU (<http://www.cbs.dtu.dk/services/barracoda>). Barracoda calculates the total reads and clonally-reduced reads for each DNA barcode (relating to its coupled pH-2 specificity). Log₂ fold changes in read counts linked to a given sample, related to the mean read counts, is compared to the baseline samples and estimated with normalization factors determined by the trimmed mean of M-values method. False-discovery rates (FDRs) were estimated using the Benjamini–Hochberg method. A p-value was calculated based on the Log₂ fold change distribution, determining the strength of the signal compared to the input, and $p < 0.001$, corresponding to $FDR < 0.1\%$, is established as the significance level determining a T cell response.

Flow cytometry

All flow cytometry experiments were carried out on Fortessa and Melody instruments (BD Biosciences). Data were analyzed in FlowJo version 10.6.1 (TreeStar, Inc.).

Statistical analyses

GraphPad Prism 8 for Mac OS X was used for graphing, statistical analyses and tools.

Acknowledgements

The authors would like to thank Bente Rotbøl and Anna Gyllenberg Burkal for excellent technical assistance, as well as all current and former members of the SRH group for scientific discussions.

Conflict of interest disclosure

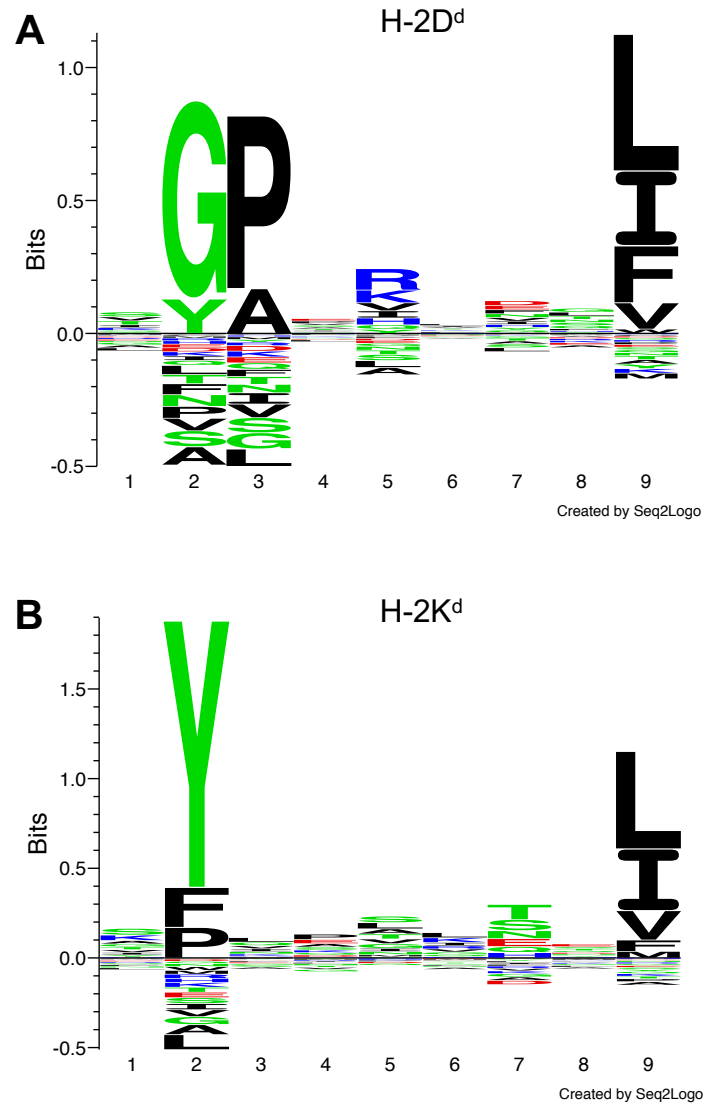
The authors declare no potential conflicts of interest.

References

- [1] J. D. Altman *et al.*, “Phenotypic Analysis of Antigen-Specific T Lymphocytes,” vol. 274, no. 5284, pp. 94–96, 1996.
- [2] R. S. Andersen *et al.*, “Parallel detection of antigen-specific T cell responses by combinatorial encoding of MHC multimers,” *Nat. Protoc.*, vol. 7, no. 5, pp. 891–902, May 2012.
- [3] B. Rodenko *et al.*, “Generation of peptide-MHC class I complexes through UV-mediated ligand exchange,” *Nat. Protoc.*, vol. 1, no. 3, pp. 1120–1132, 2006.
- [4] A. K. Bentzen *et al.*, “Large-scale detection of antigen-specific T cells using peptide-MHC-I multimers labeled with DNA barcodes,” *Nat. Biotechnol.*, vol. 34, no. 10, pp. 1037–1045, 2016.
- [5] J. C. Castle *et al.*, “Exploiting the mutanome for tumor vaccination,” *Cancer Res.*, vol. 72, no. 5, pp. 1081–1091, 2012.
- [6] S. Kreiter *et al.*, “Mutant MHC class II epitopes drive therapeutic immune responses to cancer,” *Nature*, vol. 520, no. 7549, pp. 692–696, 2015.
- [7] B. J. Hos *et al.*, “Identification of a neo-epitope dominating endogenous CD8 T cell responses to MC-38 colorectal cancer,” *Oncoimmunology*, vol. 00, no. 00, p. 1673125, Oct. 2019.
- [8] L. Aurisicchio *et al.*, “Poly-specific neoantigen-targeted cancer vaccines delay patient derived tumor growth,” *J. Exp. Clin. Cancer Res.*, vol. 38, no. 1, pp. 1–13, 2019.
- [9] S. I. S. Mosely *et al.*, “Rational selection of syngeneic preclinical tumor models for immunotherapeutic drug discovery,” *Cancer Immunol. Res.*, vol. 5, no. 1, pp. 29–41, 2017.
- [10] M. Toebes *et al.*, “Design and use of conditional MHC class I ligands,” *Nat. Med.*, vol. 12, no. 2, pp. 246–251, Feb. 2006.
- [11] G. M. Grotenbreg *et al.*, “Discovery of CD8+ T cell epitopes in Chlamydia trachomatis infection through use of caged class I MHC tetramers,” *Proc. Natl. Acad. Sci. U. S. A.*, vol. 105, no. 10, pp. 3831–3836, 2008.
- [12] E. Frickel *et al.*, “Parasite Stage-Specific Recognition of Endogenous Toxoplasma gondii –Derived CD8 + T Cell Epitopes,” *J. Infect. Dis.*, vol. 198, no. 11, pp. 1625–1633, Dec. 2008.
- [13] M. Corr, L. F. Boyd, E. A. Padlan, and D. H. Margulies, “H-2Dd exploits a four residue peptide binding motif,” *J. Exp. Med.*, vol. 178, no. 6, pp. 1877–1892, Dec. 1993.
- [14] V. Mitaksov and D. H. Fremont, “Structural definition of the H-2Kd peptide-binding motif,” *J. Biol. Chem.*, vol. 281, no. 15, pp. 10618–10625, Apr. 2006.
- [15] G. Eberl, A. Sabbatini, C. Servis, P. Romero, J. L. Maryanski, and G. Corradin, “MHC class I H-2Kd-restricted antigenic peptides: additional constraints for the binding motif,” *Int. Immunol.*, vol. 5, no. 11, pp. 1489–1492, Nov. 1993.
- [16] R. Vita *et al.*, “The Immune Epitope Database (IEDB): 2018 update,” *Nucleic Acids Res.*, vol. 47, no. D1, pp. D339–D343, Jan. 2019.
- [17] D. de Verteuil *et al.*, “Deletion of immunoproteasome subunits imprints on the transcriptome and has a broad impact on peptides presented by major histocompatibility complex I molecules,” *Mol. Cell. Proteomics*, vol. 9, no. 9, pp. 2034–2047, Sep. 2010.

- [18] N. A. Nagarajan *et al.*, “ERAAP Shapes the Peptidome Associated with Classical and Nonclassical MHC Class I Molecules.,” *J. Immunol.*, vol. 197, no. 4, pp. 1035–1043, Aug. 2016.
- [19] N. L. Dudek, C. T. Tan, D. G. Gorasia, N. P. Croft, P. T. Illing, and A. W. Purcell, “Constitutive and inflammatory immunopeptidome of pancreatic beta-cells.,” *Diabetes*, vol. 61, no. 11, pp. 3018–3025, Nov. 2012.
- [20] C. Bergmann, S. A. Stohlmann, and M. McMillan, “An endogenously synthesized decamer peptide efficiently primes cytotoxic T cells specific for the HIV-1 envelope glycoprotein,” *Eur. J. Immunol.*, vol. 23, no. 11, pp. 2777–2781, Nov. 1993.
- [21] K. Kuwano, T. J. Braciale, and F. A. Ennis, “Cytotoxic T lymphocytes recognize a cross-reactive epitope on the transmembrane region of influenza H1 and H2 hemagglutinins.,” *Viral Immunol.*, vol. 2, no. 3, pp. 163–173, 1989.
- [22] J. L. Whitton *et al.*, “Molecular analyses of a five-amino-acid cytotoxic T-lymphocyte (CTL) epitope: an immunodominant region which induces nonreciprocal CTL cross-reactivity.,” *J. Virol.*, vol. 63, no. 10, pp. 4303–4310, Oct. 1989.
- [23] N. W. Pedersen *et al.*, “CD8+ T cells from patients with narcolepsy and healthy controls recognize hypocretin neuron-specific antigens,” *Nat. Commun.*, vol. 10, no. 1, p. 837, Dec. 2019.
- [24] N. Viborg *et al.*, “T cell recognition of novel shared breast cancer antigens is frequently observed in peripheral blood of breast cancer patients,” *Oncoimmunology*, vol. 8, no. 12, p. e1663107, Dec. 2019.
- [25] A. K. Bentzen *et al.*, “T cell receptor fingerprinting enables in-depth characterization of the interactions governing recognition of peptide–MHC complexes,” *Nat. Publ. Gr.*, vol. 36, no. 12, 2018.
- [26] M. J. Selby *et al.*, “Preclinical development of ipilimumab and nivolumab combination immunotherapy: Mouse tumor models, In vitro functional studies, and cynomolgus macaque toxicology,” *PLoS One*, vol. 11, no. 9, pp. 1–19, 2016.
- [27] C. I. DeVette *et al.*, “NetH2pan: A computational tool to guide MHC peptide prediction on murine tumors,” *Cancer Immunol. Res.*, vol. 6, no. 6, pp. 636–644, 2018.
- [28] D. N. Garboczi, D. T. Hung, and D. C. Wiley, “HLA-A2-peptide complexes: refolding and crystallization of molecules expressed in *Escherichia coli* and complexed with single antigenic peptides.,” *Proc. Natl. Acad. Sci.*, vol. 89, no. 8, pp. 3429 LP – 3433, Apr. 1992.

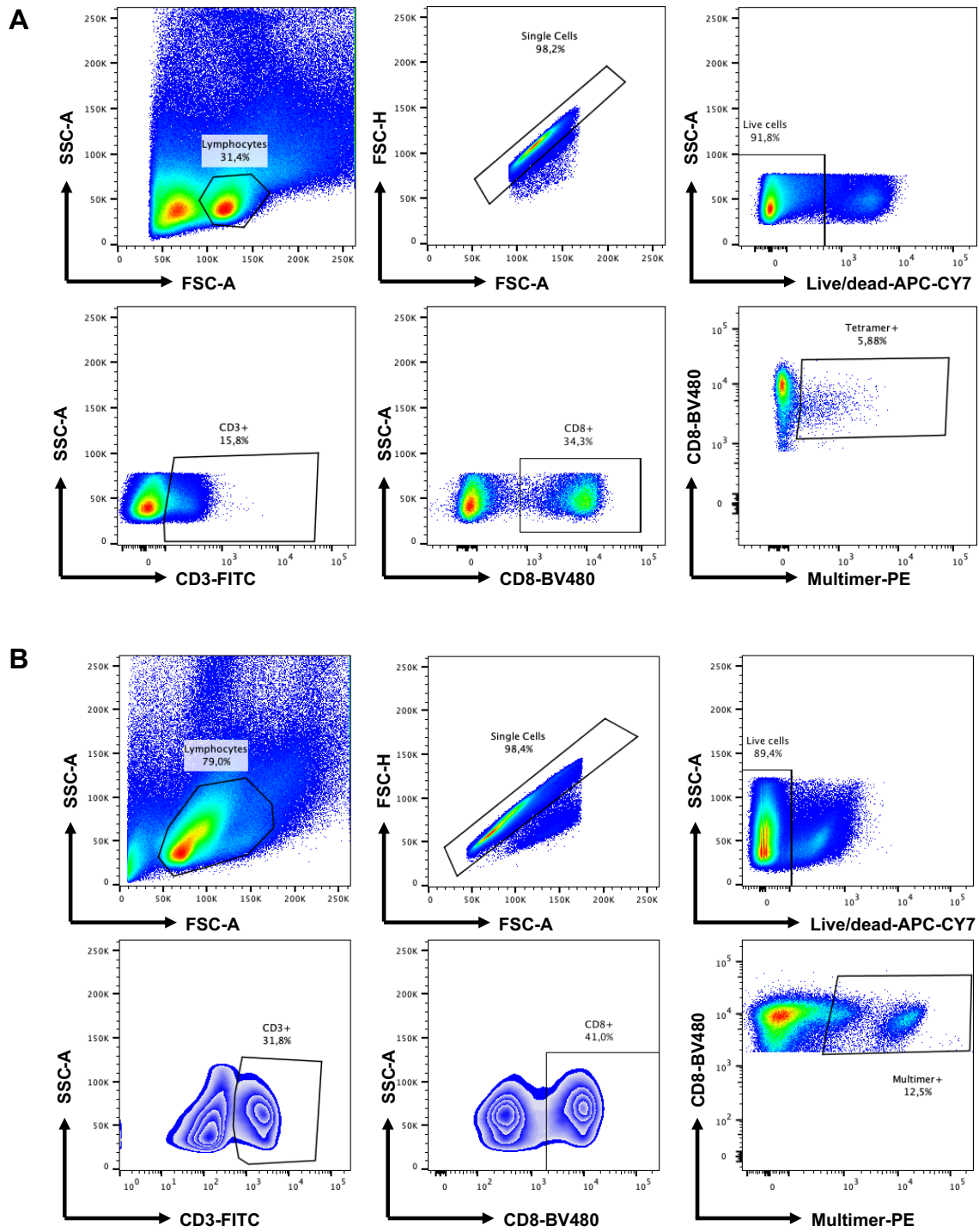
Manuscript I - Supplementary figures



Supplementary Figure 1

H-2 allele motif view based on eluted naturally presented ligands to visualize positional amino acid binding preferences of murine H-2 alleles H-2D^d (A) and H-2K^d (B). Logos created by Seq2Log

(http://www.cbs.dtu.dk/services/NetMHCpan/logos_ps.php), with H-2 ligand data from [16]–[19].



Supplementary Figure 2

FACS gating strategy, representative pH-2 multimer stainings with tetramers (A), or DNA barcode labeled multimers (B).

Manuscript I – Supplementary table

Supplementary table I: List of all peptides used to generate pH-2 multimers during this study.

Peptide name	Sequence	H-2 allele	%Rank score	pH-2 tetramers	pH-2 barcoded multimers
HIV Env ³¹¹⁻³²⁰	RGPGRAFVTI	H-2Dd	0.008	X	X
CT26_1	KADCLFTHM	H-2Dd	0.312	X	X
CT26_2	VSPKDIQLTI	H-2Dd	0.382		X
CT26_3	NNPSFPTGKM	H-2Dd	0.496		X
CT26_4	VNPAVKIVFL	H-2Dd	0.491		X
CT26_5	GGFQEFNFI	H-2Dd	0.115		X
CT26_6	MGPPGGFQEF	H-2Dd	0.432		X
CT26_7	SGPSYATY	H-2Dd	0.073		X
CT26_8	PSGPSYATYL	H-2Dd	0.113		X
CT26_9	GPSYATYL	H-2Dd	0.196		X
CT26_10	SGPSYATYLQ	H-2Dd	0.203		X
CT26_11	APSGPSYATYL	H-2Dd	0.273		X
CT26_12	YGFKKEETI	H-2Dd	0.391		X
CT26_13	ENPETSVM	H-2Dd	0.317		X
CT26_14	VNDELWATI	H-2Dd	0.269		X
CT26_15	TGPYVMMI	H-2Dd	0.383		X
CT26_16	TSPMPIL	H-2Dd	0.136		X
CT26_17	DAGPTQFTTPL	H-2Dd	0.301		X
CT26_18	TCPYCFQLL	H-2Dd	0.177		X
CT26_19	NIVQCFIAL	H-2Dd	0.445		X
CT26_20	TMPTFPHLV	H-2Dd	0.292		X
CT26_21	IMPPVGTDL	H-2Dd	0.375		X
CT26_22	STGKLLVAL	H-2Dd	0.175		X
Influenza HA ⁵¹⁸⁻⁵²⁶	IYSTVASSL	H-2Kd	0.008	X	X
CT26_23	IYQRKSDGI	H-2Kd	0.126	X	X
CT26_24	IYSRTDVL	H-2Kd	0.077		X
CT26_25	EYPSPSPL	H-2Kd	0.487		X
CT26_26	KYLSVQSQL	H-2Kd	0.003		X
CT26_27	WKYLSVQSQL	H-2Kd	0.157		X
CT26_28	KYLSVQSQLF	H-2Kd	0.298		X
CT26_29	YLSVQSQL	H-2Kd	0.312		X
CT26_30	IYVALLRVM	H-2Kd	0.046		X
CT26_31	AYVNAIEKI	H-2Kd	0.007		X
CT26_32	IYLESVAIM	H-2Kd	0.041		X
CT26_33	SIYLESVAIM	H-2Kd	0.237		X
CT26_34	SYIETLPKAI	H-2Kd	0.045		X
CT26_35	SSYIETLPKAI	H-2Kd	0.275		X
CT26_36	SYIETLPKAIK	H-2Kd	0.415		X
CT26_37	QFENLAQQL	H-2Kd	0.361		X
CT26_38	GFVVGTMTL	H-2Kd	0.263		X
CT26_39	SWDTSKKNL	H-2Kd	0.355		X
CT26_40	NYVFKAAML	H-2Kd	0.389		X
CT26_41	KYNDTPQSL	H-2Kd	0.004		X

CT26_42	EKYNDTPQSL	H-2Kd	0.298		X
CT26_43	KYNDTPQSLR	H-2Kd	0.452		X
CT26_44	QEKYNDTPQSL	H-2Kd	0.463		X
LCMV NP ₁₁₈₋₁₂₆	RPQASGVYM	H-2Ld	0.059	X	X
CT26_45	IPRDLFEGEL	H-2Ld	0.283	X	X
CT26_46	SPNTSFASDGF	H-2Ld	0.465		X
CT26_47	IGQMLQTHF	H-2Ld	0.009		X
CT26_48	SPKDIQLTI	H-2Ld	0.347		X
CT26_49	IDPLALMQAI	H-2Ld	0.220		X
CT26_50	DPLALMQAI	H-2Ld	0.477		X
CT26_51	LEHLNIVTF	H-2Ld	0.475		X
CT26_52	VPDGGAEHI	H-2Ld	0.295		X
CT26_53	FPYANVAFPHL	H-2Ld	0.169		X
CT26_54	FPYANVAF	H-2Ld	0.241		X
CT26_55	LPNILTKL	H-2Ld	0.274		X
CT26_56	SPYVYEIYMTF	H-2Ld	0.013		X
CT26_57	SPKYTLRSHF	H-2Ld	0.009		X
CT26_58	WSPKYTLRSHF	H-2Ld	0.131		X
CT26_59	SPKYTLRSHFD	H-2Ld	0.223		X
CT26_60	KEFPLLLF	H-2Ld	0.388		X
CT26_61	FPLFLLFL	H-2Ld	0.472		X
CT26_62	IPILEMQF	H-2Ld	0.105		X
CT26_63	MPEVIPILEM	H-2Ld	0.283		X
CT26_64	LPVKDELLCQL	H-2Ld	0.427		X
CT26_65	QPMASRFF	H-2Ld	0.113		X
CT26_66	QPTSPPMPI	H-2Ld	0.099		X

3. MANUSCRIPT II

DNA based neo-epitope vaccination induces tumor control in the CT26 syngeneic mouse model

Preclinical and clinical evidence support the notion of mutation-derived neo-epitopes as crucial targets for immunotherapy in cancer. In manuscript II, we established a vaccination-based platform in the syngeneic CT26 model, which is suitable for neo-epitope screening and detection. Here, multi-neo-epitope vaccination with DNA plasmid was found to be more anti-tumor effective than neo-peptides + TLR3 ligand poly IC. This was mirrored by a strong induction of CD8+ T cells by neo-epitope DNA vaccination. The framework presented here, will provide valuable feedback to neo-epitope prediction and selection algorithms.

The research presented in manuscript II represent current results from an ongoing study. We intend to extend the manuscript with further analyses to dissect immunogenicity of neo-epitopes in the CT26 syngeneic mouse model. Specifically, future analyses will address which of the neo-epitopes are driving anti-tumor effects and whether the therapeutic effect is mediated by CD4+ or CD8+ T cells or both via depletion studies.

DNA based neo-epitope vaccination induces tumor control in the CT26 syngeneic mouse model

Authors: Nadia Viborg^{1,2}, Marina Barrio Calvo², Stine Friis², Thomas Trolle², Christian Skjødt Hansen², Jens Kringelum², Sine Reker Hadrup¹ and Birgitte Rønø²

Affiliations:

¹ Department of Health Technology, Technical University of Denmark, Lyngby, Denmark

² Evaxion Biotech, Copenhagen, Denmark

Corresponding author: Birgitte Rønø, PhD, Senior Director, Cancer Immunotherapy, Evaxion Biotech,

Bredgade 34E, 1260 Copenhagen K, Phone: +45 31207309, Email: br@evaxion-biotech.com

Financial support: This research was funded in part by the Industrial Researcher programme, Innovation Fund Denmark

Number of figures: 4

Number of tables: 1

Number of supplementary figures: 2

Abstract

Cancer vaccines can be employed to engage T cell mediated immune recognition and elimination of tumors. Despite extensive past attempts, it has proven challenging to mediate substantial anti-tumor activity in the clinic with cancer vaccines. Recently, several clinical and preclinical discoveries position mutation derived neo-epitopes as important targets for effective immune responses against tumors. As such, personalized cancer vaccines with neo-epitopes delivered as synthetic peptides or RNA have reached the clinic with promising preliminary results and induction of neo-antigen specific T cells. However, the majority of *in silico* predicted neo-epitopes are not immunogenic, and we are yet to uncover the rules that govern neo-epitope immunogenicity. Research in murine preclinical models continuously increased our understanding of neo-epitopes and their potential therapeutic applicability. In this project, we set out to test DNA and peptide delivery platforms for their ability to induce neo-epitopes immunogenicity and anti-tumor effects in the syngeneic CT26 model. Our data demonstrate that prophylactic neo-epitope DNA vaccination confers anti-tumor immunity in the CT26 tumor model, whereas neo-peptide vaccination adjuvanted by poly IC does not. This is mirrored by a preferential induction of neo-epitope specific CD8⁺ T cells by DNA vaccination, which is skewed towards CD4⁺ T cells with neo-peptide vaccination. DNA vaccination confers a versatile platform that allows encoding of multiple neo-epitopes in a single formulation, a feasible strategy for robust neo-epitope vaccination, and thus a pipeline to validate neo-epitopes for immunogenicity and therapeutic applicability.

Introduction

T cells are acknowledged to play an essential role in immunological recognition and rejection of tumors [1]. Mutation derived T cell epitopes, also known as neo-epitopes, are being thoroughly explored as targets in cancer as they differentiate aberrant tumor tissue from the healthy self. Neo-epitope specific T cells have been reported in peripheral blood and tumor infiltrating lymphocytes (TILs) in patient with various cancers [2]–[6]. Furthermore, durable response to checkpoint inhibitor (CPI) therapy and good cancer prognosis have been related to tumor mutational burden or neo-epitope load and intratumoral presence of T cells [7]–[12]. This underlines the relevance of understanding and further investigating neo-epitope expression and subsequent T cell recognition in cancer therapy and immune monitoring.

With tumor-restricted expression, neo-epitopes are theorized as ideal therapeutic cancer targets minimally affected by immune tolerance and with limited risk of autoimmune adverse events. Therapeutic cancer vaccination with patient specific neo-epitopes offers a promising strategy to harness immune responses against a tumor. Such personalized strategies have recently been pursued in clinical trials with encouraging results when delivering the patient specific neo-epitopes loaded on autologous dendritic cells [13], encoded by RNA [14], [15] or neo-peptide pools adjuvanted by polyinosinic-polycytidylic acid, and poly-L-lysine (poly-ICLC) [16], [17]. In each clinical trial, several neo-epitopes were able to enhance existing or induce *de novo* T cells responses, confirming immunogenicity of neo-epitopes in humans. Interestingly, the majority of the T cell responses observed in these clinical trial with RNA and peptide delivery were MHC class II restricted and thus recognized by CD4⁺ T cells.

Preclinical research in murine models have contributed to our understanding of the dynamic interplay between T cells and neo-epitopes. There are several neo-epitope descriptions of relevance in therapeutic syngeneic tumor models based on common inbred strains C57BL/6 and BALB/c such as CT26 [18], [19], MC38 [20], [21], and B16-F10 [22]. These syngeneic tumor models represent different tissue origins and harbor diverse levels of immunogenicity and sensitivity to immunotherapy [23]. Various vaccination strategies have been employed to induce neo-epitope specific immunity in these syngeneic platforms of which some provide tumor growth control. One approach is synthetic neo-peptides adjuvanted by the Toll-like receptor (TLR) 3 agonist polyinosinic-polycytidylic acid (poly IC) or CpG, shown to induce anti-tumor immunity and growth delay in MC38 and B16-F10 models [20]–[22]. Another is delivery of neo-epitope encoding RNA,

with inherent self-adjuvating properties via TLR7 stimulation tested in CT26, B16-F10, and 4T1 models [19], [24]. Recent reports further position DNA based neo-epitope immunization as a relevant approach with induced immunity and anti-tumor effect in CT26, B16-F10, MC38, and Lewis lung carcinoma models [25]–[28]. In these studies, neo-epitopes were encoded by DNA plasmids or an adenoviral vector, delivered either alone or in combination with CPIs.

DNA vaccination harbors self-adjuvating effects via the innate DNA sensing machinery of mammalian cells. This directs the immune response towards Th1-like immunity which is preferable in therapies for cancer and viral infections [29]–[31]. Antigens delivered in DNA format have direct access to the MHC class I processing and presentation pathway in transfected cells, which is essential for induction of cytotoxic CD8⁺ T cells. Exogenous antigen delivery via peptides or whole protein will be presented by MHC class II on APCs and require cross presentation to reach MHC class I and CD8⁺ T cell priming [32]. Cross presentation can be promoted by interferons (IFN) in the surrounding milieu during antigen uptake by antigen presenting cells, and has been shown to be more efficient for synthetic long peptides than whole proteins [33], [34]. Delivery systems and adjuvants are commonly employed to facilitate efficient vaccination with various antigen formats. For DNA vaccination, delivery systems can protect against potential degradation of the DNA plasmid after injection and increase transfection efficiency [35]. Nonionic block co-polymers form micelle-like structures with DNA and enhance gene delivery to several tissues [36], [37]. Block co-polymers potentially augment immunogenicity of DNA via directing immune responses on the Th1/Th2 axis based on their chemical components/structure [38]. Synthetic peptides have low inherent immunogenicity on their own, why there is a need to co-formulate with adjuvants or carriers. A well described adjuvant for peptide delivery is poly IC, a double stranded RNA analogue and a facilitator of Th1-like adaptive immunity [39], [40] which has been described to induce anti-tumor immune responses [41], [42].

In this study, we set out to investigate immunogenicity and anti-tumor efficacy of *in silico* predicted neo-epitopes in the CT26 tumor model. Our aim is to obtain a drug development-like preclinical platform suitable for screening the large putative neo-epitope libraries resulting from mutational mapping and *in-silico* based prediction algorithms. Via this approach, we wish to expand our understanding of what characterizes a good neo-epitope with therapeutic applicability, which will be fed back to the neo-epitope prediction and selection algorithm. Here, we have compared two

delivery modalities of a set of CT26 neo-epitopes; neo-plasmid DNA vaccination with and without block co-polymer facilitated delivery, and neo-peptide vaccination adjuvanted by poly IC.

Results

Prophylactic vaccination with CT26 neo-epitope DNA and block co-polymer inhibits tumor growth and shows higher immunogenicity than neo-peptides + poly IC

We decided on five neo-epitopes to investigate in immunization studies based on mapping of nonsynonymous somatic mutations in the CT26 tumor cell line. The neo-epitopes selected all span a somatic mutation and encode all together the five peptides with the best *in silico* predicted affinity to MHC class II (H-2-IA^d). The expression of the five peptides was also confirmed by RNA sequencing. Each neo-epitope sequence contains ≥ 1 predicted strong binder for H-2^d class I and class II alleles, thus is potentially able to induce both CD4⁺ and CD8⁺ T cell responses as it is reported to be important in murine tumor models [19], [43].

To find the superior delivery platform for our CT26 neo-epitopes, we initially compared delivery as DNA encoding neo-epitopes or neo-peptides. Plasmid DNA encoding the five CT26 neo-epitope sequences (from here on: neo-pentatope DNA) was formulated with nonionic block co-polymer Lutrol to possibly enhance longevity of the plasmid DNA after injection and thereby increase antigen expression and exposure. This approach was benchmarked to delivery of CT26 neo-peptides formulated with poly IC. To overcome the inherent challenge of inducing a potent CD8⁺ T cell response with peptide-based vaccination, we set out to mimic the course of viral infections by exposing the mice to high-dose neo-peptides + poly IC. This set up is inspired by previous reports of successful cross presentation and generation of antigen specific CD8⁺ T cells by cluster vaccination with peptide antigens [44]. We have previously demonstrated that this cluster-priming approach of high dose neo-peptide delivery is more immunogenic and induce more functional T cells compared to conventional prime-boost and lower peptide doses (supplementary figure S1). Additionally, we have across several previous studies not observed anti-tumor effects in the CT26 tumor model of poly IC adjuvant delivered alone (data not shown).

In a small prophylactic setup we compared the induced T cell responses and anti-tumor effect of intramuscularly (i.m) immunized BALB/c mice with 100 μ g of neo-pentatope DNA + Lutrol (n = 5) or Lutrol only (n = 4), with the responses obtained in mice immunized intraperitoneally (i.p.) with 50 μ g of each neo-peptide + 40 μ g of poly IC (n = 5).

The mice in the neo-peptide group underwent cluster priming vaccination schedule consisting of immunizations on four consecutive days followed by weekly boosts. The mice in the neo-pentatope DNA group received weekly immunizations over the course of the experiment. Three to four weeks after priming, mice were inoculated with 5×10^5 CT26 tumor cells s.c. in the right flank (Fig. 1A). The vaccination approaches were validated for anti-tumor effect by monitoring tumor growth until majority of tumors in the control group reached the maximum allowed size (18 days after tumor cell inoculation). Mice immunized with neo-pentatope DNA + Lutrol developed considerably smaller or no tumors compared to mice immunized with Lutrol (Fig. 1B). Interestingly, immunization with neo-peptides + poly IC conferred no anti-tumor effect, and these mice developed tumor to the same extent as the control group. To explore if the differences in anti-tumor efficacy between the two neo-epitope based deliveries could be explained by their ability to induce CT26 epitope recognizing CD8⁺ T cells, we exploited the MHC tetramer staining methodology. PE and APC fluorochrome conjugated MHC class I tetramers were loaded with a confirmed H-2K^d restricted minimal epitope (KFKASRASI) derived from the C22 neo-epitope (present both in the DNA and peptide based CT26 vaccines) and added to tail vein whole blood in conjunction with anti-CD3 and anti-CD8 antibodies. In samples collected two weeks after priming we observed high frequent tetramer-specific CD8⁺ T cells in mice immunized with neo-pentatope DNA + Lutrol compared to neo-peptides + poly IC and Lutrol only groups (Fig. 1D). Epitope recognition is an important step towards anti-tumor immunity, however, to induce cancer cell killing a functional response is required. To compare the functional T cell responses induced by the two delivery methodologies, splenocytes from all groups were re-stimulated with immunization-relevant neo-peptide pool (five 27-mers) for IFN γ enzyme linked immunospot (ELISPOT) assay. By ELISPOT we observed significantly more IFN γ spot forming units (SFUs) in mice immunized with neo-pentatope DNA + Lutrol than neo-peptides + poly IC (Fig. 1C). To further interrogate T cell immunogenicity, splenocytes were re-stimulated with the immunization-relevant neo-peptide pool for intracellular cytokine staining (ICS) assay to identify IFN γ and tumor necrosis factor (TNF) α producing CD4⁺ and CD8⁺ T cells. Neo-pentatope DNA + Lutrol immunization resulted in high frequencies of single- and double-cytokine producing CD8⁺ T cells and in lower frequencies of cytokine producing CD4⁺ T cells (Fig. 1E). Neo-peptides + poly IC immunization led to convincing frequencies of IFN γ cytokine producing CD4⁺ T cells but less double-cytokine producing CD4⁺ T cells. With neo-peptide immunization, cytokine producing CD8⁺ T cells could not be measured after peptide stimulation. Based on these results, neo-pentatope DNA + Lutrol offers a more immunogenic and specific CD8⁺ T cell inducing platform for neo-

epitope immunization and we therefore set out to further explore the ability of neo-pentatope DNA vaccination to induce anti-tumor immunity.

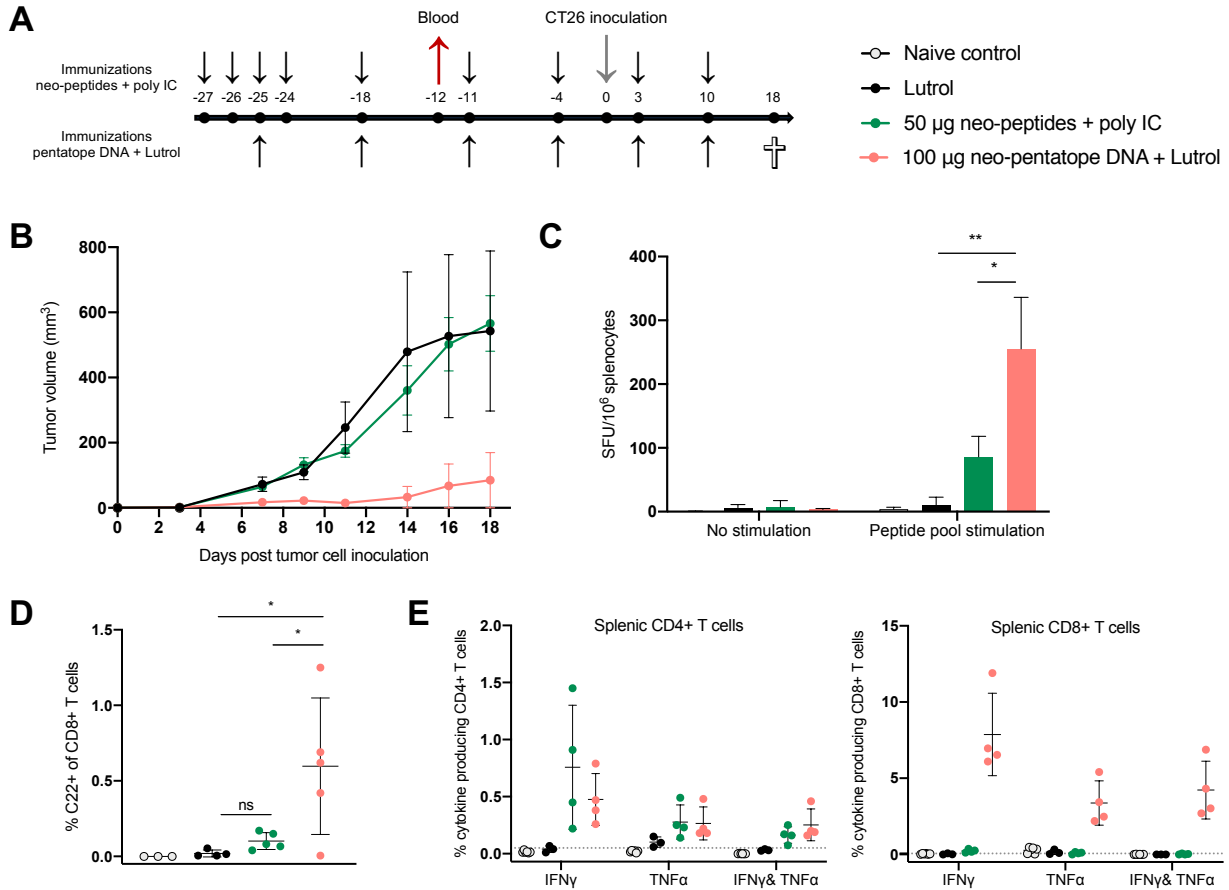


Figure 1. *In vivo* and *ex vivo* efficacy of vaccination with neo-epitope as DNA + co-polymer or peptides + poly IC. (A) Schematic representation of the timeline in the *in vivo* experiment. Groups of BALB/c mice were immunized prophylactically with 100 μg of neo-pentatope DNA + Lutrol (n = 5), 50 μg of neo-peptides + 40 μg of poly IC (n = 5), or Lutrol only (n = 4), before s.c. inoculation with CT26 tumor cells. Naïve control mice (no immunizations and no tumor inoculation) were housed together with experimental mice in a mixed cage setup. **(B)** Group mean tumor growth curves (in mm³) ± standard error of the mean (SEM). **(C)** IFN γ ELISPOT on bulk splenocytes from mice terminated at study day 18 after re-stimulation with immunization-relevant peptide pool (n = 3 to 5 mice per group, run in duplicates). **(D)** Tail vein blood collected in EDTA coated tubes was stained on study day -12 with an MHC tetramer (loaded with H-2K^d restricted minimal epitope *KFKASRASI* from the C22 neo-peptide), to monitor frequency of antigen specific CD8⁺ T cells induced by immunization. **(E)** Peptide pool re-stimulation and intracellular cytokine staining for IFN γ and TNF α producing CD4⁺ and CD8⁺ T cells on bulk splenocytes (n = 3 to 4 mice per group). Dotted line represents average cytokine production in unstimulated samples. Statistics: ordinary ANOVA with Sidak's multiple comparisons test (C and D), *p < 0.05, **p < 0.01.

Higher doses of DNA vaccination induces better CT26 tumor protection

Next, we investigated whether there is a dose-response dependency of immunogenicity and CT26 tumor control of neo-pentatope DNA vaccination. Moreover, we investigated whether the anti-tumor effects were driven by a specific immune response to the neo-pentatope or if it also could be attributed innate immunity of DNA on its own. To test this, we prophylactically immunized BALB/c mice weekly i.m. with 100 μg (n = 8), 20 μg (n = 12) or 2 μg (n = 12) neo-pentatope DNA + Lutrol or 100 μg of empty plasmid“mock” DNA + Lutrol (n = 8). Non-immunized (untreated) CT26 bearing mice were included as control group (n = 12) (Fig. 2A). For specific neo-pentatope DNA we observed a dose-dependent anti-tumor response, with 100 μg neo-pentatope DNA leading to smaller tumor end volume than 20 μg and 2 μg (Fig. 2B-D). There was no anti-tumor effect observed of mock DNA + Lutrol immunizations compared to untreated controls (Fig. 2B-D). This result indicates that the anti-tumor effect is driven by the immunization with CT26 neo-epitopes and not by the innate immunogenicity of the DNA on its own. Two weeks after the first immunization, MHC tetramer staining of tail vein blood disclosed the presence of C22 specific CD8⁺ T cells only for 100 μg and 20 μg neo-pentatope DNA groups (Fig. 2E). Five weeks after first immunization, upon termination of the mice, we detected in splenocytes vaccine specific dose-dependent induction of double-cytokine producing CD8⁺ T cells, and to a lesser extend CD4⁺ T cells upon stimulation with the vaccine-relevant peptides (Fig. 2F). Hence, we decided to continue with the highest dose of neo-pentatope DNA in our analyses and conclude that the observed anti-tumor effect is attributed to the neo-pentatope DNA and not to unspecific immune stimulation by the plasmid DNA itself.

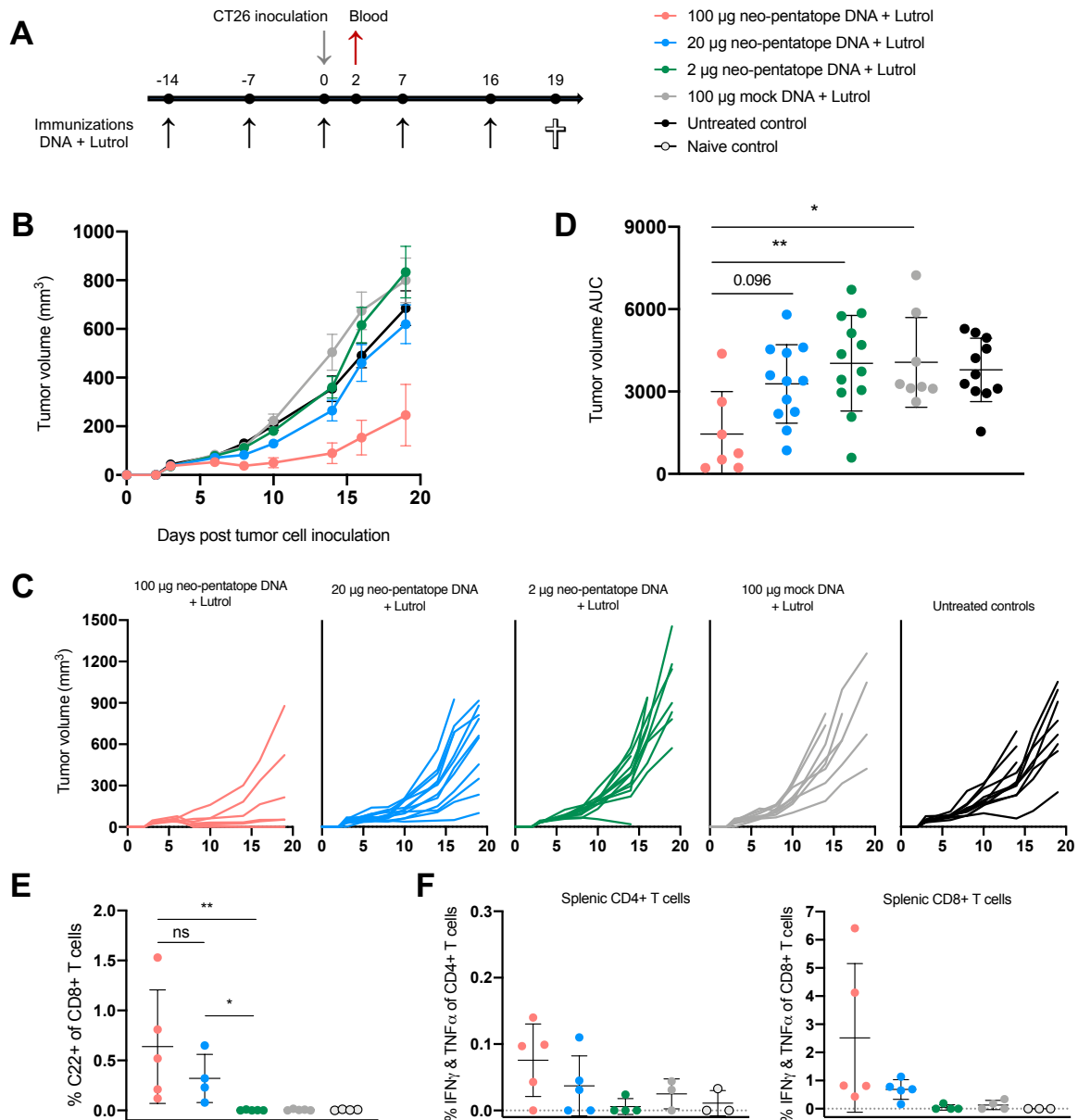


Figure 2. Prophylactic immunization with 100 µg neo-pentatope DNA + Lutrol confers better protection against CT26 tumor growth than lower doses, and there is no effect of immunizing with empty pVAX1 (“mock”) plasmid DNA + Lutrol. (A) Schematic representation of the timeline in the *in vivo* experiment. Groups of BALB/c mice were immunized prophylactically with 100, 20, or 2 µg of pentatope DNA + Lutrol (n = 8 to 12), or 100 µg of mock DNA + Lutrol (n = 8), before s.c. inoculation with CT26 tumor cells. Untreated CT26 bearing mice were included as controls (n = 12), and naïve control mice were housed together with experimental mice in a mixed cage setup. (B) Group mean tumor growth curves (in mm³) ± SEM. (C) Individual mouse tumor growth curves (in mm³). (D) Area under the tumor growth curve (AUC) for individual mice by group. (E) Tail vein blood collected in EDTA coated tubes was stained on study day 2 with an MHC tetramer (loaded with H-2K^d restricted minimal epitope *KFKASRSI* from the C22 neo-peptide), to monitor frequency of antigen specific CD8+ T cells induced by immunization. (F) Peptide pool re-stimulation and intracellular cytokine staining for IFN γ and TNF α producing CD4+ and CD8+ T cells on bulk splenocytes (n = 3 to 5 mice per group). Dotted line represents average cytokine production in unstimulated samples. Statistics: ordinary ANOVA with Sidak’s multiple comparisons test (D), non-parametric Kruskal-Wallis with Dunn’s multiple comparisons test (E), *p < 0.05, **p < 0.01.

Clinical grade co-polymer Kolliphor performs similarly to Lutrol and increases early onset immunogenicity compared to naked DNA

To increase potential clinical translatability of the observed anti-tumor effect of neo-pentatope DNA formulated with a co-polymer, we tested the clinical grade block co-polymer Kolliphor. Kolliphor's ability to facilitate neo-pentatope DNA delivery in the CT26 tumor model was compared to the anti-tumor effect induced by the polymer Lutrol and by naked neo-pentatope on its own. We prophylactically immunized BALB/c mice weekly i.m. with 100 µg neo-pentatope DNA + Lutrol or Kolliphor, 100 µg of naked neo-pentatope DNA, 100 µg of mock DNA + Kolliphor, or Kolliphor only (n = 13 per group) (Fig. 3A). The majority of mice immunized with naked neo-pentatope DNA and neo-pentatope DNA + Lutrol or Kolliphor showed similar substantial tumor growth control, compared to mock DNA and Kolliphor immunized mice (Fig. 3B-D). Two weeks after the first immunization, a tail vein blood MHC tetramer staining revealed presence of C22 specific CD8⁺ T cells in the groups immunized with naked neo-pentatope DNA and neo-pentatope DNA + Lutrol or Kolliphor, albeit the level was significantly lower for naked neo-pentatope DNA at this timepoint (Fig. 3E). This is indicative of polymer facilitated increase of plasmid immunogenicity by adjuvating effects or prevention of degradation. Upon endpoint (21 days after tumor cell inoculation) we stimulated splenocytes with peptide pool, and performed ICS assay to investigate differences in T cell functionality between the groups. We detected similar specific induction of double-cytokine producing CD8⁺ and CD4⁺ T cells by neo-pentatope DNA with and without co-polymers (Fig. 3F). At endpoint high dose neo-pentatope DNA were thus equally immunogenic and anti-tumor efficient with and without co-polymer facilitated delivery. Clinical grade co-polymer Kolliphor performed similarly to Lutrol, and is therefore used for future experiments.

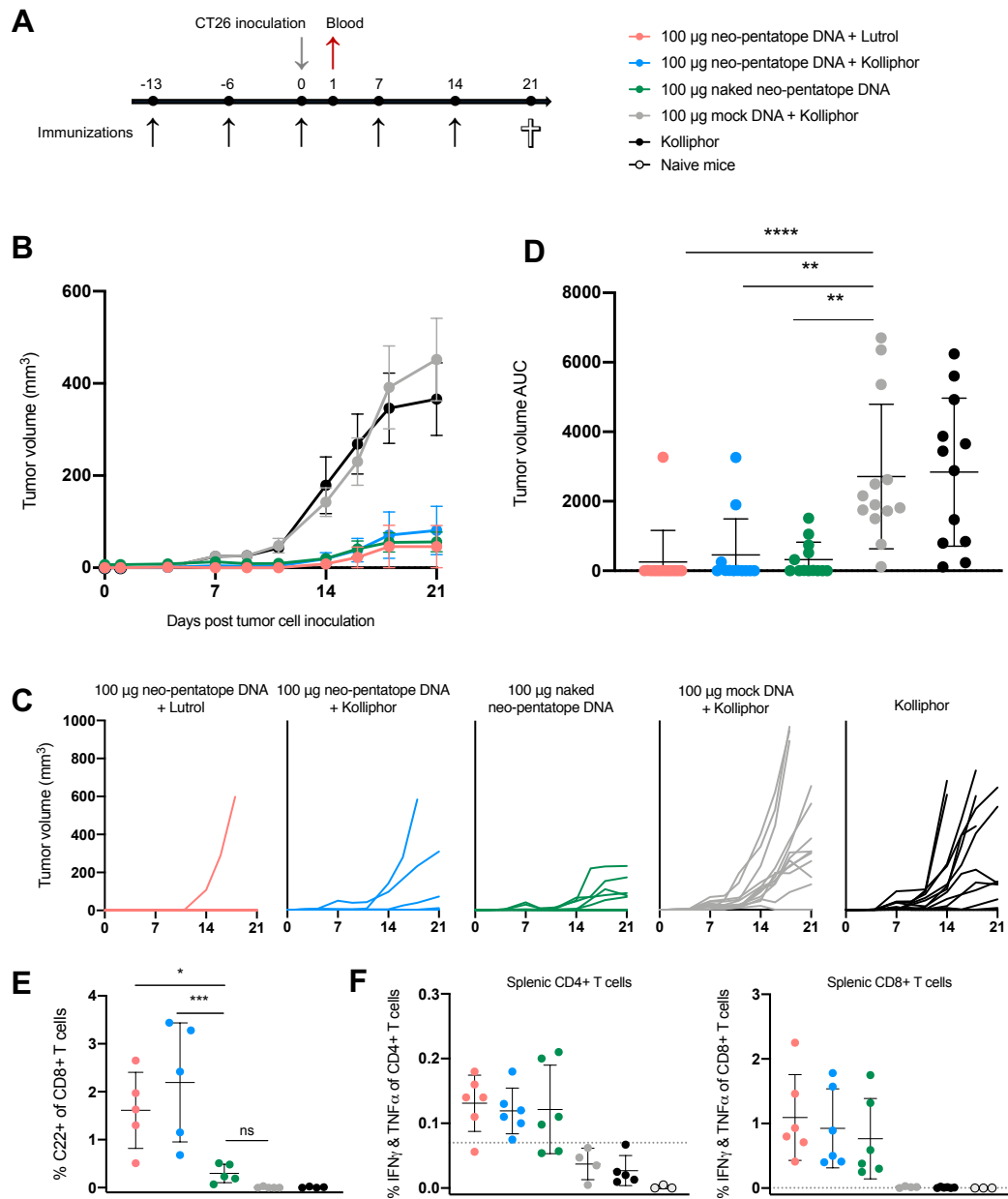


Figure 3. Clinical-grade co-polymer Kolliphor performs similarly to Lutrol in tumor growth control. (A) Schematic representation of the timeline in the *in vivo* experiment. Groups of BALB/c mice were immunized prophylactically with 100 µg of pentatope DNA + Lutrol or Kolliphor (n = 13 per group), 100 µg of naked pentatope DNA (n = 13), 100 µg of mock DNA + Lutrol (n = 13), or Kolliphor only (n = 13), before s.c. inoculation with CT26 tumor cells. Naïve control mice were housed together with experimental mice in a mixed cage setup. (B) Group mean tumor growth curves (in mm³) ± SEM. (C) Individual mouse tumor growth curves (in mm³). (D) Area under the tumor growth curve (AUC) for individual mice by group. (E) Tail vein blood collected in EDTA coated tubes was stained on study day 1 with an MHC tetramer (loaded with H-2K^d restricted minimal epitope *KFKASRSI* from the C22 neo-peptide), to monitor frequency of antigen specific CD8+ T cells induced by immunization. (F) Peptide pool re-stimulation and intracellular cytokine staining for IFN γ and TNF α producing CD4+ and CD8+ T cells on bulk splenocytes (n = 4 to 6 mice per group). Dotted line represents average cytokine production in unstimulated samples. Statistics: non-parametric Kruskal-Wallis with Dunn's multiple comparisons test (D), ordinary ANOVA with Sidak's multiple comparisons test (E), *p < 0.05, **p < 0.01, ***p < 0.001, ****p < 0.0001.

Neo-pentatope DNA vaccinated mice retain long-term tumor growth control

For the study described in the previous paragraph a subset of mice, immunized with neo-pentatope DNA with and without co-polymers, with small or no tumors were kept alive until 44 days after CT26 cell inoculation. Majority of the mice remained tumor free until day 44 (data not shown). Tail vein blood from these mice was MHC tetramer stained on study day 42. Here, we observed presence of neo-peptide C22 specific CD8⁺ T cells at levels comparable to what observed in the early blood staining (Fig. 3E and data not shown). This is indicative of long lasting anti-tumor effects of neo-pentatope DNA immunization possibly via immunological memory.

Prophylactic vaccination outperforms therapeutic vaccination and two epitopes drive the observed neo-pentatope immunogenicity

We next investigated the ability of the neo-pentatope DNA vaccine to induce tumor control in a therapeutic setting, and compare it with the robust anti-tumor effect of the same vaccine administered prophylactically. We immunized BALB/c mice weekly i.m. with 100 µg neo-pentatope DNA + Kolliphor or 100 µg of naked neo-pentatope DNA either prophylactically or therapeutically (n = 13 per group) relative to CT26 tumor cell inoculation (Fig. 4A). The prophylactic treatment started two weeks prior tumor cell inoculation while the therapeutic treatment was initiated after detection of palpable tumors. Mice injected with Kolliphor only, following the prophylactic immunization schedule were included as a negative control (n = 13). Similarly to Fig. 3B prophylactic immunization with neo-pentatope DNA ± Kolliphor resulted in tumor growth control for the majority of mice in both groups (Fig. 4B-D). Therapeutic immunization, however, offered no anti-tumor effect compared to Kolliphor only controls, apparent by tumor growth curves (Fig. 4B-D) and tumor volume AUC (Fig. 4C). Immune monitoring via tail vein blood MHC tetramer staining was carried out three weeks after the first prophylactic immunization and 5 days after the first therapeutic immunization. Tetramer staining revealed presence of C22 specific CD8⁺ T cells after prophylactic immunization, again the level was significantly lower for naked neo-pentatope DNA than neo-pentatope DNA + Kolliphor group (Fig. 4E). To dissect the contribution of CD4⁺ and CD8⁺ T cells to neo-pentatope immunogenicity, splenocytes were subjected to peptide pool re-stimulation and ICS. At endpoint, we detected similar specific induction of double-cytokine producing CD4⁺ T cells across prophylactic and therapeutic groups (Fig. 4F), albeit at a slightly higher frequency for prophylactic immunization with neo-pentatope DNA + Kolliphor. The same tendency was observed for CD8⁺ T cells, where prophylactic immunization with naked neo-

pentatope DNA and neo-pentatope DNA + Kolliphor induced more double-cytokine producers than therapeutic immunization. Lastly, splenocytes from prophylactic immunized groups were re-stimulated with neo-pentatope corresponding peptide pool or individual neo-peptides (C22, C23, C25, 30, C38) for IFN γ ELISPOT to deconvolute immunogenicity. C22 and C23 neo-epitopes from the neo-pentatope were the main drivers of observed immunogenicity (Fig. 4G), with a smaller contribution from peptide C25. IFN γ spot counts were similar for naked neo-pentatope DNA and neo-pentatope DNA + Kolliphor groups.

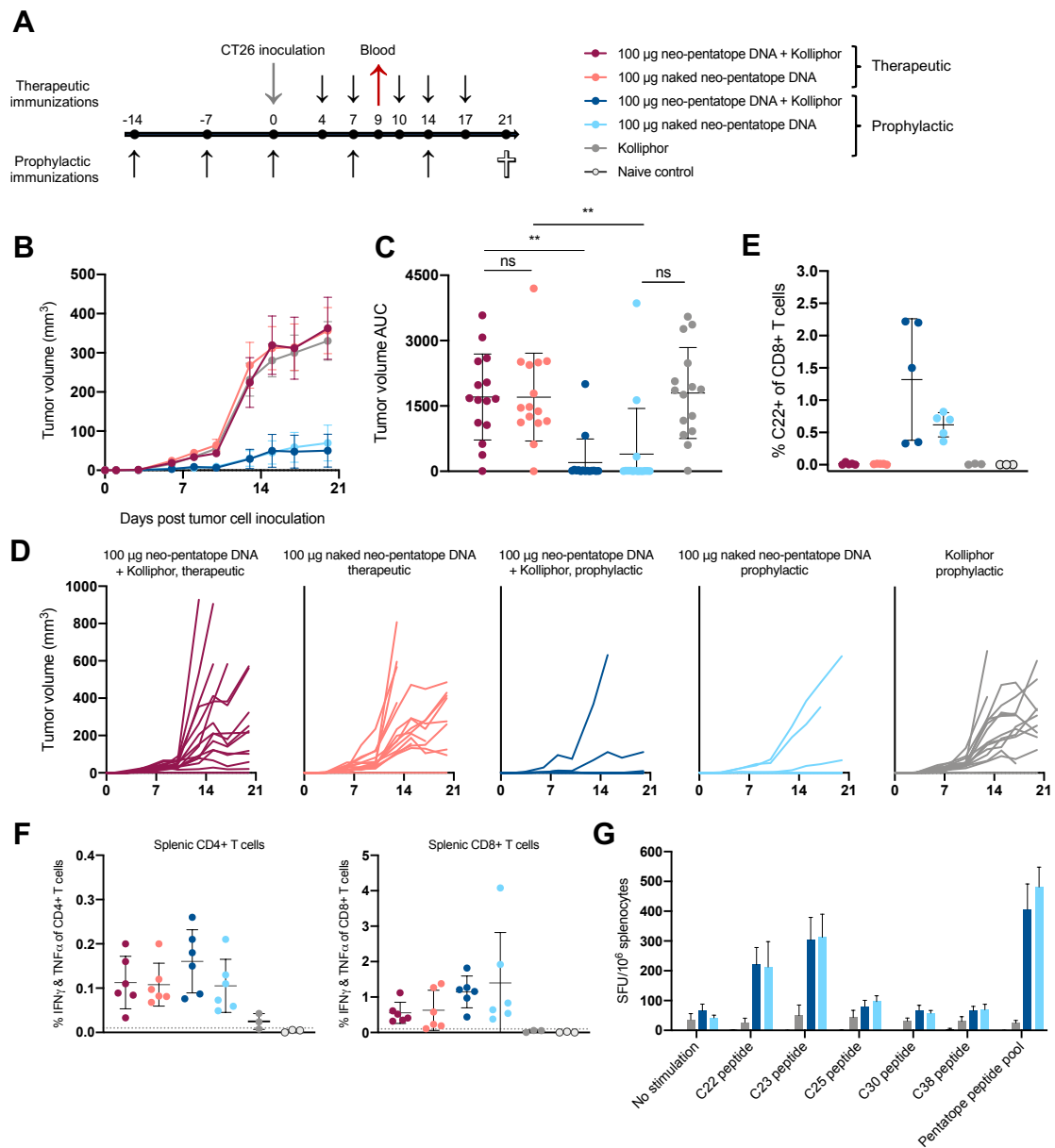


Figure 4. CT26 anti-tumor effect is obtained only by prophylactic and not therapeutic immunization with neo-pentatope DNA. (A) Schematic representation of the timeline in the *in vivo* experiment. Groups of BALB/c mice were immunized prophylactically or therapeutically with 100 µg of neo-pentatope DNA ± Kolliphor (n = 13 per group), before s.c. inoculation with CT26 tumor cells. Naïve control mice (no immunizations and no tumor inoculation) were housed together with experimental mice in a mixed cage setup. (B) Group mean tumor growth curves (in mm³) ± SEM. (C) Area under the tumor growth curve (AUC) for individual mice by group. (D) Individual mouse tumor growth curves (in mm³). (E) Tail vein blood collected in EDTA coated tubes was stained on study day 9 with an MHC tetramer (loaded with H-2K^d restricted minimal epitope *KFKASRASI* from the C22 neo-peptide), to monitor frequency of antigen specific CD8⁺ T cells induced by immunization. (F) Peptide pool re-stimulation and intracellular cytokine staining for IFN γ and TNF α producing CD4⁺ and CD8⁺ T cells on bulk splenocytes (n = 4 to 6 mice per group). Dotted line represents average cytokine production in unstimulated samples. (G) IFN γ ELISPOT on bulk splenocytes from prophylactically immunized mice after re-stimulation with immunization-relevant peptide pool or individual peptides (n = 3 to 6 mice per group, run in duplicates). Statistics: non-parametric Kruskal-Wallis with Dunn's multiple comparisons test (C), *p < 0.05, **p < 0.01.

Discussion

In this study we demonstrate a comparison between vaccination with five CT26 tumor neo-epitopes in the form of neo-plasmid DNA and neo-peptides. Our first observation was that prophylactic vaccination with neo-epitope DNA and co-polymer Lutrol provided protection against CT26 tumor challenge, whereas prophylactic neo-peptide + poly IC vaccination did not. This was flanked by higher immunogenicity of neo-pentatope DNA vaccination as apparent by MHC tetramer staining of peripheral blood and two *ex vivo* functional assays for cytokine production upon re-stimulation. Interestingly, we observed by ICS that neo-pentatope DNA preferentially induced cytokine producing CD8⁺ T cells, whereas neo-peptides + poly IC induced cytokine producing CD4⁺ T cells upon antigen re-exposure. We further found that prophylactic protection against CT26 tumor from neo-pentatope DNA was dose-dependent, and similar high dose of mock DNA did not confer this protection. Immunogenicity of the DNA delivered neo-epitopes was also dose-dependent, apparent by MHC tetramer staining and *ex vivo* functional assays. Prophylactic neo-pentatope DNA vaccination with and without clinical grade co-polymer Kolliphor obtained similar prophylactic protection in the CT26 tumor model. Thus, co-polymer facilitated DNA delivery conferred similar protection as obtained naked pentatope DNA, albeit MHC tetramer staining of blood samples showed that Kolliphor increased early onset immunogenicity compared to naked DNA. Lastly, we found that CT26 anti-tumor effects of neo-pentatope DNA vaccination were only obtained with a prophylactic vaccination regimen, and not effective when vaccinations were initiated after tumor onset. *Ex vivo* re-stimulation and assays for cytokine production showed that prophylactic and therapeutic groups reached similar levels of vaccine induced immunogenicity, though prophylactic groups reached a slightly higher level of cytokine producing CD8⁺ T cells. We deconvoluted the vaccine induced response via individual neo-peptide re-stimulation and ELISPOT, where we observed that two of the five neo-epitopes drive the pentatope immunogenicity.

Including multiple neo-epitopes in a cancer vaccine is investigated in both mice and humans [14], [25]–[27], [45]. The multi neo-epitope approach potentially induces several clones of tumor recognizing T cells, and a broad recognition of tumor antigens is expected to have a greater protective potential in cancer. An explanation for this, is that the breadth of the anti-tumor response provides better protection in situations where tumor variants that express a certain mutation are eliminated as a result of immune pressure. Additionally, since studies have shown that far from all predicted neo-epitopes are immunogenic [46], including multiple possible hits improves chances of

raising a T cell response at all. In our investigated pentatope vaccine, only two out of five neo-epitopes were immunogenic. To investigate this further, our future studies will entail single neo-epitope immunizations to examine immunogenic and therapeutic effects of single neo-epitope delivery compared to the pentatope. With the current data, we can only speculate whether the neo-pentatope confers epitope competition, resulting in loss of immunogenicity of less dominant epitopes.

The assembly of multiple epitopes in a vaccine is somewhat easier for DNA delivery compared to synthetic peptide delivery. This is because DNA offers a versatile platform that allows encoding of multiple neo-epitopes in a single formulation, whereas synthetic neo-peptides require individual production and purification of each putative epitope. Some synthetic neo-peptides will inherently possess solubility issues, making them difficult or impossible to formulate in a vaccine without precipitation.

Reports show, that the induction of both CD4⁺ and CD8⁺ T cell responses is important for cancer immunotherapy [19], [43]. The 27-mer length neo-epitopes included in this study encompass multiple predicted MHC class I and II ligands, potentially priming both CD4⁺ and CD8⁺ T cells. As suggested by our results, neo-epitope DNA delivery offers enhanced CD8⁺ T cell reactivity than neo-peptide + poly IC. When DNA is injected intramuscularly, local resident cells (e.g. muscle and stroma) and APCs will be transfected (reference). DNA encoded antigens will then be produced inside the cells and gain access to the MHC class I pathway for presentation to CD8⁺ T cells. Peptides will naturally enter the exogenous pathway and MHC class II presentation to CD4⁺ T cells, and require cross presentation to reach the MHC class I pathway. Intracellular components of the innate DNA sensing machinery, e.g. stimulator of interferon genes (STING) and TANK binding kinase 1 (TBK1) pathways, detect plasmid DNA [29], [30], [47]. This detection is crucial for directing the adaptive immune response towards a Th1-like pathway, where CD4⁺ T cells support the development of cytotoxic CD8⁺ T cells capable of tumor destruction.

Indeed, we are able to induce both poly-functional [48] CD4⁺ and CD8⁺ T cells with neo-pentatope DNA vaccination, as apparent by the IFN γ and TNF α double producers detected via ICS. To dissect the importance of each subset of T cells for anti-tumor immunity, future neo-pentatope vaccination studies will include antibody-mediated depletion of CD4⁺ and CD8⁺ T cells.

In this study, we were not able to obtain elimination of early established CT26 tumors with therapeutic neo-pentatope DNA vaccination. Prophylactic immunization was however very efficient. We hypothesize, that the therapeutic window in the model is too short, and that the neo-pentatope DNA vaccination needs more time to establish T cell immunity [49]. Future analyses will include multiple blood samplings for immune monitoring to uncover when specific adaptive immunity kicks in. To overcome this, one could incorporate immune stimulatory sequences in the plasmid vector, encoding chemokines, cytokines, or CpG elements. A potential synergistic effect could also be obtained by combination of neo-pentatope DNA vaccination with CPI therapy [25], which could mitigate the effects of an immunosuppressive TME. Another possible approach is to use mechanical injection devices for increased DNA transfection, such as microneedles, genegun, and electroporation [50], [51]. Moreover, we only tested one combination of five neo-epitopes in the presented studies, and it is possible that other combinations of neo-epitopes would fare better in the therapeutic vaccination setting.

Preclinical models somewhat lack direct translatability to the clinic, but nonetheless provide important mechanistic lessons about the dynamic interplay between tumors and immunological recognition. DNA based vaccination has not yet been a clinical success, despite promising data from animal models [52]. However, multiple clinical trials involving personalized neo-epitope DNA vaccination are currently recruiting or ongoing [53]. Most of these entail DNA delivery with electroporation or combined with CPI therapy, and it will be interesting to follow these developments.

Herein, we present a framework to screen libraries of neo-epitopes for therapeutic relevance in syngeneic tumor models. This can be applied for neo-epitope discovery, and results can continuously feed back to improve neo-epitope prediction algorithms.

Materials and Methods

Mice

6 to 8 weeks old BALB/c JrJ females were acquired from Janvier Labs (France). The mice were acclimated for one week before initiation of experiments. The experiment was conducted under license 2017-15-0201-01209 from the Danish Animal Experimentation Inspectorate in accordance with the Danish Animal Experimentation Act (BEK nr. 12 of 7/01/2016), which is compliant with the European directive (2010/63/EU).

Cell lines

BALB/c syngeneic colon cancer cell line CT26 (#CRL2638) was purchased from ATCC and cultured in R10 medium prepared from RPMI (Gibco #72400-021) supplemented with 10% heat inactivated fetal calf serum (FCS, Gibco # 10500-064)) at 37°C and 5% CO₂ as per supplier's instructions.

Neo-epitope prediction and selection

Somatic mutations in the CT26 cell line were retrieved from previous work [18] and filtered to only include nonsynonymous mutations. Reference source protein sequences were downloaded using the Biopython Entrez module. For each somatic mutation, a 29-mer neoepitope sequence was extracted from the corresponding source protein, with the mutated amino acid (AA) at position 15. If the mutated AA was located within 15 AA of the ends of the source protein, a shorter neoepitope sequence was extracted instead. If the extracted neo-epitope sequence was shorter than 15 AAs it was discarded. Furthermore, if the annotated wildtype AA was not found at the mutated position in the reference source protein, the neoepitope was also discarded.

For each neo-epitope sequence, NetMHCIIpan-3.1[54] was used to generate MHC class II binding predictions for all overlapping 15mers towards the mouse MHC class II molecule H-2-IA^d. The 15mer with the best NetMHCIIpan %rank score was selected as representative of the neo-epitope. Neoepitopes with a gene expression >20 RPKM were ranked based on their best NetMHCIIpan %rank score and the top 5 were selected. Finally, the N- and C-terminal AAs of the selected neo-epitopes were truncated to convert the 29-mers to the final 27-mer neo-epitope sequences.

Plasmid DNA, synthetic peptides and adjuvants for immunizations

Plasmid DNA: The standard pVAX1 plasmid (containing a CMV driven expression vector and kanamycin resistance gene for selection) was acquired from Thermo Fischer (#V26020). Aldevron (North Dakota, USA) upscaled the pVAX1 plasmid with (“neo-pentatope” DNA) and without (“mock” DNA) cloning in the CT26 neo-epitope encoding construct. Plasmid inserts contained five codon optimized neo-epitope encoding DNA sequences in tandem (Table 1) connected by glycine and serine linker elements and a Kozak consensus sequence was included to effectively initiate translation. Plasmid DNA were formulated immediately prior to injection at final concentrations of 2 µg, 20 µg, and 100 µg DNA.

Peptide ID	AA sequence	Minimal epitope (H-2 allele, %rank)	In vivo use	Ex vivo use
C22	QIETQQRKFKASR <u>A</u> SILSEM <u>K</u> M <u>L</u> KEKR	KFKASRASI (H-2K ^d , 0.168) Used for H-2K ^d tetramer	Neo-pentatope DNA, neo-peptide + poly IC	Re-stimulation
C23	VILPQAPSGPSYA <u>T</u> YLQPAQAQMLTPP	-	Neo-pentatope DNA, neo-peptide + poly IC	Re-stimulation
C25	DTLSAMSNPRAMQ <u>V</u> LLQIQGLQTLAT	-	Neo-pentatope DNA, neo-peptide + poly IC	Re-stimulation
C30	DGQLELLAQGALD <u>N</u> ALSSMGALHALRP	-	Neo-pentatope DNA	Re-stimulation
C38	RLHVVKLLASAL <u>S</u> TNAAALTQELLVLD	-	Neo-pentatope DNA, neo-peptide + poly IC	Re-stimulation
EV07	GDVKIHAHKVVLA <u>N</u> ISPYFKAMFTGNL	-	Neo-peptide + poly IC	Re-stimulation

Table 1. Overview of neo-epitopes used for in vivo or ex vivo analyses during the study

Bold and underlined amino acid denotes position of point mutation. %rank of minimal peptides to H-2 allele was predicted with NetH2pan 1.0, %rank < 0.5 denotes a strong binder.

Co-polymers: Poloxamer block co-polymers Lutrol (Sigma-Aldrich, #P5556) and Kolliphor (gifted by BASF, Germany) were diluted to a final vaccine concentration of 3%.

Peptides: Lyophilized peptides were purchased from Pepscan (Lelystad, Netherlands) or Genscript (New Jersey, USA) and dissolved in DMSO to a concentration of 10 mg/ml. For *in vivo* use CT26 27-mer neo-peptides (Table 1 for full list of peptides used in the study) were formulated in Tris buffer immediately prior to immunization at final concentrations 0.4 µg, 2 µg, 10 µg, or 50 µg of each neo-peptide. Neo-peptides corresponding to vaccination antigens were used for *ex vivo* assays. From the five 27-mers used for immunization one H-2 strong binder minimal epitope was predicted (NetH2pan 1.0, %rank scores < 0.5). A minimal epitope (KFKASRASI, restricted to H-2K^d) from the C22 27-mer sequence (QIETQQRKFKASR**A**SILSEM**K**M**L**KEKR) was used to generate MHC tetramers for immune monitoring. 27-mer neo-peptides were also used for *ex vivo* re-stimulation and cytokine detection assays, described below.

Poly IC: liposome based TLR3 ligand (gifted by Dennis Christensen, Statens Serum Institut, Denmark) was mixed with peptides to a content of 40 µg poly IC per injection.

Neo-epitope immunizations

Mice were prophylactically or therapeutically immunized relative to tumor cell inoculation, i.e. therapeutic immunizations were initiated upon establishment of palpable tumors. Immunization schedules are outlined for individual studies in results section and figures. Mice were either immunized intraperitoneally (i.p.) with CT26 neo-peptides adjuvanted by poly IC in isotonic Tris buffer (9% sucrose, pH 7.4) in a total volume of 200 µl per injection, or were immunized in left and right tibialis anterior muscles (i.m.) with 2 x 50 µl CT26 neo-epitope encoding (“neo-pentatope”) or empty (“mock”) plasmid formulated with and without block co-polymers (3% final polymer concentration). Plasmid DNA and co-polymers were formulated with isotonic buffer (149 nM NaCl, 6mM KCl, 3mM CaCl₂, 2mM MgCl₂, 10mM Hepes pH 7.4, 10 mM glucose). Peptide based immunizations were performed by cluster priming (4 sequential daily immunizations) followed by up to five weekly boosts. DNA based immunizations were performed by weekly immunizations (5 to 6 in total).

Tumor challenge experiments

At the day of tumor cell inoculation (defined as study day 0), exponentially growing CT26 cells were trypsinized and washed twice in RPMI medium. 5 x 10⁵ CT26 cells, in a volume of 100 µl RPMI medium, were inoculated subcutaneously in the right flank of BALB/c mice. Once established, the tumor diameters were measured three times per week with a digital caliper. The tumor volumes were calculated using the following formula: tumor volume = $\frac{\pi}{6} * (d_1 * d_2)^{3/2}$, where d₁ and d₂ are orthogonal diameters of the tumor. The mice were euthanized by cervical dislocation when the majority of tumors in the control groups reached the maximum allowed size of 12 mm diameter in either direction or upon observed of humane endpoints. At termination, spleens were collected in cold RPMI, before processing to single cells suspensions via GentleMACS processing (Miltenyi, C-tubes #130-096-334 and Dissociater #130-093-235) and passage through a 70 µm filter (Falcon, #) before cryopreservation. Approximately two weeks after the first immunization 50-80 µl tail vein blood was drawn into EDTA coated tubes (BD #367525) from a representative number of mice from each group for *ex vivo* analyses.

IFN γ enzyme-linked immune absorbent spot (ELISPOT) assay

MultiScreen IP Filter Plates (Merck Milipore #MAIPNTR10) were coated with anti-IFN γ capture antibody (BD #551881) and blocked with R10. Approximately 5×10^5 splenocytes were added to each well and stimulated with synthetic 27-mer neo-peptides in duplicates (peptide pools or single peptides individually at 2 $\mu\text{g/ml}$ final concentration of each peptide) corresponding to the neo-epitope content of the vaccines. Cells were incubated with stimulants or R10 media overnight (12-18 hours) before addition of anti-IFN γ detection antibody (BD #551881), and signal intensification with streptavidin-HRP enzyme (BD #557630) and AEC chromogen substrate (BD #551951). ELISPOT plates were air dried and read on ELISPOT analyzer (CTL ImmunoSpot) to count spot forming units (SFU) in each well. All counts were normalized to SFU per 10^6 splenocytes.

Peptide re-stimulation and intracellular cytokine staining (ICS)

2×10^6 splenocytes were stimulated in U-bottom 96-well culture plates (Costar #3799) with R10 media or synthetic 27-mer neo-peptides (peptide pools at 5 $\mu\text{g/ml}$ final concentration of each peptide) corresponding to the neo-epitope content of the vaccines. Two hours after initiation of stimulation, protein transport was inhibited by Brefeldin A (GolgiPlug, BD #555029) and monensin (GolgiStop, BD #554724), and cells were incubated overnight (6-18 hours) at 37°C and 5% CO₂. Cells were washed, Fc receptor blocked (Biolegend #101301) 10 minutes at 4°C and surface stained for anti-CD3 (FITC, Biolegend #100305), -CD4 (PE, BD #100443), -CD8 (PerCP-CY5.5, BD #551162), and dead cells (Near IR-viability dye, Invitrogen #L10119) for 30 minutes at 4°C. Hereafter cells underwent fixation and permeabilization (eBioscience #88-8824-00) and were stained intracellularly for IFN γ (APC, BD #554413) and TNF α (BV421, BD #563387) for 30 minutes at 4°C. Samples were washed and analyzed by flow cytometry and frequencies of cytokine producing CD4⁺ and CD8⁺ T cells were determined.

MHC tetramer staining for neo-peptide specific CD8⁺ T cells

50 μl tail vein blood or $3\text{-}4 \times 10^6$ splenocytes were placed in deep 96-well plates (Sigma #575653) or U-bottom 96-well plates, respectively. Cells were Fc receptor blocked with an anti-mouse CD16/32 antibody (Biolegend #101301) 10 minutes at 4°C while MHC tetramer reagents (phycoerythrin; PE, and allophycocyanin; APC streptavidin conjugated H-2K^d(KFKASRASI) at 100 $\mu\text{g/ml}$ pMHC concentration, produced in house as previously described [55]) were centrifuged

to sediment potential MHC aggregates (10.000 rpm, 2 minutes). 1 µl of individual MHC tetramers were added to cells in a total volume of 80 µl PBS + 2% FCS and incubated for 15 minutes at 37°C. Cells were surface stained for 30 minutes at 4°C with anti-CD3 (FITC, Biolegend #100305), -CD4 (PE, BD #100443), -CD8 (PerCP-CY5.5, BD #551162), and dead cells (Near IR-viability dye, Invitrogen #L10119). Blood samples were 1-step erythrocyte-lysed and fixed (eBioscience #00-5333-57). Blood and splenocyte samples were washed in PBS + 2% FCS. Samples were moved to round bottom FACS tubes (Corning #352052) before analysis by flow cytometry and frequencies of MHC tetramer+ CD8+ T cells were determined.

Flow cytometry

All flow cytometry experiments were carried out on BD Fortessa instruments. Data were analyzed in FlowJo version 10.6.1 (BD).

Statistical analyses

GraphPad Prism 8 for Mac OS X was used for graphing, statistical analyses and tools. Data was subjected to Kolmogorov-Smirnov test for normality ($\alpha = 0.05$). Parametric data was analyzed by ordinary ANOVA with Sidak's multiple comparison correction. Non-parametric data was analyzed by Kruskal-Wallis test with Dunn's multiple comparison correction. For all results, the following levels of statistical significance are applied: * $p < 0.05$, ** $p < 0.01$, *** $p < 0.001$, **** $p < 0.0001$.

Acknowledgements

We would like to thank Bettina Eide Holm, Anne Lund, and Henriette Løwe Press for excellent technical assistance.

Disclosure of conflict of interest

NVP, MBC, SF, TT, CSH, JK, BR are employed at Evaxion Biotech.

References

- [1] P. G. Coulic, B. J. Van Den Eynde, P. Van Der Bruggen, and T. Boon, “Tumour antigens recognized by T lymphocytes: At the core of cancer immunotherapy,” *Nat. Rev. Cancer*, vol. 14, no. 2, pp. 135–146, 2014.
- [2] Y. C. Lu *et al.*, “Efficient identification of mutated cancer antigens recognized by T cells associated with durable tumor regressions,” *Clin. Cancer Res.*, vol. 20, no. 13, pp. 3401–3410, 2014.
- [3] A. Gros *et al.*, “Prospective identification of neoantigen-specific lymphocytes in the peripheral blood of melanoma patients,” *Nat. Med.*, vol. 22, no. 4, pp. 433–438, 2016.
- [4] N. McGranahan *et al.*, “Clonal neoantigens elicit T cell immunoreactivity and sensitivity to immune checkpoint blockade,” *Science*, vol. 351, no. 6280, pp. 1463–9, Mar. 2016.
- [5] S. Bobisse *et al.*, “Sensitive and frequent identification of high avidity neo-epitope specific CD8 + T cells in immunotherapy-naïve ovarian cancer,” *Nat. Commun.*, vol. 9, no. 1, p. 1092, Dec. 2018.
- [6] N. Zacharakis *et al.*, “Immune recognition of somatic mutations leading to complete durable regression in metastatic breast cancer,” *Nat. Med.*, vol. 24, no. 6, pp. 724–730, 2018.
- [7] J. Galon, “Type, Density, and Location of Immune Cells Within Human Colorectal Tumors Predict Clinical Outcome,” *Science (80-.)*, vol. 313, no. 5795, pp. 1960–1964, Sep. 2006.
- [8] L. B. Alexandrov *et al.*, “Signatures of mutational processes in human cancer,” *Nature*, vol. 500, no. 7463, pp. 415–421, Aug. 2013.
- [9] F. Duan *et al.*, “Genomic and bioinformatic profiling of mutational neoepitopes reveals new rules to predict anticancer immunogenicity,” *J. Exp. Med.*, vol. 211, no. 11, pp. 2231–2248, Oct. 2014.
- [10] M. M. Gubin *et al.*, “Checkpoint blockade cancer immunotherapy targets tumour-specific mutant antigens,” *Nature*, vol. 515, no. 7528, pp. 577–581, Nov. 2014.
- [11] M. S. Rooney, S. A. Shukla, C. J. Wu, G. Getz, and N. Hacohen, “Molecular and Genetic Properties of Tumors Associated with Local Immune Cytolytic Activity,” *Cell*, vol. 160, no. 1–2, pp. 48–61, Jan. 2015.
- [12] N. A. Rizvi *et al.*, “Cancer immunology. Mutational landscape determines sensitivity to PD-1 blockade in non-small cell lung cancer,” *Science*, vol. 348, no. 6230, pp. 124–8, Apr. 2015.
- [13] B. M. Carreno *et al.*, “A dendritic cell vaccine increases the breadth and diversity of melanoma neoantigen-specific T cells,” *Science (80-.)*, vol. 348, no. 6236, pp. 803–808, May 2015.
- [14] U. Sahin *et al.*, “Personalized RNA mutanome vaccines mobilize poly-specific therapeutic immunity against cancer,” *Nature*, vol. 547, no. 7662, pp. 222–226, 2017.
- [15] N. Hilf *et al.*, “Actively personalized vaccination trial for newly diagnosed glioblastoma,” *Nature*, vol. 565, no. 7738, pp. 240–245, Jan. 2019.
- [16] P. A. Ott *et al.*, “An immunogenic personal neoantigen vaccine for patients with melanoma,” *Nature*, vol. 547, no. 7662, pp. 217–221, 2017.
- [17] D. B. Keskin *et al.*, “Neoantigen vaccine generates intratumoral T cell responses in phase Ib glioblastoma trial,” *Nature*, vol. 565, no. 7738, pp. 234–239, Jan. 2019.
- [18] J. C. Castle *et al.*, “Immunomic, genomic and transcriptomic characterization of CT26 colorectal carcinoma,” *BMC Genomics*, vol. 15, no. 1, 2014.
- [19] S. Kreiter *et al.*, “Mutant MHC class II epitopes drive therapeutic immune responses to cancer,” *Nature*, vol.

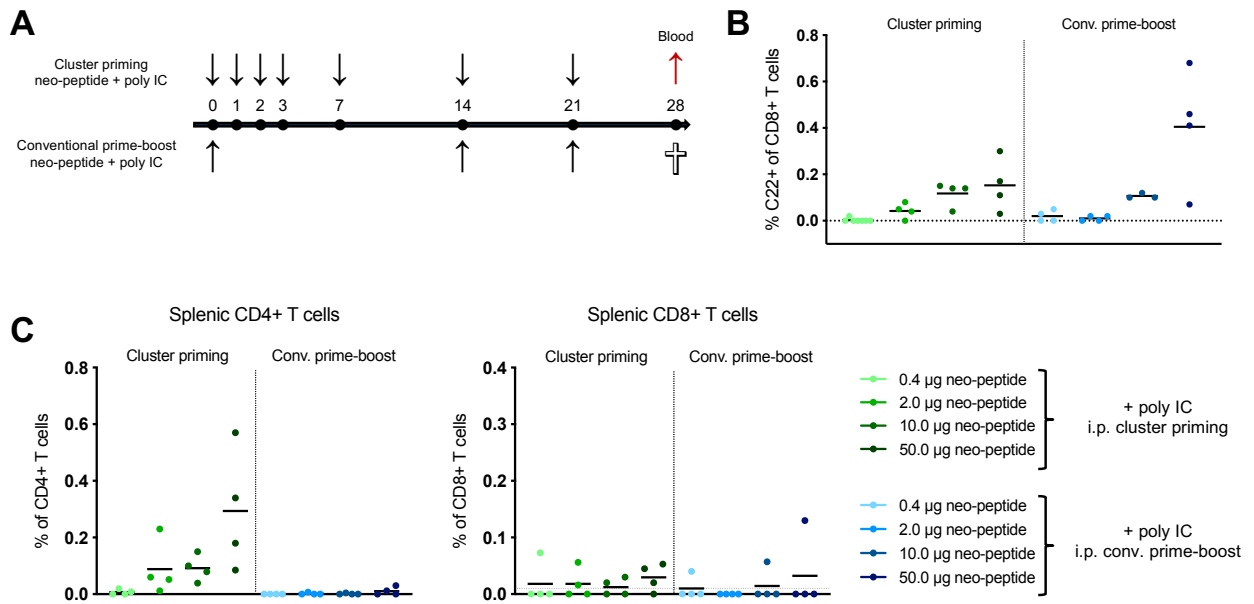
- 520, no. 7549, pp. 692–696, 2015.
- [20] M. Yadav *et al.*, “Predicting immunogenic tumour mutations by combining mass spectrometry and exome sequencing,” *Nature*, vol. 515, no. 7528, pp. 572–576, 2014.
- [21] B. J. Hos *et al.*, “Identification of a neo-epitope dominating endogenous CD8 T cell responses to MC-38 colorectal cancer,” *Oncoimmunology*, vol. 00, no. 00, p. 1673125, Oct. 2019.
- [22] J. C. Castle *et al.*, “Exploiting the mutanome for tumor vaccination,” *Cancer Res.*, vol. 72, no. 5, pp. 1081–1091, 2012.
- [23] S. I. S. Mosely *et al.*, “Rational selection of syngeneic preclinical tumor models for immunotherapeutic drug discovery,” *Cancer Immunol. Res.*, vol. 5, no. 1, pp. 29–41, 2017.
- [24] L. M. Kranz *et al.*, “Systemic RNA delivery to dendritic cells exploits antiviral defence for cancer immunotherapy,” *Nature*, vol. 534, no. 7607, pp. 396–401, 2016.
- [25] E. Tondini *et al.*, “A poly-neoantigen DNA vaccine synergizes with PD-1 blockade to induce T cell-mediated tumor control,” *Oncoimmunology*, vol. 8, no. 11, p. 1652539, 2019.
- [26] E. K. Duperret *et al.*, “A Synthetic DNA, Multi-Neoantigen Vaccine Drives Predominately MHC Class I CD8 + T-cell Responses, Impacting Tumor Challenge,” *Cancer Immunol. Res.*, vol. 7, no. 2, pp. 174–182, Feb. 2019.
- [27] L. Aurisicchio *et al.*, “Poly-specific neoantigen-targeted cancer vaccines delay patient derived tumor growth,” *J. Exp. Clin. Cancer Res.*, vol. 38, no. 1, pp. 1–13, 2019.
- [28] A. M. D’Alise *et al.*, “Adenoviral vaccine targeting multiple neoantigens as strategy to eradicate large tumors combined with checkpoint blockade,” *Nat. Commun.*, vol. 10, no. 1, pp. 1–12, 2019.
- [29] K. J. Ishii *et al.*, “TANK-binding kinase-1 delineates innate and adaptive immune responses to DNA vaccines,” *Nature*, vol. 451, no. 7179, pp. 725–729, 2008.
- [30] H. Ishikawa, Z. Ma, and G. N. Barber, “STING regulates intracellular DNA-mediated, type I interferon-dependent innate immunity,” *Nature*, vol. 461, no. 7265, pp. 788–792, 2009.
- [31] E. Raz *et al.*, “Preferential induction of a Th1 immune response and inhibition of specific IgE antibody formation by plasmid DNA immunization,” *Proc. Natl. Acad. Sci.*, vol. 93, no. 10, pp. 5141 LP – 5145, May 1996.
- [32] A. L. Ackerman and P. Cresswell, “Cellular mechanisms governing cross-presentation of exogenous antigens,” *Nat. Immunol.*, vol. 5, no. 7, pp. 678–684, Jul. 2004.
- [33] H. Zhang *et al.*, “Comparing pooled peptides with intact protein for accessing cross-presentation pathways for protective CD8+ and CD4+ T cells,” *J. Biol. Chem.*, vol. 284, no. 14, pp. 9184–9191, Apr. 2009.
- [34] R. A. Rosalia *et al.*, “Dendritic cells process synthetic long peptides better than whole protein, improving antigen presentation and T-cell activation,” *Eur. J. Immunol.*, vol. 43, no. 10, pp. 2554–2565, Oct. 2013.
- [35] M. Bello-Roufai, O. Lambert, and B. Pitard, “Relationships between the physicochemical properties of an amphiphilic triblock copolymers/DNA complexes and their intramuscular transfection efficiency,” *Nucleic Acids Res.*, vol. 35, no. 3, pp. 728–739, Jan. 2007.
- [36] A. Kabanov, J. Zhu, and V. Alakhov, “Pluronic block copolymers for gene delivery,” *Adv. Genet.*, vol. 53, pp. 231–261, 2005.
- [37] L. Desigaux *et al.*, “Nonionic amphiphilic block copolymers promote gene transfer to the lung,” *Hum. Gene*

- Ther.*, vol. 16, no. 7, pp. 821–829, Jul. 2005.
- [38] D. McIlroy *et al.*, “DNA/amphiphilic block copolymer nanospheres promote low-dose DNA vaccination.,” *Mol. Ther.*, vol. 17, no. 8, pp. 1473–1481, Aug. 2009.
- [39] M. P. Longhi *et al.*, “Dendritic cells require a systemic type I interferon response to mature and induce CD4+ Th1 immunity with poly IC as adjuvant.,” *J. Exp. Med.*, vol. 206, no. 7, pp. 1589–1602, Jul. 2009.
- [40] A. J. Currie, R. G. van der Most, S. A. Broomfield, A. C. Prosser, M. G. Tovey, and B. W. S. Robinson, “Targeting the effector site with IFN- α inducing TLR ligands reactivates tumor-resident CD8 T cell responses to eradicate established solid tumors.,” *J. Immunol.*, vol. 180, no. 3, pp. 1535–1544, Feb. 2008.
- [41] H. Il Cho, K. Barrios, Y. R. Lee, A. K. Linowski, and E. Celis, “BiVax: A peptide/poly-IC subunit vaccine that mimics an acute infection elicits vast and effective anti-tumor CD8 T-cell responses,” *Cancer Immunol. Immunother.*, vol. 62, no. 4, pp. 787–799, 2013.
- [42] H. Sultan *et al.*, “Designing therapeutic cancer vaccines by mimicking viral infections,” *Cancer Immunol. Immunother.*, vol. 66, no. 2, pp. 203–213, 2017.
- [43] E. Alspach *et al.*, “MHC-II neoantigens shape tumour immunity and response to immunotherapy.,” *Nature*, no. February, 2019.
- [44] D. A. Wick, S. D. Martin, B. H. Nelson, and J. R. Webb, “Profound CD8+ T cell immunity elicited by sequential daily immunization with exogenous antigen plus the TLR3 agonist poly(I:C),” *Vaccine*, vol. 29, no. 5, pp. 984–993, 2011.
- [45] P. A. Ott *et al.*, “An Immunogenic Personal Neoantigen Vaccine for Melanoma Patients,” *Nature*, vol. 547, no. 7662, pp. 217–221, Jul. 2017.
- [46] A. M. Bjerregaard *et al.*, “An analysis of natural T cell responses to predicted tumor neopeptides,” *Front. Immunol.*, vol. 8, no. NOV, pp. 1–9, 2017.
- [47] M. Motwani, S. Pesiridis, and K. A. Fitzgerald, “DNA sensing by the cGAS–STING pathway in health and disease,” *Nat. Rev. Genet.*, vol. 20, no. November, 2019.
- [48] W. N. Haining, “Travels in time: Assessing the functional complexity of T cells,” *Proc. Natl. Acad. Sci.*, vol. 109, no. 5, pp. 1359–1360, Jan. 2012.
- [49] M. A. Taylor *et al.*, “Longitudinal immune characterization of syngeneic tumor models to enable model selection for immune oncology drug discovery,” *J. Immunother. Cancer*, vol. 7, no. 1, p. 328, 2019.
- [50] L. Lambricht, A. Lopes, S. Kos, G. Sersa, V. Preat, and G. Vandermeulen, “Clinical potential of electroporation for gene therapy and DNA vaccine delivery.,” *Expert Opin. Drug Deliv.*, vol. 13, no. 2, pp. 295–310, 2016.
- [51] S. H. T. Jorritsma, E. J. Gowans, B. Grubor-Bauk, and D. K. Wijesundara, “Delivery methods to increase cellular uptake and immunogenicity of DNA vaccines.,” *Vaccine*, vol. 34, no. 46, pp. 5488–5494, Nov. 2016.
- [52] M. A. Kutzler and D. B. Weiner, “DNA vaccines: Ready for prime time?,” *Nat. Rev. Genet.*, vol. 9, no. 10, pp. 776–788, 2008.
- [53] A. Lopes, G. Vandermeulen, and V. Pr at, “Cancer DNA vaccines: current preclinical and clinical developments and future perspectives,” *J. Exp. Clin. Cancer Res.*, vol. 38, no. 1, pp. 1–24, 2019.
- [54] M. Andreatta, E. Karosiene, M. Rasmussen, A. Stryhn, S. Buus, and M. Nielsen, “Accurate pan-specific prediction of peptide-MHC class II binding affinity with improved binding core identification.,”

Immunogenetics, vol. 67, no. 11–12, pp. 641–650, Nov. 2015.

- [55] N. Viborg, T. S. Meldgaard, T. Tamhane, S. S. Hernandez, D. V. Albacete, and S. R. Hadrup, “H-2 multimers for high-throughput T cell interrogation and description of novel conditional ligands for H-2Dd and H-2Kd,” no. (Manuscript in preparation), 2019.

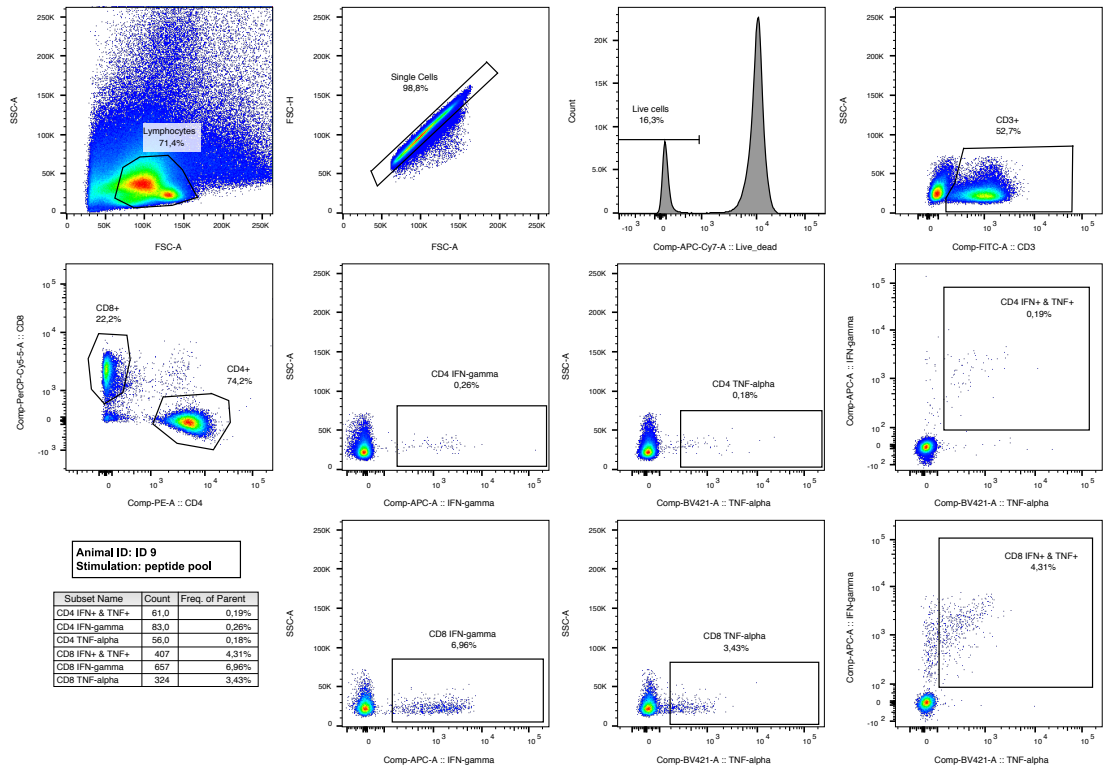
Manuscript II - Supplementary figures



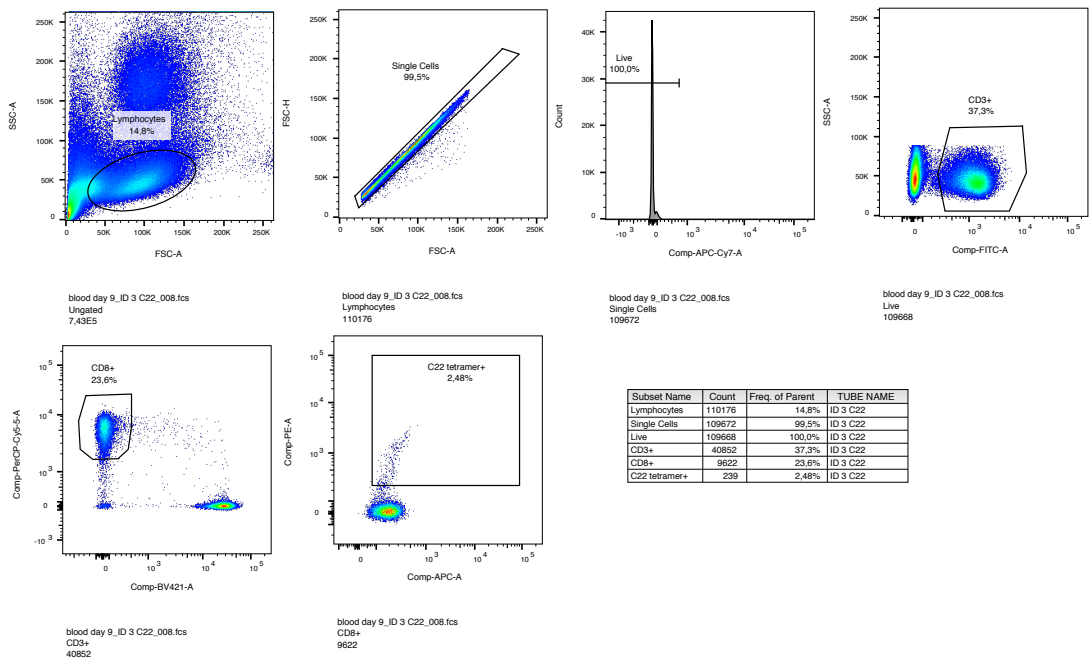
Supplementary Figure S1. Immunogenicity of single CT26 neo-peptide + poly IC depends on peptide dose and immunization schedule

Schematic representation of the timeline in the in vivo experiment and groups (**A**). BALB/c mice were immunized i.p. with 0.4, 2, 10, or 50 μg C22 neo-peptide + poly IC either following a conventional prime-boost strategy or by 4 daily cluster primings followed by weekly boosts (n = 4 mice per group). (**B**) Tail vein blood was stained 28 days after prime with an MHC tetramer (loaded with H-2K^d restricted minimal epitope KFKASRASI from the C22 neo-peptide), to monitor frequency of neo-peptide specific CD8⁺ T cells induced by immunization. (**C**) C22 neo-peptide re-stimulation and intracellular cytokine staining for IFN γ and TNF α producing CD4⁺ and CD8⁺ T cells on bulk splenocytes.

A



B



Supplementary Figure S2. FACS gating strategy

FACS gating strategy used for samples after peptide re-stimulation and intracellular cytokine staining (A).

FACS gating strategy used for samples after H-2 tetramer staining. All FACS gating was performed in FlowJo

(B).

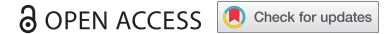
4. PAPER III

T cell recognition of novel shared breast cancer antigens is frequently observed in peripheral blood of breast cancer patients










The research enclosed in paper III describes our detection of CD8⁺ T cells specific to four novel tumor associated antigens in breast cancer patients. Breast cancer has historically been considered an immunologically silent malignancy, and furthermore harbors mid to low range prevalence of somatic mutations. The T cell landscape in breast cancer is therefore minimally described, and we set out to explore this with a high-throughput DNA barcode-labeled MHC multimer strategy. We present herein a set of interesting new T cell targets, preferentially recognized by T cells in breast cancer patients over healthy donors.

This paper was published in Oncoimmunology in August 2019.

ORIGINAL RESEARCH



T cell recognition of novel shared breast cancer antigens is frequently observed in peripheral blood of breast cancer patients

Nadia Viborg ^{a*}, Sofie Ramskov ^{a*}, Rikke Sick Andersen ^{b†}, Theo Sturm^c, Tim Fugmann ^{c‡},
Amalie Kai Bentzen ^a, Vibeke Mindahl Rafa^a, Per thor Straten ^{b,d}, Inge Marie Svane ^b, Özcan Met ^{b,d},
and Sine Reker Hadrup ^a

^aDepartment of Health Technology, Technical University of Denmark, Lyngby, Denmark; ^bCenter for Cancer Immune Therapy, Copenhagen University Hospital, Herlev, Denmark; ^cPhilochem AG, Otelfingen, Switzerland; ^dDepartment of Immunology and Microbiology, Faculty of Health and Medical Sciences, University of Copenhagen, Copenhagen, Denmark

ABSTRACT

Advances within cancer immunotherapy have fueled a paradigm shift in cancer treatment, resulting in increasing numbers of cancer types benefitting from novel treatment options. Despite originally being considered an immunologically silent malignancy, recent studies encourage the research of breast cancer immunogenicity to evaluate immunotherapy as a treatment strategy. However, the epitope landscape in breast cancer is minimally described, limiting the options for antigen-specific, targeted strategies. Aromatase, never in mitosis A-related kinase 3 (NEK3), protein inhibitor of activated STAT3 (PIAS3), and prolactin are known as upregulated proteins in breast cancer. In the present study, these four proteins are identified as novel T cell targets in breast cancer.

From the four proteins, 147 peptides were determined to bind HLA-A*0201 and -B*0702 using a combined *in silico/in vitro* affinity screening. T cell recognition of all 147 peptide-HLA-A*0201/-B*0702 combinations was assessed through the use of a novel high-throughput method utilizing DNA barcode labeled multimers.

T cell recognition of sequences within all four proteins was demonstrated in peripheral blood of patients, and significantly more T cell responses were detected in patients compared to healthy donors for both HLA-A*0201 and -B*0702. Notably, several of the identified responses were directed toward peptides, with a predicted low or intermediate binding affinity. This demonstrates the importance of including low-affinity binders in the search for epitopes within shared tumor associated antigens (TAAs), as these might be less subject to immune tolerance mechanisms.

The study presents four novel TAAs containing multiple possible targets for immunotherapy of breast cancer.

ARTICLE HISTORY

Received 10 April 2019
Revised 29 August 2019
Accepted 30 August 2019

KEYWORDS

Breast cancer; breast cancer immunogenicity; tumor associated antigens; TAAs; TAAs in breast cancer; shared tumor antigens; overexpression antigens; immunomonitoring; tumor specific CD8+ T cells; tumor specific cytotoxic T cells



Introduction

Throughout the last decade, the remarkable progress in the field of cancer immunotherapy has resulted in a paradigm shift in cancer treatment, establishing immunotherapy as the fourth pillar of treatment, next to conventional therapies; surgery, radiation, and chemotherapy. Unprecedented improvements of response rate and overall survival have been shown for an increasing range of cancer types, with various forms of immunotherapy.

Breast cancer remains the largest group of female cancers and a major cause of death, despite improvements in time of diagnosis and range of treatment options.^{1,2} Although generally considered to be poorly immunogenic, an increasing body of evidence points to a role of immunotherapy in breast cancer, especially in triple negative breast cancer, the subtype

where other treatment options are extremely limited.³ In recent years, a major focus of immune therapy has been on mutation-derived neo-antigens, with mutational burden and predicted number of neo-antigens shown to correlate with favorable clinical outcome and benefit from immune check-point therapy.⁴⁻⁶

However, the burden of somatic mutations varies greatly between tumor types,⁷ as do the chances of identifying patient-specific targetable neo-antigens, to which effector cells of the immune system can be actively directed. Breast cancers are among low mutational burden tumors and although a recent study demonstrated the presence of neo-antigen reactive T cells in tumor infiltrating lymphocytes (TILs) used to treat a breast cancer patient who obtained a complete durable regression,⁸ we would argue that the group of shared tumor associated antigens (TAAs) may play an additional role in this cancer type. TAAs are


CONTACT Sine Reker Hadrup  sirha@dtu.dk  Section for Experimental and Translational Immunology, Department of Health Technology, Technical University of Denmark, Kemitorvet Building 204, 2800 Kgs, Lyngby, Denmark

*These authors contributed equally

†Current affiliation: Department of Pathology, Odense University Hospital, Odense, Denmark

‡Current affiliation: Max Delbrück Center for Molecular Medicine, Berlin, Germany

This article has been republished with minor changes. These changes do not impact the academic content of the article.

 Supplemental data for this article can be accessed [publisher's website](#).

© 2019 The Author(s). Published with license by Taylor & Francis Group, LLC.

This is an Open Access article distributed under the terms of the Creative Commons Attribution-NonCommercial-NoDerivatives License (<http://creativecommons.org/licenses/by-nc-nd/4.0/>), which permits non-commercial re-use, distribution, and reproduction in any medium, provided the original work is properly cited, and is not altered, transformed, or built upon in any way.

of value both in the antigen-defined treatment setting, where they can act directly as targets of therapy, as well as in the antigen-undefined setting, where they can be used for immunomonitoring and potentially be able to predict treatment outcome.⁹ Few breast cancer-specific TAAs are known; those that have already been described (e.g. HER2¹⁰ and MUC1¹¹) are only expressed in subgroups of patients; and when used in vaccines, they have shown limited clinical activity, albeit modest immunological activity.² Therefore, there is an unmet need for identification of TAAs in breast cancer.

In this study we investigate aromatase, prolactin, never in mitosis A-related kinase 3 (NEK3) and protein inhibitor of activated signal transducer and activator of transcription 3 (PIAS3) as possible TAAs in breast cancer. Aromatase is the key enzyme in estrogen synthesis and is a heterodimer composed of the ubiquitously expressed flavoprotein NADPH-cytochrome P450 reductase and aromatase cytochrome P450.¹² Aromatase inhibitors are already successful in treating breast and other female cancers, underlining the relevance of investigating aromatase as a TAA.¹³ Prolactin and two of its downstream intracellular signaling proteins, NEK3 and PIAS3, are involved in breast lobulo-alveolar expansion and differentiation prior to milk synthesis and secretion.^{14,15} All four proteins have been described to have an increased expression in breast cancer compared to healthy breast tissue.^{12–16}

Results

Peptides were selected based on a combined *in silico* and *in vitro* selection pipeline

The four proteins aromatase, NEK3, PIAS3, and prolactin were selected for investigation based on a literature search, prioritizing proteins that fulfilled criteria of tissue restriction and increased expression in malignant compared to healthy breast tissue (Table 1). Aromatase mRNA levels have been shown to be significantly increased in breast cancer compared to healthy breast tissue, e.g. in a study by Harada, where mRNA levels were significantly elevated ($p < 0.01$).¹⁶ Likewise, significantly increased expression of prolactin, and the two intracellular signaling proteins, NEK3 and PIAS3, have been demonstrated in breast tumor tissue using immunohistochemistry staining. This revealed a significant difference in expression between

normal/hyperplastic epithelium and ductal carcinoma *in situ*/invasive carcinoma (t-tests, all p values < 0.02).¹⁴

Expression of all four proteins was validated in two breast ductal carcinoma cell lines (BT-549 and HCC1937), as well as in two breast adenocarcinoma cell lines (EFM-192A and MDA-MB-231) (Supplementary Figure S1). MHC class I presentation of peptides from the four proteins was investigated by mass spectrometry analysis and demonstrated presentation of peptides from PIAS3 in three of three tested cell lines (Supplementary Figure S1, Supplementary Table S3).

A library of peptides was generated based on a two-step *in silico* + *in vitro* selection process (Table 2, Supplementary Table S2). In the initial *in silico* prediction step, two available computational pipelines, SYFPEITHI and NetMHC 3.0, were used for predicting the MHC class I binding affinity of the individual peptides in the selected proteins. We identified potential HLA-A*0201 and -B*0702 binding 9- and 10-mer peptides within the sequences of the four proteins. The number of predicted peptides out of total possible peptides from each protein sequence correlated with the size of the protein, as would be expected. 415 of the total 3644 peptides were predicted with selection cut offs set to accommodate inclusion of both high and low affinity HLA-A*0201 and -B*0702 ligands (SYFPEITHI: ≥ 19 , NetMHC 3.0: ≤ 1000 nM), given that the proteins of interest are shared antigens. Previous analyses have demonstrated very low affinity epitopes of relevance in shared antigens.^{17, 18} As such, the binding of the predicted peptides was experimentally tested *in vitro* with an MHC ELISA.¹⁹ 147 of the 415 *in silico* predicted peptides were selected for further analysis, based on 50% (A*0201) and 70% (B*0702) binding affinity, compared to a reference of high affinity virus-derived ligands (Table 2, Supplementary Table S2).

Table 2. Peptide selection from the four proteins through a combined *in silico* prediction and *in vitro* binding assay.

Protein	Size (amino acids)	Total number of peptides (9- and 10-mers)	<i>In silico</i> predicted peptides ^a (9- and 10-mers)	<i>In vitro</i> selected peptides ^b (9- and 10-mers)
Aromatase	503	989	141	49
NEK3	506	995	85	36
PIAS3	628	1239	148	50
Prolactin	227	437	41	12
Total		3644	415	147

^a*In silico* prediction cut offs: SYFPEITHI score ≥ 19 and/or NetMHC 3.0 IC50 ≤ 1000 nM.

^b*In vitro* binding cut offs: A*0201: 50% of CMV control, B*0702: 70% of CMV control.

Table 1. Overview of protein targets selected for investigation as tumor associated antigens.

Protein	Full name	Normal function	Role in breast cancer	Normal expression	Increased expression	Reference
Aromatase	Aromatase	Key enzyme in estrogen synthesis. Heterodimer composed of aromatase cytochrome P450 and NADPH-cytochrome P450 reductase ^a	Enhanced tumor cell growth	Breast, ovary, testes, adipose tissue, skin, hypothalamus, placenta	Breast, endometrial & ovarian cancer	12,13,16
NEK3	Never in mitosis A-related kinase 3	Prolactin receptor-associated protein, positive regulator	Enhanced survival, motility, and invasion of tumor cells	Ubiquitous	Breast, colorectal, carcinoid & testicular cancer	14
PIAS3	Protein inhibitor of activated STAT3	Prolactin receptor-associated protein, negative regulator	Induction of malignant transformation	Ubiquitous	Breast cancer, glioma	14
Prolactin	Prolactin	Growth and differentiation hormone	Enhanced breast epithelial survival and motility, inhibition of tumor cell apoptosis	Breast, brain (pituitary gland), placenta, endometrium	Breast cancer	14,15

^aOnly aromatase cytochrome P450 is investigated in this study.

All peptides were predicted with the 3.0 version of NetMHC. However, at the time of publication, a new version had been developed (NetMHCpan 4.0). Therefore, we conducted a comparison of the prediction output from the current library of the two database versions (Supplementary Figure S2). The outputs from the two different versions of NetMHC correlated tightly, with only few outliers representing a difference in predicted affinity between the two databases.

Significantly more TAA-specific T cell responses were detected *ex vivo* in peripheral blood from breast cancer patients than in healthy donors

The 147 predicted breast cancer TAA peptides were synthesized and used to generate individual peptide MHC (pMHC) monomers with UV-mediated peptide exchange as previously described.¹⁹ We then multimerized the pMHC monomers onto a PE-labeled polysaccharide backbone, coupled to a DNA barcode, unique to each specific pMHC (as described in²⁰). We included 10 epitopes from common viruses; influenza virus (FLU), Epstein-Barr virus (EBV), or cytomegalovirus (CMV) epitopes. This yielded 157 different pMHC multimers that were used to stain cryopreserved peripheral blood from breast cancer patients (Patient cohort 1, $n = 25$) and healthy donors (Healthy Donor cohort 1, $n = 17$). Based on flow cytometry, we sorted for CD8⁺ T cells with the ability to bind to pMHC multimers, the associated DNA barcodes were amplified and the specificity of the CD8⁺ T cells could be revealed by sequencing of the DNA barcodes. T cell responses were defined as any pMHC complex enriched in the sorted T cell fraction with $p < 0.001$ (FDR < 0.1%).

We observed significantly more TAA-specific T cell responses in patient samples than in healthy donors (Figure 1(a,b)) (Fischer's exact test, A*0201: $p < 0.0001$, B*0702: $p = 0.03$). Of the total 66 TAA-specific T cell responses detected, only one did not match the HLA of the donor (sample P1.2 response to

A*0201 restricted ARO9(444) peptide). With limited patient sample material, it was particularly advantageous to screen for all multimer specificities in parallel. Across 17 healthy donors, we detected numerous T cell responses directed toward virus-derived epitopes, validating the technical feasibility and general immune competence of the healthy donor population. Yet, a minor difference was observed between immune recognition of virus-derived epitopes in patients and healthy donors.

TAA-specific T cell responses were validated by specific expansion and cluster in immunological hotspots

To validate TAA-specific T cell responses, we specifically expanded T cells from PBMCs, based on the responses observed by the DNA barcoded pMHC multimer screening. Antigen-specific T cells were stimulated using the given pMHC complex, together with a cytokine cocktail. Following this strategy, we observed T cell responses with frequencies >1% of CD8⁺ T cells detected by multimer staining, directed toward prolactin- and NEK3-derived peptides (Figure 2(a,b)). Additionally, for a subset of breast cancer samples, we enriched for TAA-restricted T cells by magnetic bead sorting, using the entire pMHC multimer library with all 147 peptide specificities. After magnetic bead enrichment, samples were analyzed by DNA barcoded pMHC multimer screening. With this strategy, a number of responses were confirmed and a number of additional responses were detected (Supplementary Figure S3(a)).

In a verification cohort of breast cancer patient samples (Patient cohort 2, $n = 18$) and healthy donors (Healthy Donor cohort 2, $n = 13$), T cell reactivity was detected in peripheral blood against the same TAAs. Samples in Patient cohort 2 and Healthy Donor cohort 2 were screened for T cell reactivity with a fluorescently labeled combinatorial-encoded pMHC multimer library *ex vivo*, and after enrichment by magnetic bead sorting. In the verification cohort, T cell responses were distributed across the four proteins (Supplementary Figure S3

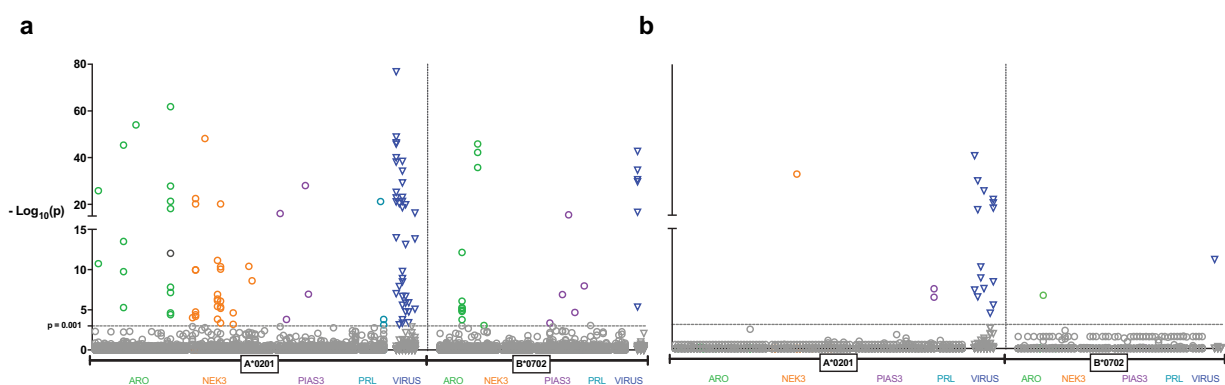


Figure 1. Detection of T cell responses to potential breast cancer TAAs and virus derived peptides.

Screening for T cell recognition by DNA barcoded pMHC multimers in peripheral blood directly *ex vivo* of 25 breast cancer patients in Patient cohort 1 (a) and 17 healthy donors in Healthy Donor cohort 1 (b). Left side, T cell responses to HLA-A*0201 restricted peptides (90 breast cancer derived peptides and 7 virus derived peptides). Right side, T cell responses to HLA-B*0702 restricted peptides (57 breast cancer derived peptides and 3 virus derived peptides). Colored circles represent T cell responses to aromatase (green), NEK3 (orange), PIAS3 (purple), and prolactin (turquoise) derived peptides. Dark blue triangles represent T cell responses to virus peptides from influenza virus, Epstein-Barr virus, or cytomegalovirus epitopes. Dark gray circle above dotted line represents HLA-A*0201 restricted response detected in a patient that is not A*0201 by HLA typing. All points lying on the same vertical axis implies multiple T cell responses to the same peptide across several donors. Data plotted on the y-axis as $-\log_{10}(p)$ of the relevant pMHC-associated DNA barcode. The horizontal dotted line represents the detection limit ($p = 0.001$ /FDR = 0.1) determining a T cell responses and all dots below are not considered as T cell responses.

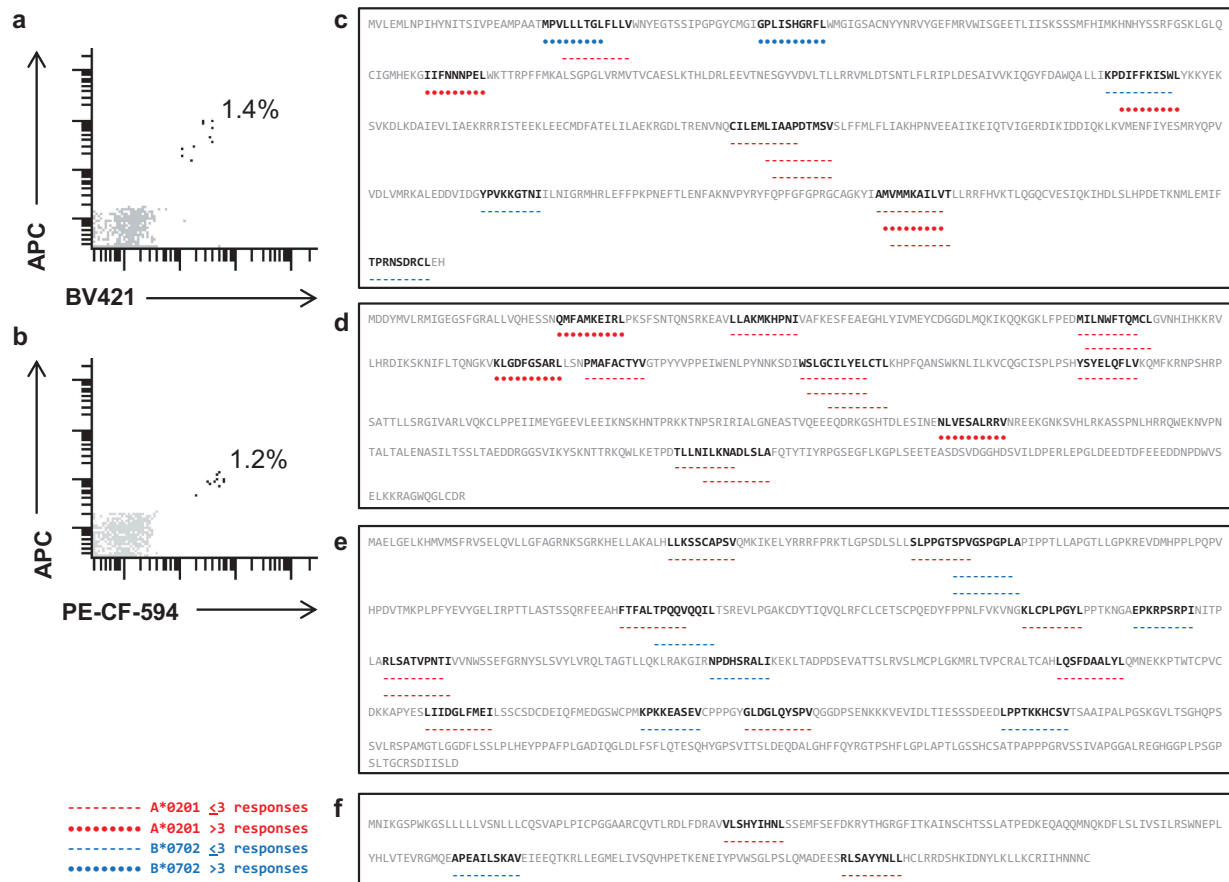


Figure 2. Validation of TAA directed T cell recognition and immunological hotspots in breast cancer antigens.

(a–b), pMHC directed expansion of T cells validated the presence of (a), A*0201 PRL9(52) specific T cells in Patient P1.8 and (b), A*0201 NEK10(329) specific T cells in Patient P1.9 from Patient cohort 1. Frequencies of pMHC multimer specific T cells out of total CD3+ CD8+ TILs are displayed.

(c–f), Protein sequences of Aromatase (c), NEK3 (d), PIAS3 (e) and prolactin (f), with immunological hotspots illustrated. Peptide sequences, for which T cell recognition was detected in Patient cohorts 1 & 2 are marked with red dashes (A*0201, < 3 responses), red dots (A*0201, > 3 responses), blue dashes (B*0702, < 3 responses), and blue dots (B*0702, > 3 responses).

(b), Supplementary Table S2) and were preferentially observed in breast cancer patients, as opposed to healthy donors.

All TAA-specific T cell responses detected directly *ex vivo* and following pMHC-specific expansion in Patient cohort 1 and 2 were mapped to their specific positions along the length of the protein sequence (Figure 2(c–f)). This analysis revealed that epitopes giving rise to T cell responses tended to cluster, indicating potential “immunological hotspots”. Evidently, the immunological hotspots covered certain regions of the protein sequences where several T cell epitopes overlapped. Furthermore, multiple T cell responses were observed toward the same epitopes and overlapping regions across multiple breast cancer patient samples, and with restriction to both HLA-A*0201 and –B*0702.

Each of the four investigated proteins contained targets of TAA-specific T cells

T cell reactivity detected in peripheral blood from breast cancer patients and healthy donors was distributed across the four proteins, with most responses toward aromatase- and NEK3-derived peptides (Figure 3(a)). In blood from

healthy donors, the number of T cell responses was significantly lower than in breast cancer patients for aromatase- and NEK3- derived peptides, and no T cell reactivity was detected toward prolactin-derived peptides. With regards to specific epitope count, it is evident that for several T cell epitopes in aromatase and NEK3, T cell reactivity was detected multiple times throughout a range of screened patients (8 unique epitopes detected for each protein, covered by 28 and 27 individual T cell responses). For PIAS3 and prolactin, the epitopes found were more unique for each donor, with less overlap in detection of the same T cell response across several samples (11 and 2 unique epitopes, respectively, covered by 12 and 3 individual T cell responses, respectively). Each protein gave rise to a similar fraction of epitopes (16–22%) when relating the number of T cell epitopes to the number of HLA binding peptides, i.e. screened for T cell recognition within each protein.

Peptides were divided into two groups, based on detection of T cell responses (response ±), to investigate potential differences in characteristics of immunogenic versus non-immunogenic peptides in this context. First, evaluating the pMHC affinity predicted by NetMHCpan 4.0 and shown as

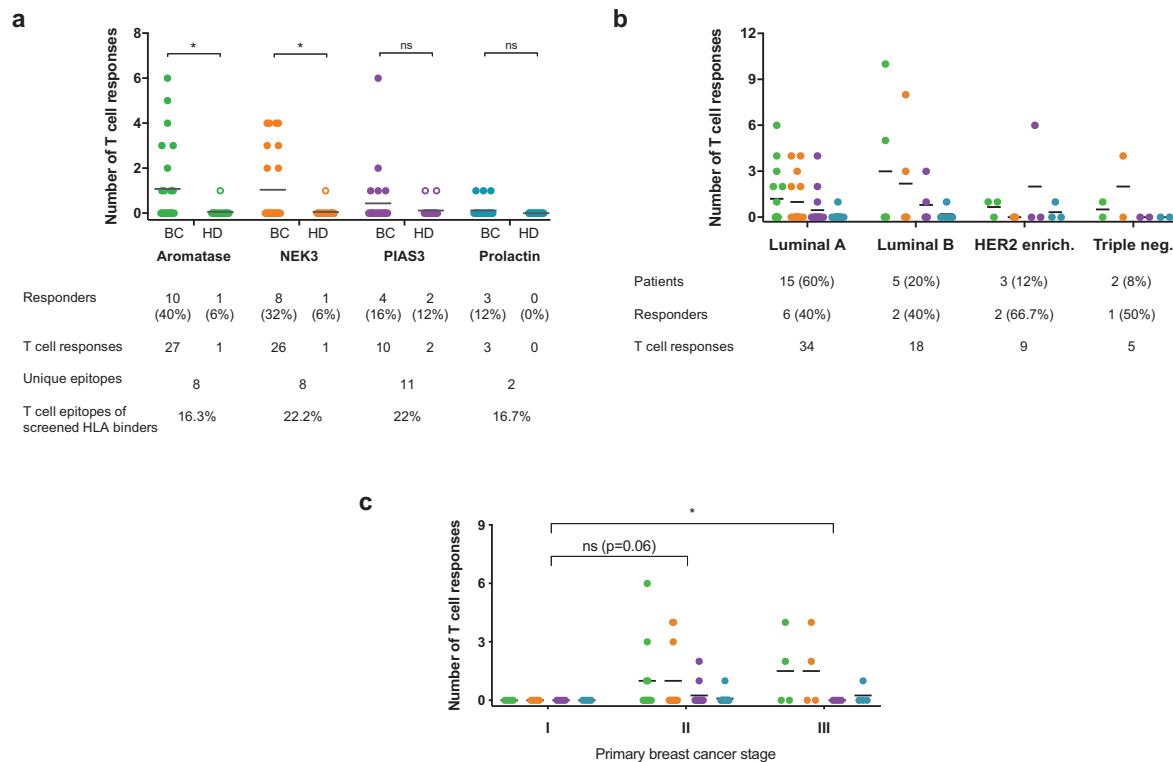


Figure 3. Distribution of detected T cell responses by protein and breast cancer subtype or stage.

Plots display distribution of T cell responses detected in breast cancer Patient cohort 1 and Healthy Donor cohort 1 *ex vivo*. (a), T cell response distribution across the four potential TAAs; aromatase (green), NEK3 (orange), PIAS3 (purple), and prolactin (turquoise). (b), Distribution of TAA specific T cell responses observed in breast cancer patients separated by breast cancer subtypes. (c), Distribution of TAA specific T cell responses observed in breast cancer patients by staging of primary tumor. Asterisks indicate significance levels (*, $p < 0.05$), nonparametric Mann-Whitney test.

nM binding affinity and % eluted ligand Rank (Supplementary Figure S4(a–b)). Second, stability was predicted by NetMHCStabpan 1.0 and shown as %Rank (Supplementary Figure S4(c)). There were no significant differences in mean predicted affinity or stability between peptides, yielding a T cell response (+) or not (-).

T cell reactivity toward breast cancer TAAs occurs independently of cancer subtype and disease stage

Breast cancer patients in cohort 1 were stratified into different molecular subtypes based on pathological examination of tumors (Supplementary Table S1). Four major subtypes of breast cancer are commonly described based on tumor cell expression of hormone receptors (estrogen receptor; ER, and progesterone receptor; PR) and growth factor HER2 as follows: luminal A (ER+ and/or PR+, HER2⁻), luminal B (ER+ and/or PR+, HER2+), HER2 enriched (ER⁻ and PR⁻, HER2+), and triple negative (ER⁻, PR⁻, HER2⁻). Breast cancer patients with TAA-specific T cell responses were observed for all subtypes and there seemed to be no preferential distribution for any particular subtype in the investigated patient cohort (Figure 3(b)). However, for certain subtypes, i.e. HER2 enriched and triple negative, the number of patients included is <5, and hence too few to firmly evaluate for potential differences.

For 20 out of 25 breast cancer patients from cohort 1 it was possible to determine disease stage based on UICC TNM

guidelines (Supplementary Table S1). Interestingly, TAA-specific T cell responses were observed in blood from patients at disease stage II and III, and none in blood from patients at stage I, with significantly more responses in disease stage III than disease stage I (Figure 3(c)). This interesting observation from a relatively small cohort of patients at each stage (I: 4 patients, II: 12 patients, and III: 4 patients), could indicate enhanced T cell reaction with higher tumor burden or metastatic disease, but such findings should be validated in a larger cohort.

Breast cancer TAA-specific T cells have functional capacity upon stimulation

To assess the functional capacity of TAA-responsive T cells in patients, we combined the DNA barcoded pMHC multimer screening with measuring cytokine production by intracellular staining, as previously described.²⁰ A selection of PBMCs from Patient cohort 1 were stimulated with 1) a pool of TAA peptides specific for each patient sample, selected based on T cell responses found by multimer screening of *ex vivo* or enriched material, or 2) a mixture of HLA matching breast cancer cell lines (BT-549, HCC1937, EFM-192A and MDA-MB-231). After stimulation, cells were stained and analyzed simultaneously for functional reactivity and T cell specificity by sorting T cells solely based on their cytokine secretion profile, IFN γ and/or TNF α secretion (ICS^{pos}) or no cytokine secretion (ICS^{neg}), after which

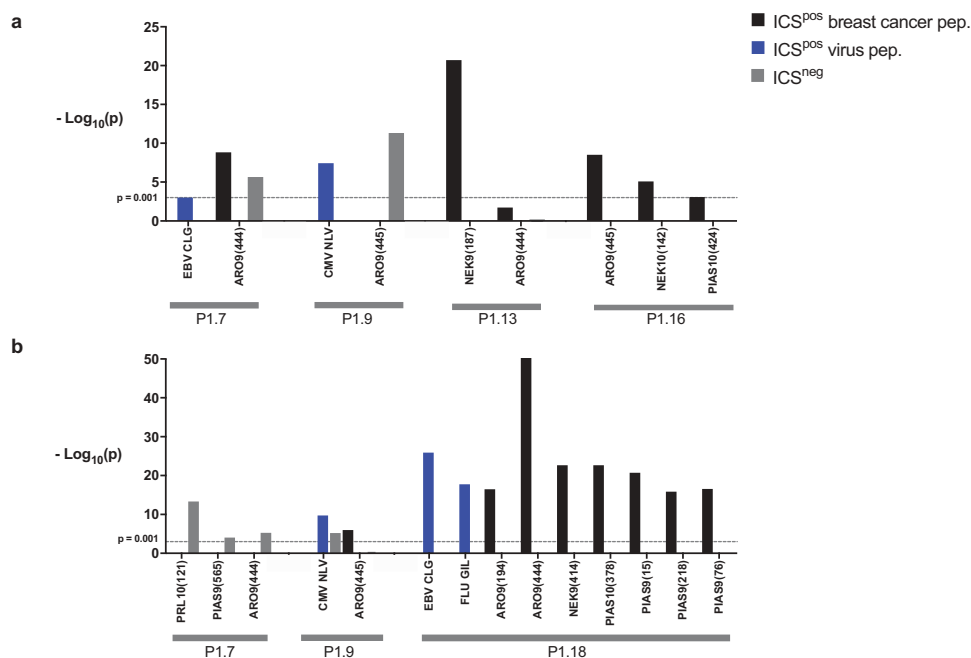


Figure 4. Functional assessment of breast cancer TAA responsive T cells.

Bar plots representing the parallel assessment of T cell specificity and functional responsiveness of breast cancer patient PBMCs from Patient cohort 1. PBMCs were stimulated with a patient specific peptide pool (a) or breast cancer tumor cell lines (b), stained with INF γ and TNF α antibodies and with DNA barcoded pMHC multimers. CD8+ T cells were sorted based on production of INF γ and/or TNF α (ICS^{POS}) versus no production of these cytokines (ICS^{NEG}). pMHC multimer binding was not included as sorting criteria. Data plotted as $-\text{Log}_{10}(p)$ of the relevant pMHC associated DNA barcode. The dotted lines represents the detection limit ($p = 0.001/\text{FDR} = 0.1$) and all bars below are not considered as T cell responses. Black bars represent T cell responses detected toward breast cancer derived peptides, blue bars represent T cell responses detected toward virus derived peptides, both in the ICS^{POS} fraction, whereas gray bars represent T cell responses detected in the ICS^{NEG} fraction.

sequencing of the pMHC associated DNA barcode uncovered the antigen specificity of the sorted T cell populations.

Patient samples stimulated with peptide pools showed presence and functional capacity of T cells specific for aromatase, NEK3, and PIAS3 peptides (Figure 4(a)). Recognition of two peptides from aromatase with overlapping sequences (ARO9 (445) and ARO9 (444), both restricted to HLA-A*0201) were present across most samples and cytokine-producing in some. Relevant virus-derived peptides were included for stimulation, with detection primarily in ICS^{POS} T cells. Stimulation with tumor cell lines showed T cells specific for all investigated TAAs, but with only functional capacity for aromatase, NEK3, and PIAS3 peptides (Figure 4(b)). Patient P1.7 had TAA-specific T cells in the ICS^{NEG} T cell fraction, whereas patient P1.18 had multiple TAA-specific T cells in the ICS^{POS} T cell fraction.

Discussion

Herein, we present the detection of CD8+ T cell responses toward peptides derived from breast cancer associated antigens. The ambition was to identify peptides from proposed breast cancer TAAs aromatase, NEK3, PIAS3, and prolactin, and validate them as T cell epitopes. This was accomplished by screening a cohort of 25 breast cancer patient samples and 17 healthy donor samples for recognition of 147 selected peptides restricted to HLA-A*0201 and -B*0702. In the primary cohort, significantly more CD8+ T cell responses were observed in breast cancer patient samples than healthy donor samples. This was uncovered by a high throughput DNA-barcode label pMHC multimer

screening; a method which enabled the investigation of hundreds of breast cancer-specific CD8+ T cells in parallel. The same strategy was recently employed to identify autoreactive T cells in narcolepsy.²¹ Our findings were confirmed in a verification cohort (18 patients, 13 healthy donors) by fluorochrome labeled pMHC multimers, where again CD8+ T cell responses to the breast cancer-derived peptides were overrepresented in patient samples versus healthy donors. Our findings across two cohorts and two technological screening platforms show strong evidence that the four investigated proteins contain CD8+ T cell targets.

Strikingly, epitopes were shared between patients, overlapped for HLA*A0201 and -B*0702 and tended to cluster along the length of the protein sequences, indicating the presence of immunological hotspots. Importantly, upon inspection of *in silico* predicted properties of peptides \pm CD8+ T cell recognition, it was evident that immunogenic peptides were not significantly better binders or more stable in the MHC complex than non-immunogenic peptides. This emphasizes the importance of evaluating the inclusion criteria when selecting peptides for T cell screening endeavors. As indicated in this study, particularly when the targets are of shared origin and the matching T cells therefore subject to stricter selection during development in the thymus, the need for including intermediate or even low affinity binders is of importance.

Several of the *ex vivo* observed CD8+ T cell responses were verified after *in vitro* expansion, with expanded responses from two patient samples validated by fluorescently-labeled pMHC multimer staining. In addition to observing CD8+ T cell responses *ex vivo*, and after specific expansion, a subset of breast cancer patient samples were further investigated for functional

capacity upon stimulation and ICS. Interestingly, the functional analysis revealed breast cancer patient CD8⁺ T cell reactivity to some of the TAA-derived peptides that were observed in *ex vivo* screenings. A limitation of the study is the lack of patient autologous tumor cells. Although we document T cell recognition of allogeneic, commercially available cancer cell lines, the pairing of patient T cells and autologous tumor cell lines would enable verification of autologous recognition. The same limitation applies to the mass spectrometry analysis, where MHC class I expression of peptides from all four proteins was investigated in three commercially-available breast cancer cell lines. Here one putative HLA-A*02:01 ligand (PIAS3; SIVAPGGAL) identified by mass spectrometry was overlapping with the T cell screening peptide library. This peptide did not result in T cell responses. Despite the limited overlap, the detection of four MHC class I embedded PIAS3 peptides does document expression and antigen-processing of PIAS3 in breast cancer.

Though breast cancer was originally considered an immunologically silent malignancy, the data reported herein and recent publications from others encourage further research of immunogenicity of breast cancer.^{22–24} In the current era of neo-epitopes and a strong focus on personalized strategies, the breast cancer TAAs investigated here provide a broader approach with potential applicability across many patients. Of note, the present study focused on HLA-A*0201 and – B*0702, where there was already some sequence-overlap between epitopes observed. Expanding the analysis to additional HLA alleles would enable coverage of a greater part of the population and possibly strengthen the tendency of immunological hotspots. For therapeutic use, the existence of immunological hotspots suggests a compelling approach, where patients could be vaccinated with a long peptide spanning a hotspot, regardless of HLA status. Such an “off-the-shelf” antigen could possibly provide an add-on to more personalized approaches, targeting e.g., neo-epitopes. Notably, we found TAA-specific T cell responses in all breast cancer subtypes suggesting that a therapy based on targeting these antigens could benefit many patients. Furthermore, TAA-specific T cell responses seem to be enhanced at more advanced stages of disease, indicating that at an early stage of breast cancer development, where tumor size is small and there is no spread to lymph nodes, these tumors are less immunogenic. Also this finding argues for enhancement of T cell reactivity by boosting the tumor specific T cells in both frequency and functionality, e.g. through checkpoint inhibition. Identification and understanding of T cell epitopes can contribute to diagnostics, immunomonitoring, and immunotherapy in cancer patients. This study provides an important contribution of four novel TAAs containing multiple epitopes in a poorly described landscape of breast cancer antigens and encourages further investigation of aromatase, NEK3, PIAS3 and prolactin in a preclinical setting, e.g. assessment of expression and immunogenicity in mouse models.

Materials and methods

Patient and healthy donor samples

Breast cancer patient samples were kindly provided by the Department of Oncology and the Center for Cancer Immune Therapy, Herlev Hospital, Denmark, with approval by the

regional ethics committee for the Capital Region of Denmark. Breast cancer patient samples came from two different cohorts, as listed in Supplementary Table S1. All patient blood samples in cohort 1 were drawn at the time of primary diagnosis, before any treatment was initiated. Patients in cohort 2 were untreated, or treated with one or more standard therapies (chemo-, radiation and endocrine), but did not receive immunotherapy prior to blood sampling. Healthy donor samples were collected by approval of the local Scientific Ethics Committee, with donor written informed consent obtained according to the Declaration of Helsinki. Healthy donor blood samples were obtained from the blood bank at Rigshospitalet, Copenhagen, Denmark. All samples were obtained anonymously.

PBMC isolation from whole blood

Peripheral blood mononuclear cells (PBMCs) from breast cancer patients and healthy donors were obtained from whole blood with density centrifugation on Lymphoprep (Axis-Shield PoC, Cat#1114544) in Leucosep tubes (Greiner Bio-One, Cat#227288) and cryopreserved at -150°C in FCS (fetal calf serum, Gibco, Cat#10500064) + 10% DMSO (dimethyl sulfoxide, Sigma-Aldrich, Cat#C6164).

HLA tissue typing

HLA class I tissue typing was determined by either flow cytometry with anti-HLA-A*02 (Abcam, Cat#ab27728) and anti-HLA-B*07 antibodies (Abcam, Cat#ab33331), PCR, or by high-resolution next generation sequencing (IMGM, Martinsried, Germany).

Tumor cell lines

Breast cancer cell lines were kindly provided by the Center for Cancer Immune Therapy, Herlev Hospital, Denmark (BT-549 and MDA-MB-231) or purchased from ATCC (HCC1937, Cat#CRL-2336) and DSMZ (EFM192A, Cat#ACC258) and grown in R10 (RPMI + GlutaMAXTM, Gibco, Cat#61870010 + 10% FCS) including 1% penicillin-streptomycin (P/S, Sigma-Aldrich, Cat#P0781).

Expression of TAAs by tumor cell lines

Expression of proteins aromatase, NEK3, PIAS3, and prolactin was investigated in breast cancer cell lines BT-549, EFM192A, HCC1937, and MDA-MB-231 by intracellular staining with anti-aromatase (Bioss, Cat#bs-1292R), anti-NEK3 (Abcam, Cat#83221), anti-PIAS3 (Abcam, Cat#ab77231) and anti-prolactin (Lifespan Biosciences, Cat#LS-C209024) antibodies, with analysis by flow cytometry. Tumor cells were harvested and washed twice in R10, once in PBS + 2% FCS. Thereafter, cells were permeabilized and fixated with the Transcription Factor Buffer Set (BD, Cat#562574) and stained for 30 min at 4°C with specific antibodies or isotype/stain control antibodies. Following, cells were washed twice in PBS + 2% FCS and stained with secondary antibodies when relevant, washed twice in PBS + 2% FCS and finally fixated in 1% paraformaldehyde (PFA, Santa Cruz Biotechnology, Cat#sc-281692) until analysis.

Endogenous peptide presentation on tumor cell lines

The endogenous MHC class I immunopeptidomes of the breast cancer cell lines BT-549, EFM-192A and MDA-MB-231 were analyzed by MHC immunoaffinity chromatography (MHC-IAC) followed by liquid chromatography-mass spectrometry (LC-MS) as detailed in Supplementary Methods. Briefly, each cell line was subjected to two parallel MHC-IACs using 108 cells per analysis and employing the W6/32 antibody. Peptides were measured at a Q Exactive (Thermo Scientific) using a top 10 data dependent acquisition strategy, and data were processed with Proteome Discoverer version 1.4 employing Sequest HT and Percolator to achieve a false discovery rate of 5%.

In silico HLA-A*0201 and -B*0702 binding affinity and stability prediction of peptides

The binding affinity and stability to HLA-A*0201 and HLA-B*0702 of 9- and 10- amino acid peptides from the four investigated proteins were predicted by SYFPEITHI,²⁵ NetMHC 3.0,²⁶ NetMHCpan 4.0²⁷ and NetMHCstabpan 1.0.²⁸ Peptides with a binding score ≥ 19 in SYFPEITHI and/or ≤ 1000 nM in NetMHC 3.0 were analyzed.

Peptides

All breast cancer associated and virus-derived peptides were purchased from Pepscan (Pepscan Presto BV, Lelystad, Netherlands) and dissolved to 10 mM in DMSO. A full list of breast cancer associated peptides used in the study can be found in Supplementary Table S2. The following virus-derived peptides were included in the study; HLA-A*0201 restriction: CMV pp65 (NLVPMVATV), CMV IE1 (VLEETSVML), EBV BMF1 (GLCTLVAML), EBV BRLF1 (YVLDHLIVV), EBV LMP2 (CLGGLTMV), EBV LMP2 (FLYALALL), FLU MP (GILGFVFTL), HIV pol (ILKEPVHGV), HLA-B*0702 restriction: CMV pp65 (RPHERNGFTV), CMV pp65 (TPRVTGGGAM), EBV EBNA (RPPFIRLL).

In vitro affinity testing and selection of peptides

The experimental binding of *in silico* predicted peptides was assessed by MHC ELISA, as previously described by Rodenko et al.¹⁹ Briefly, biotinylated peptide-HLA (pHLA)-A*0201/B*0702 complexes were generated by UV-mediated peptide exchange and incubated on streptavidin (Invitrogen, Cat#S888)-coated Maxisorp plates (NUNC, Cat#44-2404-21) for 1 h at 37°C. The pHLA complexes were then incubated with horseradish peroxidase-conjugated β_2 microglobulin (β_2m) antibody (Acris GmbH, Cat# 604HRP) for an additional 1 h at 37°C, binding only to correctly folded peptide-MHC (pMHC) molecules. Plates were washed and a colorimetric reaction was initiated by the addition of tetramethylbenzidine peroxidase substrate (KPL, Cat#506606). Finally, the optical density (OD) of each well was measured at 405 nm by an ELISA reader (Epoch microplate spectrophotometer, Bio-Tek) and values were normalized to the OD

of a CMV-derived virus peptide with a known high binding affinity by the formula,

$$\text{Index value} = \frac{OD_{\text{peptide}} - OD_{\text{PBS}}}{OD_{\text{CMVcontrol peptide}}}$$

HLA-binding peptides were selected based on their ability to rescue the A*0201/B*0702 molecule from degradation after UV-mediated cleavage of the conditional ligand and compared to that of a CMV virus-derived control with known high binding affinity. The threshold for selection was set at 50% (A*0201) and 70% (B*0702) of the binding affinity of the respective virus-derived peptides.

MHC monomer production and generation of specific pMHC multimers

The production of MHC monomers was performed as previously described by Hadrup et al.²⁹ In brief, HLA-A*0201 and -B*0702 heavy chains and human β_2m light chain were expressed in bacterial BL21 (DE3) pLysS strain (Novagen, Cat# 69451) and purified as inclusion bodies. After solubilization, A*0201/B*0702 inclusion bodies were refolded with β_2m light chain and a UV-sensitive ligand,^{30,31} and the folded monomers were biotinylated with BirA biotin-protein ligase standard reaction kit (Avidity, 318 LLC-Aurora, Colorado) and purified using a size-exclusion column (Waters, BioSuite125, 13 μ m SEC 21.5 \times 300 mm) and HPLC (Waters 2489). Specific pMHC monomers were generated by UV-induced peptide exchange³⁰ and multimerized with fluorochrome-conjugated streptavidin or coupled to dextramer according to specific protocols.

Enrichment of pMHC-specific T cells by magnetic bead sorting

Cryopreserved PBMCs were thawed and washed in R10 media containing DNase (40 U/ml, Stem Cell Technologies, Cat#07900) before incubation with PE (phycoerythrin)-coupled pMHC multimers (0.1 mg of each specificity) for 1 h at 4°C. Hereafter, cells were washed twice in R10 and incubated 15 min at 4°C with anti-PE microbeads (Miltenyi Biotec, Cat#130-048-801). Cells were washed twice after incubation, resuspended in 0.5 mL RPMI with DNase and applied to magnetic separation columns (MS; Miltenyi Biotec; Cat#130-042-201) placed in a magnetic field of a magnetic-activated cell sorting (MACS) separator through a 30 μ m pre-separation filter. After washing, cells were flushed out in 2mL X-vivo (Lonza, Cat#Be04-418Q), 5% human serum, 100 U/mL IL-2 (Proleukin; Novartis, Cat#200-02), 15 ng/mL IL-15 (Peprotech, Cat#200-15), centrifuged and resuspended in 200 μ L of the same media containing 5×10^4 feeder cells, prepared and irradiated from the negative fraction during separation and 5×10^3 anti-CD3/CD28-coated Dynabeads (Invitrogen, Cat#111.31.D). Enriched cells were cultured in 96-well plates for 2–3 weeks, with bi-weekly change of medium and analyzed by pMHC multimer-specific T cell detection methods.

pMHC-specific expansion of T cells

Cryopreserved PBMCs were thawed and washed in R10 media, resuspended and cultured in X-vivo + 5% human serum. Cells were stimulated twice a week with the given pMHC complex, IL-2 and IL-21, all co-complexed on a dextran molecule for expansion of specific T cell populations and analyzed after two weeks by combinatorial fluorescently-encoded pMHC multimers.

Detection of pMHC-specific T cells by combinatorial fluorescently-encoded MHC multimers

The combinatorial encoding method and gating strategy is described in detail by Andersen et al.³² Briefly, a UV exchange reaction was carried out for each selected HLA-A*0201/B*0702 peptide ligand, followed by multimerization on two different streptavidin-conjugated fluorochromes. Thus, each of the peptide specificities was assigned a unique two-color combination. Five different streptavidin-conjugated fluorochromes were used for detection of specific T cells in Patient cohort 1: PE (phycoerythrin, Biolegend, Cat#405203), APC (allophycocyanin, Biolegend, Cat#405207), PE-Cy7 (phycoerythrin-cyanin 7, Biolegend, Cat#405206), PE-CF594 (BD, Cat#562284), and BV421 (brilliant violet, Biolegend, Cat#405226). Nine streptavidin-conjugated fluorochromes were used for detection of specific T cells in Patient cohort 2 and Healthy Donor cohort 2: PE, APC, PE-Cy7, BV421, Q-dot 585 (quantum dot, Invitrogen: Q10111MP), Q-dot 605 (Invitrogen, Cat#Q10101MP), Q-dot 625 (Invitrogen, Cat#A10196), Q-dot655 (Invitrogen: Q10121MP) and Q-dot705 (Invitrogen, Cat#Q10161MP). Breast cancer and healthy donor PBMCs were stained with a panel of up to 36 combinatorially encoded pMHC-multimers at a time, followed by staining with an antibody mix consisting of either CD8-BV480 (BD, Cat#566121 (clone RPA-T8)) in Patient cohort 1 or CD8-PerCP (Invitrogen, Cat#MHCD0831) in Patient cohort 2 and Healthy Donor cohort 2, dump channel antibodies CD4-FITC (CD4- fluorescein isothiocyanate, BD, Cat#345768), CD14-FITC (BD, Cat#345784) CD19-FITC (BD, Cat#345776), CD16-FITC (BD, Cat#335035) and CD40-FITC (Bio-rad, Cat#MCA1590F), and the dead cell marker LIVE/DEAD Fixable Near-IR (Invitrogen, Cat#L10119). Multimer positive T cell responses were gated as single, live, CD8⁺, FITC⁻ (dump channel), multimer color 1⁺, multimer color 2⁺, and negative for the remaining multimer colors, and defined by a minimum of 10 dual color positive events.

Detection of pMHC-specific T cells by barcoding

DNA-barcoded pMHC multimers were used to screen for T cell recognition against 157 pMHC specificities in a single sample. The method is described in detail in Bentzen et al.²⁰ Briefly, a UV exchange reaction was carried out for each selected HLA-A*0201/B*0702 peptide ligand, as described above. Each generated pMHC complex was coupled to DNA barcode- and PE-labeled dextran backbones, so that each specific peptide was encoded by a unique DNA barcode. Breast cancer and healthy donor PBMCs were stained with a pool of all barcoded MHC-multimers and an antibody mix of CD8-BV480, dump channel antibodies CD4-FITC, CD14-FITC, CD19-FITC, CD16-FITC, and CD40-FITC,

and the dead cell marker LIVE/DEAD Fixable Near-IR. Multimer-specific T cells were then sorted as single, live, CD8⁺, FITC⁻ (dump channel), PE⁺ fraction of cells, pelleted by centrifugation and cryopreserved at -80°C. DNA barcodes were amplified from the cell pellet and from a stored aliquot of the pMHC multimer reagent pool (used as baseline for comparison) by PCR, purified with a QIAquick PCR Purification kit (Qiagen, Cat#28104) and sequenced (Sequetech) using an Ion Torrent PGM 316 or 318 chip (Life Technologies). Sequencing data were processed by the software package Barracoda, available online at www.cbs.dtu.dk/services/barracoda. This tool identifies barcodes used in a given experiment, assigns sample ID and pMHC specificity to each barcode, and counts the total number of reads and clonally-reduced reads for each pMHC-associated DNA barcode. Log₂ fold changes in read counts mapped to a given sample relative to the mean read counts mapped to triplicate baseline samples are estimated with normalization factors determined by the trimmed mean of M-values method. False-discovery rates (FDRs) were estimated using the Benjamini-Hochberg method. A *p*-value is calculated based on the Log₂ fold change distribution, determining the strength of the signal compared to the input. Also, *p* < 0.001, corresponding to FDR < 0.1%, is established as the significance level determining a T cell response.

Functional assessment of pMHC-specific T cells by barcoding and intracellular flow cytometry

The functionality of pMHC-specific T cells was tested by combining intracellular cytokine staining (ICS) with a DNA barcode-based pMHC multimer staining, as previously described in Bentzen et al.²⁰ Briefly, patient-derived PBMCs were stimulated with either pre-stimulated IFN γ (PreproTech, Cat#300-02) breast cancer cell lines at a 10:1 ratio (PBMCs:cell lines), a pool of peptides with known reactivity in the specific patient or a leucocyte activation cocktail (LAC, BD, Cat#550583) positive control for 4 h at 37°C. After stimulation, cells were stained with barcoded MHC multimers, followed by staining with extracellular surface antibodies: CD3-FITC (BD, Cat#345763), CD8-BV480, and dead cell marker LIVE/DEAD Fixable Near-IR. Hereafter cells were permeabilized with the Intracellular Fix and Perm kit (eBioscience, Cat#88-8824-00), stained with intracellular antibodies TNF α -PE-Cy7 (BioLegend, Cat#502930) and IFN γ -APC (BD, Cat#341117), and fixated in 1% PFA until analysis.

Flow cytometry

All flow cytometry experiments were carried out on LSRII, Fortessa, and AriaFusion instruments (BD Biosciences). Data were analyzed in FACSDiva Software version 8.0.2 (BD Biosciences) and FlowJo version 10.4.2 (TreeStar, Inc.)

Statistical analyses

GraphPad Prism 7 for Mac OS X was used for graphing, statistical analyses and tools. This study included the D'agostino-Pearson omnibus normality test, unpaired parametric T-test

(following log-transformation to reach Gaussian distribution as needed), nonparametric Mann-Whitney test, Fischer's exact test, and Pearson's correlation coefficient.

Acknowledgments

We would like to thank all breast cancer patients and healthy donors for contributing blood samples to this study; Tina Seremet, Bente Rotbøl, Tripti Tamhane, Anna Gyllenberg Burkal, and Julien Candrian for excellent technical assistance, as well as all current and former members of the SRH group for scientific discussions.



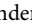

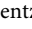
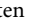
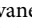

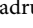
Disclosure of interest

The authors declare no potential conflicts of interest.

Funding

This research was funded in part through the Independent Research fund Danmarks Frie Forskningsfond (DK) (Grant no. DFF – 4004-00422) and the European Research Council, StG 677268 NextDART.

ORCID

Nadia Viborg  <http://orcid.org/0000-0001-9471-0895>
 Sofie Ramskov  <http://orcid.org/0000-0001-9413-8673>
 Rikke Sick Andersen  <http://orcid.org/0000-0001-7237-2215>
 Tim Fugmann  <http://orcid.org/0000-0002-7447-7480>
 Amalie Kai Bentzen  <http://orcid.org/0000-0002-5184-3054>
 Per thor Straten  <http://orcid.org/0000-0002-4731-4969>
 Inge Marie Svane  <http://orcid.org/0000-0002-9451-6037>
 Özcan Met  <http://orcid.org/0000-0002-3256-7592>
 Sine Reker Hadrup  <http://orcid.org/0000-0002-5937-4344>

References

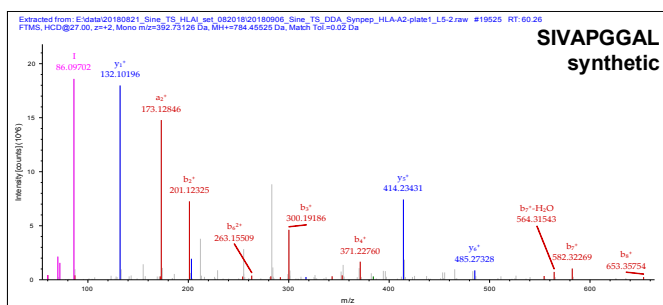
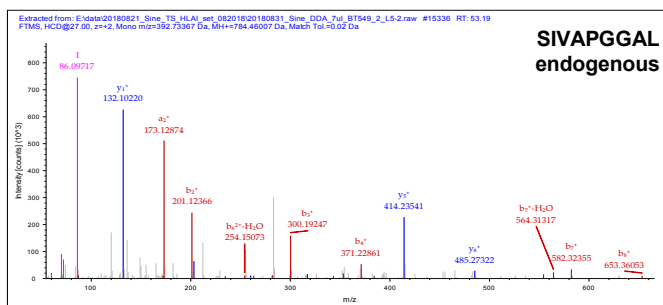
- Bray F, Ferlay J, Soerjomataram I, Siegel RL, Torre LA, Jemal A. Global cancer statistics 2018: GLOBOCAN estimates of incidence and mortality worldwide for 36 cancers in 185 countries. *CA Cancer J Clin.* 2018;68:394–424. doi:10.3322/caac.v68.6.
- Emens LA. Breast cancer immunotherapy: facts and hopes. *Clin Cancer Res.* 2018;24:511–520. doi:10.1158/1078-0432.CCR-16-3001.
- Nathan MR, Schmid P. The emerging world of breast cancer immunotherapy. *Breast.* 2017;37:200–206. doi:10.1016/j.breast.2017.05.013.
- Rooney MS, Shukla SA, Wu CJ, Getz G, Hacohen N. Molecular and genetic properties of tumors associated with local immune cytolytic activity. *Cell.* 2015;160:48–61. doi:10.1016/j.cell.2014.12.033.
- Brown SD, Warren RL, Gibb EA, Martin SD, Spinelli JJ, Nelson BH, Holt RA. Neo-antigens predicted by tumor genome meta-analysis correlate with increased patient survival. *Genome Res.* 2014;24:743–750. doi:10.1101/gr.165985.113.
- Mcgranahan N, Furness AJS, Rosenthal R, Ramskov S, Lyngaa R, Saini SK, Jamal-Hanjani M, Wilson GA, Birkbak NJ, Hiley CT, et al. Clonal neoantigens elicit T cell immunoreactivity and sensitivity to immune checkpoint blockade. *Science.* 2016;351:1463–1469. doi:10.1126/science.aaf1490.
- Alexandrov LB, Nik-Zainal S, Wedge DC, Aparicio SAJR, Behjati S, Biankin AV, Bignell GR, Bolli N, Borg A, Børresen-Dale A-L, et al. Signatures of mutational processes in human cancer. *Nature.* 2013;500:415–421. doi:10.1038/nature12477.
- Zacharakis N, Chinnasamy H, Black M, Xu H, Lu Y-C, Zheng Z, Pasetto A, Langhan M, Shelton T, Prickett T, et al. Immune recognition of somatic mutations leading to complete durable regression in metastatic breast cancer. *Nat Med.* 2018;24:724–730. doi:10.1038/s41591-018-0040-8.
- Bjoern J, Lyngaa R, Andersen R, Hölmich LR, Hadrup SR, Donia M, Svane IM. Influence of ipilimumab on expanded tumour derived T cells from patients with metastatic melanoma. *Oncotarget.* 2017;8:27062–27074. doi:10.18632/oncotarget.v8i16.
- Krishnamurti U, Silverman J. HER2 in breast cancer: a review and update. *Adv Anat Pathol.* 2014;21:100–107. doi:10.1097/PAP.0000000000000015.
- Nath S, Mukherjee P. MUC1: A multifaceted oncoprotein with a key role in cancer progression. *Trends Mol Med.* 2014;20:332–342. doi:10.1016/j.molmed.2014.02.007.
- Bulun SE, Chen D, Lu M, Zhao H, Cheng Y, Demura M, Yilmaz B, Martin R, Utsunomiya H, Thung S, et al. Aromatase excess in cancers of breast, endometrium and ovary. *J Steroid Biochem Mol Biol.* 2007;106:81–96. doi:10.1016/j.jsbmb.2007.05.027.
- Bulun SE, Lin Z, Imir G, Amin S, Demura M, Yilmaz B, Martin R, Utsunomiya H, Thung S, Gurates B, et al. Regulation of aromatase expression in estrogen-responsive breast and uterine disease: from bench to treatment. *Pharmacol Rev.* 2005;57:359–383. doi:10.1124/pr.57.3.6.
- McHale K, Tomaszewski JE, Puthiyaveettil R, Livolsi VA, Clevenger CV. Altered expression of prolactin receptor-associated signaling proteins in human breast carcinoma. *Mod Pathol.* 2008;21:565–571. doi:10.1038/modpathol.2008.7.
- Gill S, Peston D, Vonderhaar BK, Shousha S. Expression of prolactin receptors in normal, benign, and malignant breast tissue: an immunohistological study. *J Clin Pathol.* 2001;54:956–960. doi:10.1136/jcp.54.12.956.
- Harada N. Aberrant expression of aromatase in breast cancer tissues. *J Steroid Biochem Mol Biol.* 1997;61:175–184. doi:10.1016/S0960-0760(97)80010-6.
- Speiser DE, Baumgaertner P, Voelter V, Devevre E, Barbey C, Rufer N, Romero P. Unmodified self antigen triggers human CD8 T cells with stronger tumor reactivity than altered antigen. *PNAS.* 2008;105:3849–3854. doi:10.1073/pnas.0800080105.
- Lesterhuis WJ, Schreiber G, Scharenborg NM, Brouwer HM-LH, Gerritsen M-JP, Croockewit S, Coulie PG, Torensma R, Adema GJ, Figdor CG, et al. Wild-type and modified gp100 peptide-pulsed dendritic cell vaccination of advanced melanoma patients can lead to long-term clinical responses independent of the peptide used. *Cancer Immunol Immunother.* 2011;60:249–260. doi:10.1007/s00262-010-0942-x.
- Rodenko B, Toebes M, Hadrup SR, van Esch WJE, Molenaar AM, Schumacher TNM, Ovaa H. Generation of peptide-MHC class I complexes through UV-mediated ligand exchange. *Nat Protoc.* 2006;1:1120–1132. doi:10.1038/nprot.2006.121.
- Bentzen AK, Marquard AM, Lyngaa R, Saini SK, Ramskov S, Donia M, Such L, Furness AJS, McGranahan N, Rosenthal R, et al. Large-scale detection of antigen-specific T cells using peptide-MHC-I multimers labeled with DNA barcodes. *Nat Biotechnol.* 2016;34:1037–1045. doi:10.1038/nbt.3662.
- Pedersen NW, Holm A, Kristensen NP, Bjerregaard A-M, Bentzen AK, Marquard AM, Tamhane T, Burgdorf KS, Ullum H, Jennum P, et al. CD8+ T cells from patients with narcolepsy and healthy controls recognize hypocretin neuron-specific antigens. *Nat Commun.* 2019;10:1–12. doi:10.1038/s41467-019-08774-1.
- Mahmoud SMA, Paish EC, Powe DG, Macmillan RD, Grainge MJ, Lee AHS, Ellis IO, Green AR. Tumor-infiltrating CD8+ lymphocytes predict clinical outcome in breast cancer. *J Clin Oncol.* 2011;29:1949–1955. doi:10.1200/JCO.2010.30.5037.
- Savas P, Virassamy B, Ye C, Salim A, Mintoff CP, Caramia F, Salgado R, Byrne DJ, Teo ZL, Dushyanthen S, et al. Single-cell profiling of breast cancer T cells reveals a tissue-resident memory subset associated with improved prognosis. *Nat Med.* 2018;24:986–993. doi:10.1038/s41591-018-0078-7.
- Schmid P, Adams S, Rugo HS, Schneeweiss A, Barrios CH, Iwata H, Diéras V, Hegg R, Im S-A, Shaw Wright G, et al. Atezolizumab and nab-paclitaxel in advanced triple-negative breast cancer. *N Engl J Med.* 2018;379:2108–2121. doi:10.1056/NEJMoa1809615.

25. Rammensee H-G, Bachmann J, Emmerich NPN, Bachor OA, Stevanovic S. SYFPEITHI: database for MHC ligands and peptide motifs. *Immunogenetics*. 1999;50:213–219. doi:10.1007/s002510050595.
26. Lundegaard C, Lamberth K, Harndahl M, Buus S, Lund O, Nielsen M. NetMHC-3.0: accurate web accessible predictions of human, mouse and monkey MHC class I affinities for peptides of length 8–11. *Nucleic Acids Res*. 2008;36:509–512. doi:10.1093/nar/gkn202.
27. Jurtz V, Paul S, Andreatta M, Marcatili P, Peters B, Nielsen M. NetMHCpan-4.0: improved peptide–MHC class I interaction predictions integrating eluted ligand and peptide binding affinity data. *J Immunol*. 2017;199:3360–3368. doi:10.4049/jimmunol.1700893.
28. Nielsen M, Lundegaard C, Blicher T, Lamberth K, Harndahl M, Justesen S, Røder G, Peters B, Sette A, Lund O, et al. NetMHCpan, a method for quantitative predictions of peptide binding to any HLA-A and -B locus protein of known sequence. *PLoS One*. 2007;2:e796. doi:10.1371/journal.pone.0000796.
29. Hadrup SR, Toebes M, Rodenko B, Bakker AH, Egan DA, Ovaa H, Schumacher TN. High-throughput T-cell epitope discovery through MHC peptide exchange. *Methods Mol Biol*. 2009;524:383–405.
30. Toebes M, Coccorsis M, Bins A, Rodenko B, Gomez R, Nieuwkoop NJ, van de Kastele W, Rimmelzwaan GF, Haanen JBAG, Ovaa H, et al. Design and use of conditional MHC class I ligands. *Nat Med*. 2006;12:246–251. doi:10.1038/nm1360.
31. Bakker AH, Hoppes R, Linnemann C, Toebes M, Rodenko B, Berkers CR, Hadrup SR, van Esch WJE, Heemskerk MHM, Ovaa H, et al. Conditional MHC class I ligands and peptide exchange technology for the human MHC gene products HLA-A1, -A3, -A11, and -B7. *PNAS*. 2008;105:3825–3830. doi:10.1073/pnas.0709717105.
32. Andersen RS, Kvistborg P, Frøsig TM, Pedersen NW, Lyngaa R, Bakker AH, Shu CJ, Straten PT, Schumacher TN, Hadrup SR. Parallel detection of antigen-specific T cell responses by combinatorial encoding of MHC multimers. *Nat Protoc*. 2012;7:891–902. doi:10.1038/nprot.2012.037.

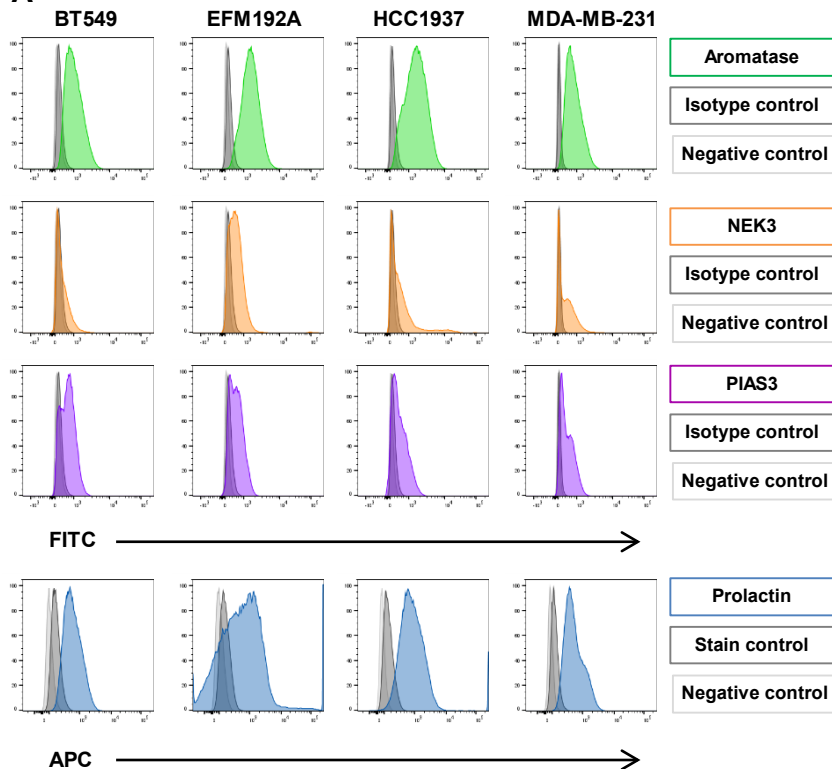
Supplementary Figure S1. Aromatase, NEK3, PIAS3 and prolactin protein and endogenous MHC class I peptide expression in breast cancer cell lines.

A, Characterization of aromatase (1st panel), NEK3 (2nd panel), PIAS3 (3rd panel) and prolactin (4th panel) protein expression in breast cancer cell lines BT549, EFM192A, HCC1937 and MDA-MB-231 by flow cytometry. **B**, MS2 spectra of SIVAPGGAL, a putative HLA-A*02:01 ligand. The upper panel shows the MS2 spectrum obtained from the BT-549 cell line, whereas the lower MS2 spectrum depicts the MS2 spectrum of synthetic SIVAPGGAL. **C**, MS2 spectra of endogenous PIAS3 peptides putatively derived from MHC allotypes other than HLA-A*02:01 and HLA-B*07:02. The upper panel shows the MS2 spectrum of ASEVCPGGY containing a cysteinylated cysteine and was obtained from the BT-549 cell line, the middle panel displays the MS2 spectrum of RFEEAHFTF obtained from the EFM192A cell line, and the lower panel depicts the MS2 spectrum of GELIRPTTL derived from MDA-MB-231.

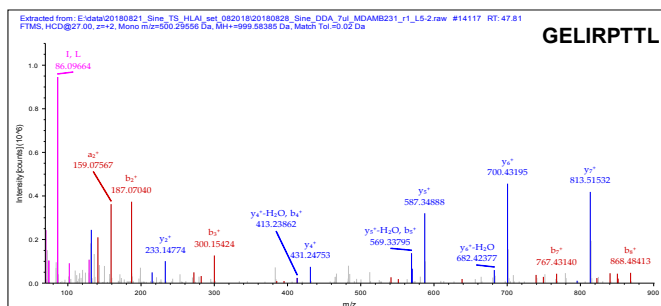
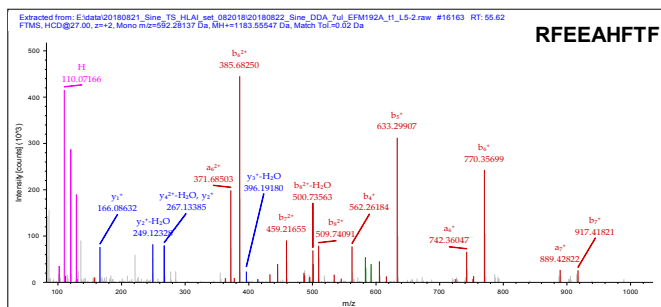
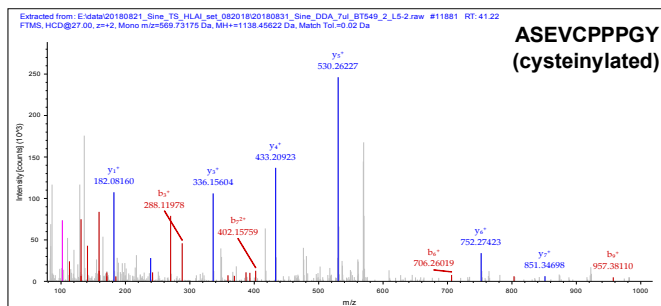
B

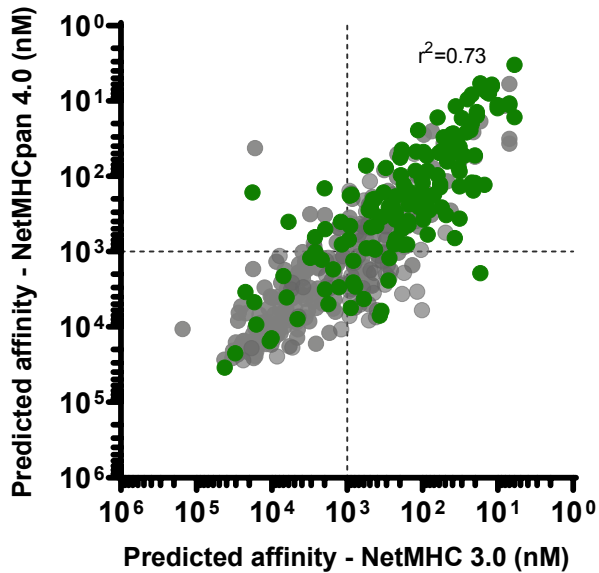


A

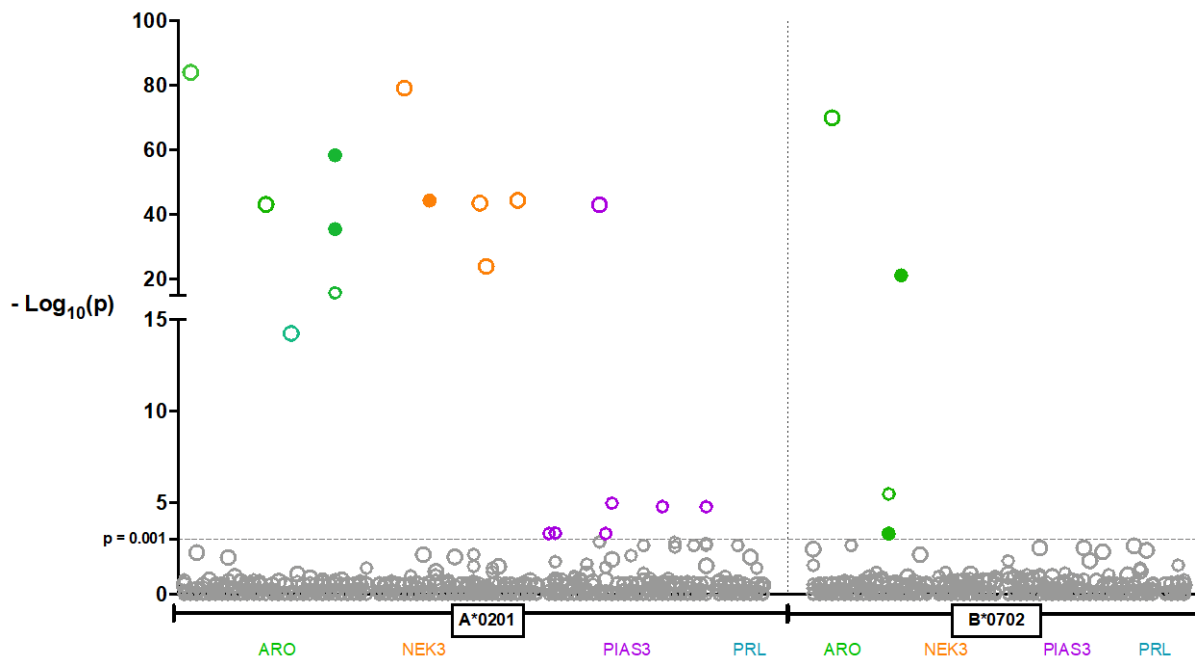
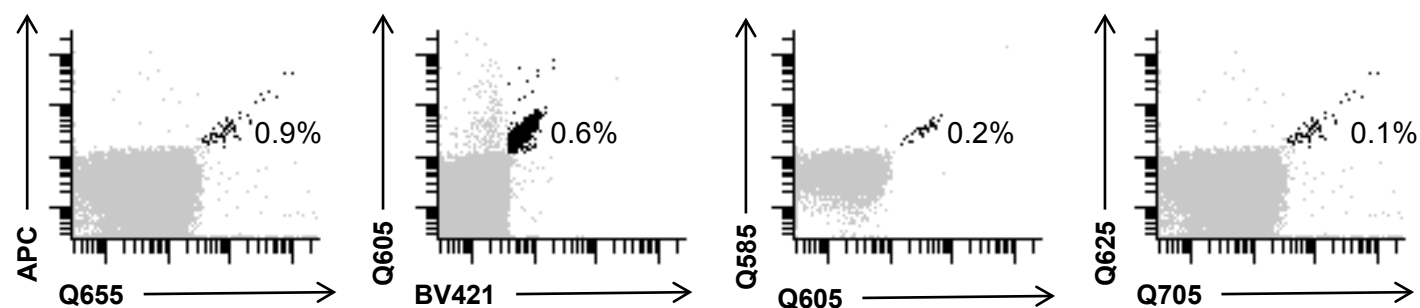


C



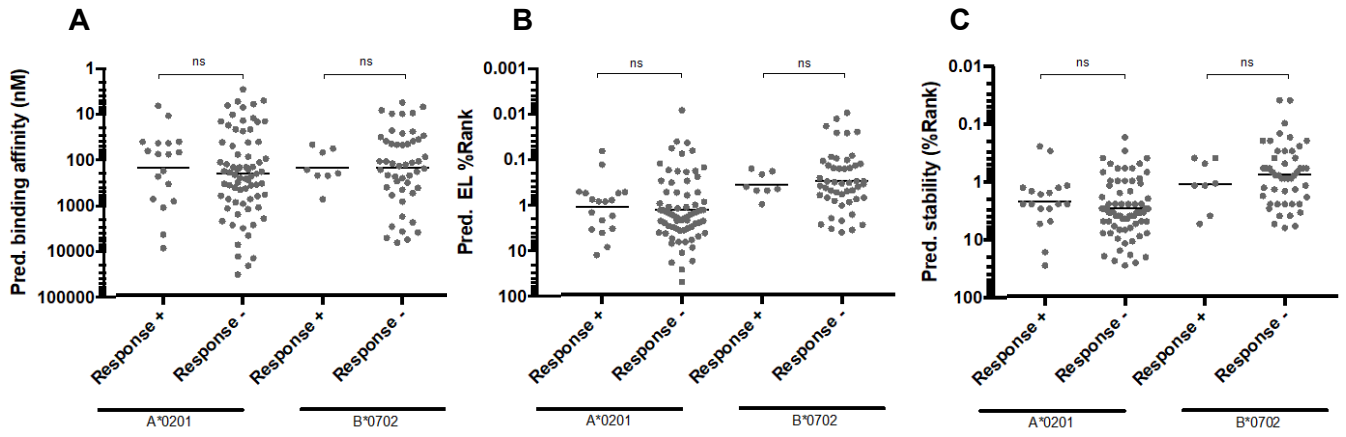
A**Supplementary Figure S2.****Similarities in predicted MHC binding affinity from different versions of NetMHC.**

Correlation of binding affinity estimated with NetMHC 3.0, which was used for the original *in silico* selection of predicted binders to HLA-A*0201 and -B*0702 and state-of-the-art NetMHCpan 4.0. Green dots represent peptides that passed the *in vitro* MHC-ELISA and were included in the T cell screening library. Gray dots represent peptides that did not qualify for T cell screening based on MHC-ELISA results. Dotted lines represent conventional cut-off criteria for intermediate affinity MHC binders (<1000 nM). Peptides with predicted affinities >1000 nM were included based on SYFPEITHI prediction values instead of NetMHC. Pearson correlation coefficient calculated on log transformed data ($p < 0.0001$).

A**B****Supplementary Figure S3.****Specific expansion of TAA T cell responses.**

A, T cell responses to potential breast cancer TAAs detected in samples after pMHC based MACS enrichment of 17 breast cancer patient samples from Patient cohort 1. The left side, T cell responses to HLA-A*0201 restricted peptides (90 breast cancer derived peptides). Right side, T cell responses to HLA-B*0702 restricted peptides (57 breast cancer derived peptides). Colored circles represent T cell responses to aromatase (green), NEK3 (orange), PIAS3 (purple), and prolactin (turquoise) derived peptides. The horizontal dotted line represents the detection limit ($p = 0.001/\text{FDR} = 0.1$) determining a T cell responses and all dots below are not considered as T cell responses. All points lying on the same vertical axis implies multiple T cell responses to the same peptide across several donors. Filled circles represent specific T cell responses found in a given breast cancer patient sample directly *ex vivo* and verified after pMHC based enrichment.

B, Enrichment of pMHC multimer specific T cells after MACS sorting in breast cancer patients from Patient cohort 2. From left to right: A*0201 ARO9(305) specific T cells in patient P2.5, A*0201 AR010(304) specific T cells in patient P2.5, A*0201 NEK10(418) specific T cells in patient P2.8 and B*0702 PIAS9(85) specific T cells in patient P2.12. Frequencies of pMHC multimer specific T cells out of total CD3+CD8+ TILs are displayed.



Supplementary Figure S4.

T cell recognition cannot be explained by predicted MHC binding affinity or stability of peptides.

Comparison of peptides for which a T cell response was detected (Response +) vs. not detected (Response -), in terms of predicted MHC binding affinity, using NetMHCpan 4.0 (A) and %EL Rank (B), and pMHC stability %Rank using NetMHCstabpan 1.0 (C). Asterisks indicate significance levels, unpaired parametric T test on log transformed values.

Supplementary Materials and Methods

Endogenous peptide presentation on tumor cell lines

Cells

The breast cancer cell lines, BT-549, MDA-MB-231 and EF192A, used for mass spectrometry analyses, expressed the following HLA class I alleles; BT-549: A*01:01, A*02:01, B*15:17, B*56, C*03:03 and C*07:01; EFM-192A: A*01:01, A*24:02, B*07:02, B*39:01, C*07:02 and C*12:03; MDA-MB-231: A*02:01, A*02:17, B*40:02, B*41:01, C*0202, C*17:01 (1). All cells were cultured in R10 medium + 1% P/S. For harvesting, cells were washed in PBS for 5 min, loosened with 0.25% trypsin-EDTA (Gibco, Cat#25200056) for maximum 15 min at 37°C, resuspended in R10 and washed three times in PBS. They were then incubated for 1 h on ice in lysis buffer (0.5% IGEPAL CA-630 (Sigma-Aldrich, Cat#I8896), 0.25% sodium deoxycholate (Sigma-Aldrich, Cat#D6750), 1 mM EDTA (ethylenediaminetetraacetic acid, Sigma-Aldrich, Cat#798681) 0.2 mM iodoacetamide (Sigma-Aldrich, Cat#I6125), 1 mM PMSF (phenylmethanesulfonyl fluoride, Sigma-Aldrich, Cat#P7626), Roche Complete Protease Inhibitor Cocktail (Sigma-Aldrich, Cat# 11697498001) in PBS). Lysates were cleared by centrifugation at 21,000 g for 30 min at 4°C and stored at -80°C.

MHC-IAC and desalting

We used the W6/32 monoclonal antibody (2) to purify peptide-HLA-A, -B, and -C complexes. W6/32 was purified from HB-95 hybridoma supernatant using Protein-A sepharose, and it was coupled to AminoLink Plus Coupling Resin (Thermo Scientific) following the manufacturer's instructions. The supernatant of the cell lysate was slowly rotated with the W6/32 resin for 2 h at 4 °C. The resin was washed at 4 °C with lysis buffer, followed by buffer A (150 mM NaCl, 20 mM Tris, pH 7.5), buffer B (400 mM NaCl, 20 mM Tris, pH 7.5), a second buffer A treatment and was finally washed with buffer C (20 mM Tris, pH 8.0). Peptide-MHC complexes were eluted with 0.1 M acetic acid.

Peptides were desalted and separated from MHC proteins using C₁₈ Macro SpinColumns (Harvard Apparatus) prewashed with 50% acetonitrile. We equilibrated and washed the C₁₈ columns with 0.1% TFA and eluted using 30% acetonitrile / 0.1% TFA followed by vacuum-centrifugation.

LC-MS measurements

The fully dried samples were solved in 11 µl 3% CH₃CN / 0.1% HCOOH, and 7 µl thereof were injected into the LC-MS system. The Q Exactive was coupled online to an EASY-nLC 1000 (both Thermo Scientific) via a nanoelectrospray ion source (Nanospray Flex, Proxeon). Peptides were loaded at 800 bar and then separated at a flow rate of 300 nl/min on a 15 cm x 50 µm column with C₁₈ beads of 2 µm

44 diameter (Acclaim PepMap RSLC, Thermo Scientific). The linear gradient of 120 min
45 ranged from 0% to 30% CH₃CN in 0.1% HCOOH. MS1 scans were acquired at a
46 resolution of 70,000 at 200 Th. The measured MS1 *m/z* range was 250 Th - 2000
47 Th, and only 2+ and 3+ charged precursors were allowed for fragmentation. The ten
48 most abundant precursors from every MS1 scan were selected for higher-energy
49 collisional dissociation (HCD) using an isolation width of 2 Th, and they were then
50 dynamically excluded from repeated fragmentation for 15 s. We applied a normalized
51 collision energy of 27%, and we recorded MS2 spectra at a resolution of 17,500 at
52 200 Th. Automatic Gain Control targets were 3,000,000 ions to be reached in
53 maximal 80 ms for MS1 and 100,000 ions to be reached in maximal 240 ms for MS2.
54

55 **LC-MS data analysis**

56 MS data were processed with Proteome Discoverer 1.4.1.14 from Thermo Fisher.
57 We utilized Sequest (3) HT for searching the LC-MS data allowing an MS1 mass
58 error of 10 ppm and an MS2 mass error of 0.02 Da. Oxidation of methionine and
59 cysteinylolation of cysteine were set as variable modifications. The target protein
60 database contained the human reference proteome downloaded from
61 www.uniprot.org on 7 July 2017 (93,563 proteins). Our peptide spectral match false
62 discovery rate (PSM FDR) cut-off of ≤5% was calculated by Percolator (4) using the
63 reversed target protein sequences as a decoy database. The MS2 spectra of the
64 four identified peptides from PIAS3 were manually checked taking alternative peptide
65 suggestions from Proteome Discoverer into account. The putative HLA-A*02:01
66 ligand SIVAPGGAL was additionally validated by acquiring the MS2 spectrum of its
67 synthetic form (see Supplementary Figure S1). Peptides differing only in the
68 modification status of methionine or cysteine were considered as equal for peptide
69 counting.

70

- 71 1. Boegel S, Löwer M, Bukur T, Sahin U, Castle JC. A catalog of HLA type, HLA
72 expression, and neoepitope candidates in human cancer cell lines. *Oncoimmunology*.
73 2014;3:1–12.
- 74 2. Barnstable CJ, Bodmer WF, Brown G, Galfre G, Milstein C, Williams AF, et al.
75 Production of monoclonal antibodies to group A erythrocytes, HLA and other human
76 cell surface antigens-new tools for genetic analysis. *Cell*. 1978;14:1–20.
- 77 3. Eng JK, McCormack AL, Yates JR. An Approach to Correlate Tandem Mass Spectral
78 Data of Peptides with Amino Acid Sequences in a Protein Database. *Am Soc Mass*
79 *Spectrometry*. 1994;5:976–89.
- 80 4. Käll L, Canterbury JD, Weston J, Noble WS, MacCoss MJ. Semi-supervised learning
81 for peptide identification from shotgun proteomics datasets. *Nat Methods*.
82 2007;4:923–5.

83

Supplementary Tables

Supplementary Table S1. Patient and healthy donor characteristics.

Cohort	Patient/healthy donor ID	Age	HLA-A*0201, B*0702 type	Molecular subtype	Disease stage	Treatment ^d (+)
P1 (Patient cohort 1)	P1.1	71	A*0201 (+), B*0702 (+) ^a	HER2 enriched	1	
	P1.2	61	A*0201 (-), B*0702 (-) ^a	HER2 enriched	2	
	P1.3	40	A*0201 (+), B*0702 (-) ^a	Luminal B	2	
	P1.4	71	A*0201 (-), B*0702 (+) ^a	Luminal A	2	
	P1.5	45	A*0201 (+), B*0702 (-) ^a	Luminal A	1	
	P1.6	65	A*0201 (-), B*0702 (+) ^a	Luminal A	1	
	P1.7	43	A*0201 (+), B*0702 (+) ^b	Luminal A	2	
	P1.8	84	A*0201 (+), B*0702 (+) ^a	Luminal A	3	
	P1.9	53	A*0201 (+), B*0702 (+) ^a	Luminal B	2	
	P1.10	39	A*0201 (+), B*0702 (+) ^a	Luminal A	3	
	P1.11	53	A*0201 (+), B*0702 (+) ^a	Luminal B	2	
	P1.12	71	A*0201 (+), B*0702 (-) ^b	Luminal A	2	
	P1.13	56	A*0201 (+), B*0702 (-) ^a	Luminal A	3	
	P1.14	58	A*0201 (+), B*0702 (+) ^a	Luminal A	NA	
	P1.15	49	A*0201 (+), B*0702 (+) ^a	Triple negative	2	
	P1.16	55	A*0201 (+), B*0702 (+) ^a	Luminal A	NA	
	P1.17	72	A*0201 (+), B*0702 (+) ^a	Luminal A	2	
	P1.18	51	A*0201 (-), B*0702 (+) ^b	Luminal A	1	
	P1.19	50	A*0201 (+), B*0702 (+) ^b	Luminal B	NA	
	P1.20	70	A*0201 (-), B*0702 (+) ^a	Triple negative	3	
	P1.21	65	A*0201 (+), B*0702 (+) ^a	HER2 enriched	NA	
	P1.22	86	A*0201 (+), B*0702 (-) ^b	Luminal A	2	
	P1.23	58	A*0201 (+), B*0702 (+) ^b	Luminal A	2	
	P1.24	75	A*0201 (+), B*0702 (+) ^a	Luminal A	NA	
	P1.25	69	A*0201 (+), B*0702 (-) ^b	Luminal B	2	
HD 1 (Healthy Donor cohort 1)	HD1.1		A*0201 (+), B*0702 (-) ^b			
	HD1.2		A*0201 (+), B*0702 (-) ^b			
	HD1.3		A*0201 (+), B*0702 (-) ^b			
	HD1.4		A*0201 (+), B*0702 (-) ^b			
	HD1.5		A*0201 (+), B*0702 (-) ^b			
	HD1.6		A*0201 (+), B*0702 (-) ^b			
	HD1.7		A*0201 (+), B*0702 (-) ^b			
	HD1.8		A*0201 (-), B*0702 (+) ^b			
	HD1.9		A*0201 (+), B*0702 (-) ^b			
	HD1.10		A*0201 (-), B*0702 (+) ^b			
	HD1.11		A*0201 (+), B*0702 (+) ^b			
	HD1.12		A*0201 (+), B*0702 (-) ^b			
	HD1.13		A*0201 (+), B*0702 (+) ^b			
	HD1.14		A*0201 (+), B*0702 (-) ^b			
	HD1.15		A*0201 (+), B*0702 (+) ^b			
	HD1.16		A*0201 (+), B*0702 (+) ^b			
	HD1.17		A*0201 (-), B*0702 (+) ^b			
P2 (Patient cohort 2)	P2.1	62	A*0201 (+), B*0702 (-) ^c			+
	P2.2	51	A*0201 (+), B*0702 (-) ^c			+
	P2.3	61	A*0201 (+), B*0702 (+) ^c			+
	P2.4	47	A*0201 (+), B*0702 (+) ^c			+
	P2.5	46	A*0201 (+), B*0702 (-) ^c			+
	P2.6	44	A*0201 (+), B*0702 (+) ^c			+
	P2.7	N/A	A*0201 (+), B*0702 (+) ^c			+
	P2.8	64	A*0201 (+), B*0702 (+) ^c			+
	P2.9	32	A*0201 (+), B*0702 (+) ^c			+
	P2.10	58	A*0201 (+), B*0702 (+) ^c			+
	P2.11	58	A*0201 (+), B*0702 (+) ^c			+
	P2.12	56	A*0201 (+), B*0702 (+) ^c			+
	P2.13	65	A*0201 (+), B*0702 (+) ^c			+
	P2.14	62	A*0201 (+), B*0702 (-) ^{c,a}			+
	P2.15	59	A*0201 (+), B*0702 (-) ^{c,a}			+
P2.16	51	A*0201 (+), B*0702 (-) ^{c,a}			+	

	P2.17	65	A*0201 (+), B*0702 (-) ^{c,a}
	P2.18	56	A*0201 (+), B*0702 (-) ^{c,a}
HD2 (Healthy Donor cohort 2)	HD2.1		A*0201 (-), B*0702 (+) ^c
	HD2.2		A*0201 (+), B*0702 (+) ^c
	HD2.3		A*0201 (+), B*0702 (+) ^c
	HD2.4		A*0201 (-), B*0702 (+) ^c
	HD2.5		A*0201 (-), B*0702 (+) ^c
	HD2.6		A*0201 (-), B*0702 (+) ^c
	HD2.7		A*0201 (+), B*0702 (+) ^c
	HD2.8		A*0201 (+), B*0702 (+) ^c
	HD2.9		A*0201 (+), B*0702 (-) ^c
	HD2.10		A*0201 (+), B*0702 (-) ^c
	HD2.11		A*0201 (+), B*0702 (-) ^c
HD2.12		A*0201 (+), B*0702 (-) ^c	
HD2.13		A*0201 (+), B*0702 (-) ^c	

^aHLA type determined by flow cytometry.

^bHLA type determined by sequencing.

^cHLA type determined by PCR.

^dPrior treatments included chemo-, radiation and endocrine therapy. No patients were treated with immunotherapy.

NA: disease stage classification not possible due to lack of information.

Supplementary Table S2. Total list of all investigated possible TAA peptides from all four proteins.

Peptide IDs were given according to the protein of origin, 9-/10-mer and position of 1st amino acid. Peptides predicted to bind to both HLA-A*0201 and –B*0702 are shown in italics. Peptides selected for T cell screens are shown in bold.

HLA	Protein	Peptide ID	Sequence	SYFPEITHI ^a (score)	Net MHC 3.0 ^b (nM)	NetMHCpan 4.0 (nM)	NetMHCpan 4.0 (rank score)	NetMHCstabpan 1.0 (rank score)	MHC ELISA (rank score)	Response ^c (+ (P1/P2))
A*0201	CMV pp65	CMV (NLV)	NLVPVMVATV	30	N/A	26	0	0	3	
	Aromatase	ARO9(65)	FLWMGIGSA	24	36	12	0	0	4	
		ARO9(320)	FLIAKHPNV	25	6	3	0	0	5	
		ARO10(275)	CMDFATELIL	18	338	346	8	8	14	
		ARO9(331)	AIIKEIQTV	28	96	47	0	0	25	
		ARO9(12)	NITSIVPEA	18	281	2396	2	2	26	
		ARO9(194)	VMLDTSNTL	25	35	46	0	0	27	
		ARO9(52)	YCMGIGPLI	14	947	688	2	2	29	
		ARO9(299)	CILEMLIAA	21	193	96	3	3	29	
		ARO10(330)	EAIKEIQTV	19	22232	3418	4	4	30	
		ARO9(20)	AMPAATMPV	22	6	16	1	1	31	
		ARO10(304)	LIAAPDTMSV	24	112	254	1	1	35	+ (P2)
		ARO9(271)	KLEECMDFA	16	32	363	3	3	40	
		ARO9(5)	MLNPIHYN	22	17	6	0	0	47	
		ARO9(79)	RVYGEFMRV	17	114	24	0	0	48	
		ARO9(275)	CMDFATELI	17	105	209	3	3	49	
		ARO10(299)	CILEMLIAAP	19	16846	4650	31	31	53	+ (P1)
		ARO10(443)	AMVMMKAILV	20	102	107	3	3	54	+ (P2)
		ARO9(232)	DIFFKISWL	22	15880	9224	11	11	55	+ (P1, P2)
		ARO9(30)	LLTGLFLLV	25	30	17	1	1	56	+ (P1)
		ARO9(445)	VMMKAILVT	19	58	127	1	1	59	+ (P2)
		ARO9(437)	CAGKYIAMV	21	1270	2939	11	11	65	
		ARO9(167)	SLKTHLDRL	25	1522	1710	2	2	66	
		ARO9(444)	MVMMKAILV	16	60	49	1	1	68	+ (P1)
		ARO9(305)	IAAPDTMSV	24	475	470	1	1	69	+ (P2)
		ARO9(441)	YIAMVMMKA	18	153	236	1	1	71	
		ARO9(132)	IIFNNNP	24	86	84	0	0	72	+ (P1)
		ARO10(413)	FTLENFAKNV	18	196	56	2	2	73	
		ARO10(331)	AIIKEIQTVI	20	776	2908	3	3	77	
		ARO9(310)	TMSVSLFFM	16	32	86	3	3	79	
		ARO10(346)	KIDDIQKLK	23	236	800	1	1	82	
		ARO10(35)	FLLVWNYEGT	18	20	54	4	4	84	
		ARO10(436)	GCAGKYIAMV	21	6508	8217	12	12	87	
		ARO10(295)	NVNQCILEML	19	1519	5697	14	14	89	
		ARO10(250)	DLKDAIEVLI	19	12004	8449	7	7	95	
		ARO10(228)	LIKPDIFFKI	21	674	822	5	5	96	
		ARO10(195)	MLDTSNTLFL	21	7	37	1	1	98	
		ARO10(169)	KTHLDRLEEV	21	1758	1198	3	3	101	
		ARO9(352)	KLKVMENFI	19	3593	1354	3	3	102	
		ARO9(250)	DLKDAIEVL	23	14612	13035	5	5	109	
		ARO10(373)	VMRKALEDDV	19	3172	8417	15	15	117	
		ARO10(257)	VLIAEKRRRI	21	5779	17998	13	13	129	
		ARO9(258)	LIAEKRRRI	23	15951	20985	14	14	133	
		ARO10(306)	AAPDTMSVSL	21	4580	13776	10	10	134	
		ARO9(29)	LLLTGLFLL	30	7	6	0	0	135	
		ARO10(148)	FMKALSGPGL	20	164	155	2	2	138	
		ARO9(220)	YFDAWQALL	14	457	187	1	1	139	
		ARO10(156)	GLVRMVTVCA	17	521	1915	9	9	144	
		ARO10(203)	FLRIPLDESA	17	848	199	1	1	145	
		ARO10(159)	RMVTVCAESL	20	94	326	4	4	147	
		ARO10(470)	SIQKIHDL	23	1427	6268	6	6	148	
		ARO10(344)	DIKIDDIQKL	22	42273	27112	12	12	150	
		ARO10(151)	ALSGPGLVRM	24	1077	984	1	1	153	
		ARO10(354)	KVMENFIYES	15	305	604	6	6	156	
		ARO9(24)	ATMPVLLLT	18	569	594	2	2	160	
		ARO9(283)	ILAEKRGDL	27	9140	6741	5	5	166	
		ARO10(187)	VLTLRRVML	22	6701	1737	10	10	170	
		ARO10(20)	AMPAATMPVL	21	42	285	3	3	172	
		ARO9(36)	LLVWNYEGT	17	791	1604	7	7	175	

	ARO9(150)	KALSGPGLV	19	3616	4206	5	5	177	
	ARO10(355)	VMENFIYESM	14	418	941	6	6	182	
	ARO10(442)	IAMVMMKAIL	19	6257	3091	19	19	184	
	ARO9(28)	VLLLTGLFL	24	285	155	1	1	188	
	ARO9(443)	AMVMMKAIL	22	1166	1245	4	4	198	
	ARO10(25)	TMPVLLLTGL	23	261	474	7	7	201	
	ARO9(303)	MLIAAPDTM	18	182	209	1	1	203	
	ARO10(283)	ILAEKRGDLT	20	7703	11960	11	11	208	
	ARO10(205)	RIPLDESAIV	20	3859	1006	2	2	209	
	ARO9(58)	PLISHGRFL	19	17500	12429	8	8	211	
	ARO9(332)	IIEKIQTVI	19	6366	5685	3	3	214	
	ARO9(23)	AATMPVLLL	21	10302	8692	7	7	218	
	ARO9(446)	MMKAILVTL	25	52	36	1	1	219	
	ARO10(446)	MMKAILVTL	21	72	78	4	4	223	
	ARO9(188)	LTLRRVML	20	12623	10599	14	14	224	
	ARO9(186)	DVLTLLRRV	20	14321	11734	9	9	226	
	ARO9(182)	SGYVDVLT	20	10396	11249	6	6	230	
	ARO9(35)	FLLVWNYEG	16	320	83	3	3	231	
	ARO9(170)	THLDRLEEV	19	11002	15724	11	11	232	
	ARO10(462)	TLQGQCVESI	26	172	856	4	4	234	
	ARO9(414)	TLENFAKNV	19	5794	2336	2	2	235	
	ARO9(339)	VIGERDIKI	21	2562	5586	3	3	236	
	ARO10(441)	YIAMVMMKAI	20	359	440	7	7	237	
	ARO10(395)	ILNIGRMHRL	24	932	787	2	2	238	
	ARO9(345)	IKIDDIQKL	21	16405	24301	8	8	239	
	ARO10(445)	VMMKAILVTL	28	7	32	1	1	242	
	ARO9(207)	PLDESAIVV	19	3812	1715	1	1	243	
	ARO10(363)	SMRYQPVVDL	25	3481	1328	2	2	245	
	ARO9(95)	LIISKSSM	19	3537	7434	8	8	246	
	ARO10(29)	LLLTGLFLLV	25	8	11	1	1	247	
	ARO9(153)	SGPGLVRMV	19	28324	20957	14	14	248	
	ARO10(239)	WLYKKEYKSV	22	129	304	4	4	249	
	ARO9(313)	VSLFFMLFL	14	937	2632	12	12	250	
	ARO10(88)	WISGEETLII	19	2070	4923	11	11	251	
	ARO10(282)	LILAEKRGDL	22	17787	19054	24	24	252	
	ARO10(454)	LLRRFHVKTL	27	5358	4168	15	15	254	
	ARO9(311)	MSVSLFFML	11	926	352	6	6	255	
	ARO10(131)	GIIFNNPEL	23	752	2044	2	2	256	
	ARO9(454)	LLRRFHVKTL	21	16441	10164	13	13	257	
	ARO10(453)	TLLRRFHVKTL	20	3324	5895	14	14	258	
	ARO10(178)	VTNESGYVDV	20	4496	10738	11	11	259	
	ARO9(317)	FMLFLIAKH	19	8354	12450	20	20	260	
	ARO10(4)	EMLNPIHYNI	16	906	177	3	3	261	
	ARO9(314)	SLFFMLFLI	24	17	18	1	1	261	
	ARO9(300)	ILEMLIAAP	19	25105	5320	9	9	262	
	ARO10(271)	KLEECMDFAT	17	372	1293	7	7	263	
	ARO10(5)	MLNPIHYNIT	18	906	418	4	4	264	
	ARO10(28)	VLLLTGLFLL	27	75	25	1	1	265	
	ARO10(310)	TMSVSLFFML	18	32	63	5	5	267	
	ARO10(312)	SVSLFFMLFL	17	656	702	9	9	268	
	ARO10(314)	SLFFMLFLIA	17	116	97	5	5	269	
NEK3	NEK9(226)	YSYELQLV	16	14	8	0	0	1	+ (P1)
	NEK10(104)	ILNWFTQMCL	23	55	46	3	3	2	+ (P1)
	NEK9(151)	LLSNPMAFA	19	121	47	1	1	7	
	NEK10(407)	WLKETPDLLL	21	2625	1003	2	2	8	
	NEK9(97)	KLFPEDMIL	24	39	27	0	0	8	
	NEK9(425)	SLAFQTYTI	26	63	16	0	0	9	
	NEK9(414)	TLLNILKNA	19	424	198	1	1	10	+ (P1)
	NEK10(160)	CTYVGTPYYV	16	97	373	7	7	12	
	NEK9(187)	SLGCILYEL	29	22	8	0	0	15	+ (P1)
	NEK9(301)	ALGNEASTV	24	469	288	0	0	17	
	NEK9(269)	IIMEYGEEV	26	12	6	0	0	19	
	NEK10(142)	KLGDFGSARL	24	55	258	1	1	20	+ (P1)

	NEK10(150)	RLLSNPMAFA	18	58	140	1	1	23	
	NEK9(90)	KIKQQKGKL	20	41685	34481	25	25	36	
	NEK10(186)	WSLGCILYEL	21	555	72	6	6	37	+ (P1)
	NEK10(53)	LLAKMKHPNI	23	274	1217	7	7	39	+ (P1)
	NEK10(213)	KVCQGCISPL	19	2155	1274	12	12	43	
	NEK10(28)	QMFAMKEIRL	19	149	194	3	3	44	+ (P1)
	NEK9(103)	MILNWFQTM	14	100	163	3	3	44	+ (P2)
	NEK9(155)	PMAFACTYV	16	517	278	6	6	57	+ (P1)
	NEK10(329)	NLVESALRRV	26	450	884	2	2	58	+ (P1)
	NEK10(418)	ILKNADLSLA	19	3055	1205	4	4	63	+ (P2)
	NEK10(221)	PLPSHYSYEL	20	4539	7824	15	15	67	
	NEK10(371)	ALTALENASI	23	225	679	3	3	70	
	NEK10(268)	EIIMEYGEEV	19	5960	400	3	3	76	
	NEK9(190)	CILYELCTL	25	1165	798	10	10	81	+ (P1,P2)
	NEK10(366)	NVPNTALTAL	19	9006	13190	13	13	93	
	NEK9(110)	QMCLGVNHI	23	8659	1346	4	4	94	
	NEK9(270)	IMEYGEEVL	20	2713	847	2	2	100	
	NEK10(134)	FLTQNGKVKL	24	309	601	1	1	107	
	NEK10(269)	IIMEYGEEVL	23	111	462	1	1	108	
	NEK10(325)	SINENLVESA	23	465	2824	3	3	111	
	NEK10(260)	LVQKCLPPEI	17	576	2304	16	16	114	
	NEK10(69)	FEAEGHLYIV	20	1596	2386	6	6	114	
	NEK9(418)	ILKNADLSL	24	669	430	1	1	116	
	NEK10(189)	GCILYELCTL	19	17640	1698	11	11	120	
	NEK9(250)	TLLSRGIVA	16	619	1185	1	1	122	
	NEK10(300)	IALGNEASTV	22	4313	1467	2	2	124	
	NEK9(211)	ILKVCQGCI	19	10329	3904	2	2	125	
	NEK9(379)	SILTSSLTA	19	740	1972	4	4	136	
	NEK9(377)	NASILTSSL	19	11707	16784	17	17	142	
	NEK10(168)	YVPEIWENL	18	300	456	1	1	143	
	NEK9(407)	WLKETPDTL	23	3069	318	0	0	145	
	NEK9(455)	SVDGGHDSV	22	2473	1595	1	1	152	
	NEK10(417)	NILKNADLSL	23	1468	4278	6	6	154	
	NEK10(415)	LLNILKNADL	25	2379	1653	9	9	159	
	NEK9(135)	LTQNGKVKL	22	19777	21714	12	12	164	
	NEK10(132)	NIFLTQNGKV	21	3874	1975	8	8	165	
	NEK9(372)	LTALENASI	20	3270	5993	7	7	169	
	NEK9(206)	SWKNLILKV	19	28235	22990	13	13	176	
	NEK9(325)	SINENLVES	21	7128	7182	5	5	179	
	NEK10(250)	TLLSRGIVAR	19	23113	15255	13	13	180	
	NEK10(251)	LLSRGIVARL	28	92	160	1	1	186	
	NEK10(210)	LILKVCQGCI	20	1951	3366	27	27	187	
	NEK9(252)	LSRGIVARL	20	19628	19707	14	14	191	
	NEK10(349)	HLRKASSPNL	21	4663	8660	9	9	196	
	NEK9(330)	LVESALRRV	19	7626	12072	10	10	199	
	NEK10(179)	YNNKSDIWSL	19	10130	17082	20	20	201	
	NEK9(251)	LLSRGIVAR	21	24993	16822	13	13	204	
	NEK9(184)	DIWSLGCIL	19	14064	8795	14	14	207	
	NEK10(322)	DLESINENLV	19	15053	17498	13	13	227	
	NEK9(441)	FLKGPLSEE	19	27751	8179	7	7	231	
	NEK10(205)	NSWKNLILKV	18	570	1596	7	7	240	
	NEK9(469)	RLEPGLDEE	19	32961	25608	16	16	244	
PIAS3	PIAS9(15)	RVSELQVLL	19	456	203	0	0	13	
	PIAS10(106)	LLGPKREVDM	20	9971	14031	12	12	16	+ (P1)
	PIAS9(345)	HLQSFDAAL	24	177	128	0	0	18	
	PIAS9(79)	SLPPGTSPV	28	23	24	0	0	22	+ (P1, P2)
	PIAS10(160)	FTFALTPQQV	16	33	77	2	2	28	+ (P1)
	PIAS9(569)	FLGPLAPTL	27	15	7	0	0	32	
	PIAS9(249)	RLSATVPNT	19	426	937	2	2	33	
	PIAS9(347)	QSFDAALYL	13	820	1315	2	2	34	
	PIAS10(494)	VLRSPAMGTL	23	6956	2095	4	4	41	
	PIAS10(44)	LLKSSCAPSV	24	123	84	4	4	42	+ (P1)
	PIAS10(346)	LQSFDAALYL	12	862	174	2	2	44	+ (P2)

PIAS9(37)	LLAKALHLL	29	19	14	0	0	45	
PIAS10(378)	LIIDGLFMEI	23	22	20	1	1	46	+ (P1, P2)
PIAS10(275)	YLVRQLTAGT	19	158	796	6	6	50	
PIAS10(616)	SLTGCRSDII	21	1762	4925	14	14	51	
PIAS9(76)	SLLSLPPGT	21	225	303	1	1	52	
PIAS10(424)	GLDGLQYSPV	23	39	49	0	0	60	+ (P1)
PIAS9(69)	TLGSPDLSL	25	156	390	0	0	61	
PIAS9(214)	KVNGKLCPL	23	1948	501	4	4	62	
PIAS10(477)	ALPGSKGVL	20	10588	15292	10	10	64	
PIAS10(249)	RLSATVPNTI	21	227	373	1	1	70	+ (P1)
PIAS10(325)	LMCPLGKMRL	22	2642	638	5	5	74	
PIAS9(218)	KLCPLPGYL	24	917	180	1	1	75	+ (P2)
PIAS10(36)	ELLAKALHLL	24	1206	400	4	4	78	
PIAS10(520)	FPLGADIQGL	20	17854	163	1	1	80	
PIAS10(241)	PINITPLARL	22	30290	22157	20	20	83	
PIAS10(399)	FMEDGSWCPM	13	95	28	1	1	90	
PIAS9(246)	PLARLSATV	24	3494	1769	3	3	91	
PIAS10(379)	IIDGLFMEIL	22	614	441	3	3	92	
PIAS10(510)	SLPLHEYPPA	17	954	444	4	4	97	
PIAS9(11)	VMSFRVSEL	24	76	324	1	1	99	
PIAS10(280)	LTAGTLLQKL	26	2760	4589	11	11	103	
PIAS10(485)	LTSGHQSSV	20	1715	11953	14	14	104	
PIAS10(163)	ALTPQQVQI	25	475	2737	2	2	105	
PIAS9(379)	IIDGLFMEI	23	215	51	0	0	106	
PIAS10(502)	TLGGDFLSSL	28	112	222	1	1	110	
PIAS10(10)	MVMSFRVSEL	21	47	115	4	4	112	
PIAS9(470)	VTSAAIPAL	21	261	1760	2	2	115	
PIAS9(503)	LGGDFLSSL	20	14557	14771	13	13	118	
PIAS10(141)	LIRPTTLAST	24	12565	14132	25	25	119	
PIAS10(469)	SVTSAIPAL	21	622	3343	5	5	122	
PIAS10(68)	KTLGSPDLSL	22	1380	1397	2	2	122	
PIAS10(69)	TLGSPDLSLL	26	214	780	2	2	128	
PIAS10(128)	TMKPLPFYEV	22	217	102	2	2	132	
PIAS10(271)	SLSVYLVRQL	26	218	228	3	3	137	
PIAS10(210)	NLFVKVNGKL	23	1820	2799	5	5	138	
PIAS10(499)	AMGTGGDFL	20	1201	2744	6	6	140	
PIAS9(317)	ATTSLRVSL	20	8881	9184	7	7	141	
PIAS9(302)	ALIKEKLT	21	1344	1482	1	1	145	
PIAS10(114)	DMHPPLPQPV	19	8361	4011	6	6	146	
PIAS10(602)	ALREGHGGPL	24	7768	8818	8	8	149	
PIAS9(99)	TLLAPGTL	23	286	303	0	0	151	
PIAS9(382)	GLFMEILSS	19	1293	472	1	1	155	
PIAS10(320)	SLRVSLMCPL	22	881	168	8	8	157	
PIAS10(92)	PLAPIPPTL	21	3102	3012	2	2	158	
PIAS9(308)	LTADPDSEV	22	2420	3065	3	3	161	
PIAS10(100)	LLAPGTLLGP	22	4438	3607	8	8	162	
PIAS9(105)	TLLGPKREV	27	3305	1684	1	1	163	
PIAS9(36)	ELLAKALHL	21	4415	1886	2	2	168	
PIAS9(92)	PLAPIPPTL	24	1184	428	0	0	174	
PIAS9(271)	SLSVYLVRQ	19	2568	16547	14	14	178	
PIAS9(377)	SLIIDGLFM	19	445	656	1	1	183	
PIAS10(285)	LLQKLRAKGI	20	4842	5464	17	17	185	
PIAS9(252)	ATVPNTIVV	20	1288	1337	1	1	189	
PIAS10(71)	GPSDLSLLSL	19	29812	15935	18	18	190	
PIAS9(281)	TAGTLLQKL	21	17299	25742	19	19	191	
PIAS9(52)	SVQMKIKEL	22	10607	12782	6	6	197	
PIAS9(328)	PLGKMRLTV	20	14160	9775	7	7	202	
PIAS9(3)	ELGELKHMV	21	4615	2117	2	2	205	
PIAS9(225)	YLPPTKNGA	20	1467	1883	1	1	206	
PIAS9(521)	PLGADIQGL	22	8005	11052	6	6	209	
PIAS9(477)	ALPGSKGVL	24	16369	14417	8	8	210	
PIAS9(191)	QLRFCLCET	19	6295	3477	25	25	212	
PIAS9(242)	INITPLARL	21	32345	20528	14	14	213	

		PIAS9(616)	SLTGCRSDI	21	6679	7393	11	11	215	
		PIAS10(564)	GTPSHFLGPL	19	7685	5872	17	17	216	
		PIAS10(104)	GTLLGPKREV	19	14432	6853	3	3	217	
		PIAS10(307)	KLTADPDSEV	22	95	316	1	1	217	
		PIAS9(100)	LLAPGTLG	21	3849	3770	4	4	219	
		PIAS9(378)	LIIDGLFME	19	7116	6386	8	8	220	
		PIAS9(221)	PLPGYLPPT	19	4671	2946	7	7	221	
		PIAS9(324)	SLMCPGKGM	24	1955	327	2	2	222	
		PIAS9(595)	SIVAPGGAL	22	22029	6582	4	4	225	
		PIAS9(171)	QILTSREVL	20	9599	14816	12	12	228	
		PIAS10(302)	ALIKEKLTAD	19	27274	19428	13	13	233	
		PIAS9(333)	RLTVPCRAL	21	12349	2988	5	5	253	
Prolactin		PRL9(52)	VLSHYIHNL	27	10	12	0	0	6	+ (P1)
		PRL9(122)	PLYHLVTEV	25	325	163	0	0	11	
		PRL9(153)	RLLEGMELI	24	13	7	0	0	16	
		PRL10(153)	RLLEGMELIV	25	19	16	0	0	21	
		PRL9(132)	GMQEAPAI	20	146	160	0	0	22	
		PRL9(139)	AILSKAIVEI	25	408	455	1	1	24	
		PRL9(192)	RLSAYYNLL	22	32	45	0	0	38	+ (P1)
		PRL9(115)	ILRSWNEPL	22	139	224	2	2	42	
		PRL9(157)	GMELIVSQV	22	308	456	1	1	85	
		PRL9(118)	SWNEPLYHL	21	27144	6428	3	3	86	
		PRL9(185)	QMADEESRL	21	317	1040	1	1	88	
		PRL10(114)	SILRSWNEPL	22	555	627	7	7	113	
		PRL9(110)	SLIVSILRS	19	2815	3621	4	4	121	
		<i>PRL10(175)</i>	<i>YPVWSGLPSL</i>	<i>19</i>	<i>16548</i>	<i>42</i>	<i>0</i>	<i>0</i>	<i>123</i>	
		PRL10(51)	VVLSHYIHNL	22	162	343	17	17	126	
		PRL10(42)	TLRDLFDRAV	22	1361	745	3	3	127	
		PRL9(209)	KIDNYLKLL	23	209	1033	1	1	130	
		PRL9(202)	CLRRDSHKI	21	152223	10544	11	11	131	
		<i>PRL10(82)</i>	<i>AINSCHTSSL</i>	<i>23</i>	<i>515</i>	<i>4932</i>	<i>11</i>	<i>11</i>	<i>134</i>	
		PRL9(35)	GAARCQVTL	21	8548	11959	13	13	167	
		PRL10(194)	SAYYNLLHCL	21	782	5518	15	15	171	
		PRL9(108)	FLSLIVSIL	25	21	26	1	1	173	
		PRL9(45)	DLFDRAVVL	23	3857	2248	1	1	181	
		PRL10(102)	QMNQKDFLSL	22	136	1501	5	5	188	
		PRL9(154)	LLEGMELIV	24	509	236	1	1	192	
		PRL9(195)	AYYNLLHCL	19	6747	9773	11	11	193	
		PRL9(125)	HLVTEVRGM	19	4653	5341	3	3	194	
		PRL9(173)	EIYPVWSGL	19	11018	5615	5	5	195	
		PRL9(176)	PVWSGLPSL	21	1656	1572	2	2	200	
		PRL10(132)	GMQEAPAIL	23	266	1030	1	1	207	
		PRL9(213)	YLKLLKCRI	20	7459	2576	8	8	229	
		PRL10(213)	YLKLLKCRII	19	9803	4079	23	23	241	
		PRL10(110)	SLIVSILRSW	20	23774	15402	16	16	266	
B*0702	CMV pp65	CMV (RPH)	RPHERNGFTV	17	N/A	34	0	0	26	
	Aromatase	ARO9(307)	APDTMSVSL	25	30	51	0	1	2	
		ARO9(422)	VPYRYFPQF	18	41	27	0	0	5	
		ARO9(407)	FPKPNEFTL	21	187	44	0	0	10	
		ARO9(26)	MPVLLLTGL	21	47	63	0	1	11	+ (P1)
		ARO9(21)	MPAATMPVL	24	25	9	0	0	12	
		ARO9(493)	TPRNSDRCL	22	28	53	0	0	13	+ (P2)
		ARO10(193)	RVMLDTSNTL	12	187	500	1	1	23	
		ARO9(386)	YPVKKGTNI	19	20	52	0	0	29	+ (P1)
		ARO10(7)	NPIHYNITSI	17	85	592	1	1	30	
		ARO9(480)	HPDETKNML	21	81	281	0	1	32	
		ARO10(17)	VPEAMPAATM	18	87	53	0	1	33	
		ARO10(21)	MPAATMPVLL	24	46	36	0	1	37	
		ARO10(307)	APDTMSVSLF	20	152	439	0	2	47	
		ARO10(57)	GPLISHGRFL	21	73	184	0	1	48	+ (P1)
		ARO9(154)	GPGLVRMVT	19	903	455	1	6	49	
		ARO10(409)	KPNEFTLENF	17	279	259	0	1	51	
		ARO10(386)	YPVKKGTNII	18	15	129	0	0	53	

	ARO10(86)	RVWISGEETL	11	368	7062	5	7	55	
	ARO10(230)	KPDIFFKISW	12	891	5571	2	6	56	+ (P1, P2)
	ARO10(26)	MPVLLLTGLF	17	49	557	2	4	62	
	ARO10(145)	RPFMFKALSG	13	605	461	3	5	64	
	ARO10(433)	GPRGCAGKYI	20	99	122	0	1	65	
	ARO10(493)	TPRNSDRCLE	13	678	5053	5	13	70	
	ARO9(57)	GPLISHGRF	16	519	431	0	3	72	
	ARO10(206)	IPLDESAIV	18	614	3035	1	1	78	
	ARO10(154)	GPGLVRMTV	19	212	647	1	1	80	
	ARO10(306)	AAPDTMSVSL	14	559	293	0	5	85	
	ARO10(47)	IPGPGYCMGI	19	1677	3032	1	5	93	
	ARO9(325) ^d	HPNVEEAI	17	1893	1312	1	1	96	
	ARO9(206) ^d	IPLDESAIV	18	1108	2614	1	1	102	
	ARO9(23) ^d	AATMPVLLL	18	4392	7228	2	13	112	
	ARO9(17)	VPEAMPAAT	19	304	1980	2	7	116	
NEK3	NEK9(367)	VPNTALTAL	22	13	8	0	0	1	
	NEK9(222)	LPSHYSYEL	22	52	30	0	1	3	
	NEK9(294)	NPSRIRIAL	24	12	6	0	0	4	
	NEK9(148)	SARLLSNPM	9	34	44	0	0	15	
	NEK9(288)	TPRKTNPNS	15	22	120	1	1	21	
	NEK9(241)	NPSHRPSAT	19	17	1921	2	3	24	
	NEK9(355)	SPNLHRRQW	11	37	660	1	1	44	
	NEK9(177)	LPYNNKSDI	16	70	174	0	2	45	
	NEK10(245)	RPSATLLSR	16	350	6051	6	4	52	
	NEK9(169)	VPPEIWENL	20	6305	4038	1	4	54	
	NEK10(288)	TPRKTNPNSR	14	412	7396	7	3	58	
	NEK9(377)	NASILTSSL	13	382	1120	1	6	60	
	NEK9(245)	RPSATLLS	17	164	466	0	1	64	
	NEK9(411)	TPDTLLNIL	21	700	590	0	3	67	
	NEK10(241)	NPSHRPSATT	19	117	3376	3	4	68	
	NEK10(177)	LPYNNKSDIW	10	440	3517	2	4	71	
	NEK10(243)	SHRPSATLL	15	511	8107	4	2	74	
	NEK10(154)	NPMAFACTYV	19	747	549	2	3	99	
	NEK9(165)	TPYYVPPEI	17	417	347	0	4	107	
	NEK9(466)	DPERLEPGL	21	18539	18989	4	23	109	
	NEK9(243)	SHRPSATTL	14	314	2742	1	1	114	
PIAS3	PIAS9(85)	SPVGS PGPL	23	7	11	0	0	6	+ (P2)
	PIAS9(565)	TPSHFLGPL	23	10	11	0	0	7	
	PIAS9(65)	FPRKTLGPS	14	35	33	1	1	8	
	PIAS9(406)	CPMKPKKEA	21	1976	144	1	3	9	
	PIAS10(276)	LVRQLTAGTL	12	48	327	2	1	14	
	PIAS10(461)	LPPTKKHCSV	16	180	803	3	1	16	+ (P1)
	PIAS9(609)	GPLPSGPSL	23	26	26	0	0	17	
	PIAS9(234)	EPKRPSRPI	21	93	221	1	1	18	+ (P1)
	PIAS9(409)	KPKKEASEV	18	191	51	0	0	18	+ (P1)
	PIAS10(10)	MVMSFRVSEL	12	483	243	2	1	19	
	PIAS9(245)	TPLARLSAT	18	63	96	1	1	22	
	PIAS9(296)	NPDHSRALI	19	108	246	0	6	25	+ (P1)
	PIAS9(124)	HPDVTMKPL	22	32	40	0	1	27	
	PIAS10(409)	KPKKEASEVC	13	820	2550	2	0	28	
	PIAS9(585)	TPAPPGRV	21	226	355	0	3	31	
	PIAS10(240)	RPINITPLAR	14	595	4245	3	3	34	
	PIAS9(94)	APIPPTLLA	25	248	246	0	3	35	
	PIAS9(214)	KVNGKLCPL	14	553	902	2	1	36	
	PIAS10(71)	GPSDL SLLSL	24	32	135	0	1	38	
	PIAS10(490)	QPSSVLRSPA	20	98	205	2	1	39	
	PIAS10(587)	APPPGRVSSI	20	21	153	0	1	40	
	PIAS9(237)	RPSRPINIT	22	224	184	1	1	42	
	PIAS9(165)	TPQQVQQIL	20	303	77	0	0	43	+ (P1)
	PIAS10(85)	SPVGS PGPLA	19	271	249	1	4	50	+ (P1)
	PIAS10(611)	LPSGSLTGC	15	903	4474	3	5	57	
	PIAS10(327)	CPLGKMRLTV	21	588	208	2	1	59	
	PIAS10(602)	ALREGHGGPL	15	300	693	2	1	61	

	PIAS10(91)	GPLAPIPPTL	22	928	155	1	12	63	
	PIAS10(245)	TPLARLSATV	18	144	99	1	1	66	
	PIAS9(121)	QPVHPDVTM	21	310	457	0	1	69	
	PIAS10(316)	VATTSLRVSL	13	186	3611	3	3	73	
	<i>PIAS10(520)</i>	<i>FPLGADIQGL</i>	22	2768	770	1	2	75	
	PIAS9(240)	RPINITPLA	19	246	174	0	2	76	
	PIAS9(478)	LPGSKGVL	20	877	3103	2	9	77	
	PIAS9(91)	GPLAPIPPT	22	7819	1138	1	7	79	
	<i>PIAS10(469)</i>	<i>SVTSAAIIPAL</i>	12	399	5930	4	3	81	
	PIAS9(62)	RRRFRKTL	17	286	1509	1	5	82	
	<i>PIAS10(320)</i>	<i>SLRVSLMCPL</i>	13	488	1736	14	1	83	
	PIAS10(475)	IPALPGSKGV	18	119	388	1	1	86	
	PIAS10(65)	FPRKTLGSPD	14	336	1345	7	9	86	
	PIAS9(611)	LPSGSLTG	19	1880	2064	1	13	86	
	PIAS10(143)	RPTTLASTSS	12	104	944	3	3	87	
	<i>PIAS9(15)</i>	<i>RVSELQVLL</i>	15	919	3284	1	7	88	
	PIAS9(588)	PPPGRVSSI	19	1187	10702	3	6	88	
	<i>PIAS9(595)</i>	<i>SIVAPGGAL</i>	16	497	116	0	3	89	
	PIAS10(585)	TPAPPGRVS	13	871	2081	2	5	90	
	PIAS9(574)	APTLGSSHC	12	273	2239	2	4	91	
	PIAS9(431)	SPVQGGDPS	12	174	1897	2	7	92	
	PIAS10(97)	PPTLLAPGTL	20	927	7128	3	4	95	
	PIAS10(565)	TPSHFLGPLA	19	1293	483	3	7	97	
	PIAS10(511)	LPLHEYPFAF	18	185	747	1	1	98	
	PIAS9(516)	YPPAFPLGA	19	5534	3168	1	11	100	
	PIAS10(132)	LPFYEVYGE	20	493	241	1	1	103	
	PIAS9(420)	PPGYGLDGL	21	5299	18563	5	31	104	
	PIAS10(220)	CPLPGYLPPT	19	5341	2566	9	7	105	
	PIAS10(419)	PPPGYGLDGL	22	8490	24510	8	18	106	
	PIAS9(462)	PPTKKHCSV	17	101	5933	5	2	108	
	PIAS9(587)	APPPGRVSS	16	323	993	1	5	110	
	PIAS9(497)	SPAMGTLGG	14	712	1145	1	15	111	
	PIAS9(207)	FPPNLFVKV	19	3789	2937	1	6	113	
	PIAS9(143)	RPTTLASTS	11	501	481	1	4	115	
	PIAS9(311)	DPDSEVATT	19	23840	27591	8	20	117	
Prolactin	<i>PRL10(175)</i>	<i>YPVWSGLPSL</i>	21	7	11	0	0	20	
	<i>PRL9(175)</i>	<i>YPVWSGLPS</i>	14	20	121	1	3	20	
	<i>PRL10(121)</i>	<i>EPLYHLVTEV</i>	19	1957	3164	3	4	41	
	<i>PRL10(136)</i>	<i>APEAILS KAV</i>	20	99	121	1	2	46	+ (P2)
	<i>PRL10(82)</i>	<i>AINSCHTSSL</i>	13	435	1896	3	1	76	
	PRL9(29)	LPICPGGAA	21	128	50	1	0	84	
	PRL9(136)	APEAILS KA	19	1125	1147	1	6	94	
	PRL10(32)	CPGGAARCQV	20	799	1411	7	3	101	

^aPrediction cut off, SYFPEITHI: ≥ 19 .

^bPrediction cut off, NetMHC 3.0: ≤ 1000 nM.

^cResponses detected in Patient cohort 1 (+ (P1)) and 2 (+ (P2)).

^dThree peptides were included for MHC ELISA screen although not passing the prediction cut offs.

Supplementary Table S3. MHC class I presentation of peptides derived from PIAS3 in three HLA-A*02:01 or HLA-B*07:02 positive breast cancer cell lines. After MHC immunoaffinity chromatography, peptides were identified by liquid chromatography mass spectrometry (LC-MS). In the same LC-MS analyses, no MHC class I peptide ligands from aromatase, NEK3 and prolactin were identified at the applied confidence level of 5 % false discovery rate. The cysteine in ASEVCPPPGY occurred in a cysteinylated form, i.e. with a free cysteine bound to the peptide's cysteine residue via a disulfide bond.

Cell line	Total number of identified peptides	Sequence	Q-Value	PEP	XCorr	Charge	ΔM (ppm)	HLA	NetMHCpan 4.0 (nM)	SYFPEITHI (score)				
BT-549	2870	SIVAPGGAL	0.012	0.07301	2.96	2	4.70	A*0101	33178	N/A				
								A*0201	6582	22				
								B*1507	964	N/A				
								B*56	13367	N/A				
								C*0303	92	N/A				
		C*0701					18043	N/A						
		ASEVCPPPGY					0	0.00104	2.76	2	1.60	A*0101	909	N/A
												A*0201	35808	3
												B*1507	2870	N/A
												B*56	39234	N/A
C*0303	28980		N/A											
C*0701	28823	N/A												
EFM192A	4486	RFEEAHFTF	0.01	0.03169	2.06	2	1.97	A*0101	16712	N/A				
								A*2402	17	20				
								B*0702	16957	7				
								B*3901	9073	2				
								C*0702	304	N/A				
								C*1203	2440	N/A				
MDA-MB-231	3571	GELIRPTTL	0.001	0.00481	2.54	2	0.48	A*0201	28408	15				
								A*0217	36657	N/A				
								B*4002	27	N/A				
								B*4101	364	14				
								C*0202	26390	N/A				
								C*1701	36032	N/A				

PEP = posterior error probability.

5. EPILOGUE

The research presented in this thesis is tied together by the search for antigen specific T cells in the scheme of epitope discovery, immune monitoring and therapy. Each research project utilizes MHC multimers to identify relevant CD8⁺ T cells, which are the mediators of aberrant cell destruction in cancer and infections of viral and intracellular bacterial origin. During the PhD project, research has been conducted in preclinical mouse models (manuscript I-II) and a clinical cohort of breast cancer patients (paper III), all with the perspective to characterize T cell epitopes in small or large scale. As such, manuscript I describes a technology to screen for antigen specific T cells in mice, whereas manuscript II and paper III concern T cell epitope analysis in cancer settings.

For MHC multimer-based research, efficient peptide exchange technologies, such as UV-mediated peptide exchange, have facilitated rapid and high-throughput generation of larger panels of pMHC multimers in parallel. In **manuscript I** we design and validate novel conditional ligands for UV-mediated peptide exchange for two murine alleles; H-2D^d and H-2K^d. Despite there being multiple descriptions of such conditional ligands for murine and human MHC class I alleles, thus far only one allele was covered for the H-2^d haplotype (i.e. inbred BALB/c background) namely H-2L^d. This imposes technical difficulties for T cell epitope mapping in BALB/c models, because of the need for tedious individual refolding of each peptide with the H-2 allele, an obstruction for investigating large pH-2 libraries. We successfully used H-2D^d, H-2K^d, and H-2L^d to generate DNA barcode labelled pH-2 multimer panels with 72 different specificities via UV-mediated exchange. With these large pH-2 panels we screened several murine splenocyte samples for presence of specific CD8⁺ T cells. Thus, we have provided proof-of-concept of using a DNA barcode labelling system for murine pH-2 multimers, which was confirmed by multimer staining with fluorescent labels.

The novel conditional ligands described for H-2D^d and H-2K^d in manuscript I, were applicable to the neo-epitope immunogenicity investigations in **manuscript II**. Here, we

employ DNA- and peptide-based vaccination strategies with selected neo-epitopes in the syngeneic CT26 tumor model on BALB/c mice. Our data implies, that the choice of vaccine formulation and adjuvant properties is crucial, both for immunogenicity and therapeutic effects of the neo-epitopes investigated. As such, protective anti-tumor immunity was obtained by prophylactic neo-epitope DNA vaccination and not neo-peptides + poly IC. This was paralleled by neo-epitope DNA vaccination preferentially inducing cytokine reactive CD8⁺ T cells, whereas neo-peptide + poly IC vaccination induced more CD4⁺ T cells. In common for both delivery strategies, pH-2 tetramer staining disclosed presence of neo-epitope specific CD8⁺ T cells in the periphery, albeit at a significantly higher level for DNA based vaccination. Though neo-epitope specific CD8⁺ T cells were indeed present in peptide immunized mice, they were less reactive measured by bulk IFN γ ELISPOT, and ICS showed almost no IFN γ and TNF α producing CD8⁺ T cells upon re-stimulation. Conversely, DNA based neo-epitope vaccination induced significantly more IFN γ SFUs measured by ELISPOT, and impressive numbers of IFN γ and TNF α producing CD8⁺ T cells via ICS. We expect that the anti-tumor response is primarily driven by these functional CD8⁺ T cells induced by neo-epitope DNA vaccination. The question arises, whether the anti-tumor effect is driven by sheer functionality and to what extent it is a “numbers game”. It is possible, that the neo-peptide + poly IC vaccination strategy employed here induces somewhat anergic or otherwise unresponsive CD8⁺ T cells. We propose that this is in part due to innate signals present already at APC antigen uptake and priming of T cells. Exogenous peptide vaccination inherently leads to presentation by MHC class II on APCs and relies on cross presentation to reach the MHC class I pathway, as discussed in manuscript II. The addition of TLR3 agonist poly IC to the neo-peptide vaccination could be an inducer of cross presentation signals to DCs [139], [140], but in our studies this strategy primarily primed CD4⁺ T cells. Interestingly, previous reports in a different setting with the syngeneic MC38 model on C57BL/6 background suggests neo-peptide vaccination adjuvanted by poly IC and anti-CD40 antibody induces strong CD8⁺ T cell responses and anti-tumor immunity [127], [128]. Other studies have established anti-tumor potential of poly IC alone, when injected intratumorally [141]. On the other side, DNA based delivery confers direct access to the MHC class I processing and presentation pathway, since antigens are produced inside APCs, and innate DNA sensing leads to induction of Th1 like immunity. DNA delivery of neo-epitopes has in recent preclinical studies induced anti-tumor effects in other syngeneic

models with and without combination with anti-PD-1 antibody [134], [142]–[144]. We therefore think, that DNA based neo-epitope vaccination is worth pursuing further. Specifically, we will expand these studies with CD4+ and CD8+ T cell depletion to interrogate which T cell subsets are crucial for retaining anti-tumor effects observed by vaccination. We further hypothesize that we will be able to achieve anti-tumor effects with therapeutic neo-epitope DNA vaccination in combination with anti-PD-1 therapy. This synergistic combination therapy could abrogate some immune suppressive effects of the established CT26 TME and boost vaccine induced T cells. Furthermore, the CT26 tumor model has a rapid tumor onset and thus offers a short therapeutic window before mice must be euthanized for reaching humane endpoints [122], [137]. This is an important factor to consider, when talking about translatability from mice to humans, as human tumor development takes months to years.

The neo-epitopes included in our vaccination study were of 27-mer amino acid length and contain multiple *in silico* predicted MHC class I and II ligands. Preclinical studies claim that both CD4+ and CD8+ T cell responses are essential for cancer immunotherapy [126], [135], which is contradictory to the original understanding that CD8+ T cells solely drive tumor elimination [119].

Together, findings in manuscript I and II will be applicable in a preclinical framework of high-throughput neo-epitope screening. The number of putative neo-epitopes predicted by current algorithms is vast, and large-scale T cell detection technologies like the DNA barcode-labelled pMHC multimer strategy are necessary to meet this complexity. The increased understanding of immunogenic neo-epitopes will feed back to prediction algorithms, which currently rely primarily on *in silico* predicted peptide-MHC binding affinity. In time, the hope is to better define those neo-epitopes that are most likely to elicit an immune response. And furthermore, define the subset of immunogenic epitopes that are also therapeutically relevant.

An example of this framework is an ongoing project in the research group, where we are currently investigating the landscape of neo-epitope specific CD8+ T cells induced by anti-PD-1 and anti-CTLA-4 combination therapy compared to isotype control antibody in common syngeneic tumor models. The distinct antigen specific CD8+ T cell patterns induced by CPI therapy in TILs and periphery in these syngeneic models have previously not been characterized.

In **paper III** we utilize the high-throughput multimer strategy to detect CD8+ T cell responses towards previously undescribed shared overexpression antigens in breast cancer patients. This method is similar to that used in manuscript I, but with human HLAs. Breast cancer has been minimally studied in the field of immune oncology, resulting in limited knowledge of targetable T cell epitopes. But recent descriptions underline the relevance of immunological recognition of breast cancer [48], [145]–[149]. Breast cancers constitute low mutational burden tumors [150], why it is relevant to investigate non-mutated shared tumor antigens for T cell recognition. In our paper, we focus on four proteins known to be upregulated in breast cancer: aromatase, NEK3, PIAS3, and prolactin, that each contribute to cell growth, survival, and motility during malignant transformation. From these proteins, we selected 147 peptides with affinity for HLA-A*0201 and -B*0702 by combined *in silico* and *in vitro* screening. We constructed a DNA barcode labelled pHLA multimer library to screen a cohort of breast cancer patients and healthy donors for CD8+ T cell recognition to these shared antigens. Our analyses disclosed significantly more CD8+ T cell responses in breast cancer patients than healthy donors, and the peptides that gave rise to T cell responses clustered in “immunological hotspots” in the protein sequences. Interestingly, patients with more advanced disease stages also had higher numbers of CD8+ T cell responses, and specific T cells from some patients were shown to be cytokine responsive to peptide stimulation. Together these results validated the four proteins as novel tumor associated antigens, and we hypothesize their relevance for immune monitoring of breast cancer patients, potentially providing a measure of immune status or a correlate of response to immunotherapies. We found it notable, that several of the immunogenic peptides had intermediate to low predicted binding affinity to the HLA. One explanation for this, is that T cells specific to self-antigens undergo strict negative selection in the thymus, and it is therefore important to include these lower affinity binders in the search for shared epitopes to possibly circumvent tolerance. The potential applicability of this study is limited by the library’s restriction to HLA-A*0201 and -B*0702, but we are considering expanding the panel to include more HLA types. Furthermore, we are interested in investigating T cell epitopes from additional shared tumor associated antigens with relevance in breast cancer. These expansions to the pHLA library are feasible, due to the high-throughput screening method, which has previously been used for epitope mapping in human samples to detect antigen specific CD8+ T specific to: self-proteins in narcolepsy [151], neo-epitopes in non-small cell lung cancer, and shared tumor antigens in melanoma [79]. The data from

manuscript I and paper III from this thesis thus contribute to the list of applications for the high-throughput method in murine and human samples.

Perspectives of the presented work

The research contained in this thesis contributes to the field of cancer immunology by several parameters. First, by the design and validation of new conditional ligands for H-2D^d and H-2K^d and establishment of proof-of-concept of large-scale DNA barcode labelled multimer panels for BALB/c haplotype alleles. It is our expectation, that the new conditional ligands and the high-throughput technology for murine CD8⁺ T cell interrogation via pMHC-2^d multimers will assist screening purposes and antigen discovery in preclinical models of cancer, infectious diseases and autoimmunity. Second, by establishing a protective neo-epitope encoding DNA vaccination strategy in the CT26 syngeneic tumor model. This allows screening of more neo-epitopes for immunogenicity and contribution to anti-tumor effects, and can be expanded to other syngeneic models on BALB/c and C57BL/6 background. We also anticipate the DNA vaccination platform will be a great tool to investigate combination therapies. Third, by defining novel tumor associated antigens in breast cancer, where there is a lack of descriptions of T cell epitopes and immunotherapeutic strategies are less established. It could be interesting to expand the panel of putative breast cancer antigens of shared origin in future studies. Together, this research provides tools and investigations of what makes good T cell targets in cancer, which will be further discussed in the following paragraphs.

Though manuscript II and paper III take place in a murine model and patient samples, respectively, they lead to considerations on the applicability of shared and neo-epitopes. In the event of using these epitopes as immunotherapeutic T cell targets by e.g. vaccination, attention should be put on safety. For this purpose, neo-epitopes are clearly advantageous since antigen expression is limited to tumor cells and therefore there should be no adverse destruction of self-tissue. Further beneficial is that neo-epitope specific T cells are assumed to be less subjected to immune tolerance. However, using neo-epitopes therapeutically requires extensive work, since it will be a “1 patient, 1 drug” setting. Neo-epitope prediction and subsequent vaccine production is cumbersome, but worthwhile if we experience clinical benefit in the many currently ongoing personalized vaccine trials. For epitopes of shared origin, we instead have the option of interventions that will broadly benefit many patients,

and manufacturing will be less comprehensive with off-the-shelf options. This however comes with the caveat of potential adverse effects and heavy subjection to immune tolerance. Since tumor mutational load varies a lot, neo-epitope targeted strategies are not of equal relevance for every cancer.

As discussed throughout this thesis, far from all *in silico* predicted T cell epitopes are immunogenic and even less epitopes are of therapeutic relevance. Current prediction tools are now very good at predicting MHC binders, but we still do not know the determinants for a T cell epitope capable of initiating a strong CD8⁺ T cell response. Several explanations contribute to why some epitopes are not immunogenic. First, T cells specific to a given epitope might have never existed or were eliminated by negative selection. Second, specific T cells could exist, but be anergic or otherwise functionally unresponsive. Last, the epitope itself is not immunogenic enough to give rise to T cell reactivity. Future perspectives of improved epitope prediction will be contributed to by preclinical and clinical investigations alike. High-throughput technologies will support this through e.g. TCR profiling and mapping of pMHC-TCR pairs [152]. One could then imagine a framework of interrogating the naive T cell repertoire of a patient, to tailor a vaccine based on the already existing T cells. Recent reports are suggesting an additional layer of complexity, by outlining how the cancer patients' microbiome are affecting responses to anti-PD-1 therapy [153], [154]. Perhaps we will in the near future use measures like these to stratify and design personal immunotherapies to cancer patients.

As a final remark, I expect this already rapidly developing field to advance with knowledge of how we can utilize the immune system to combat cancer. The cancer-immunity interplay is indeed intricate and multifaceted, and I believe that insights into how we can tune adaptive responses via innate stimuli, will take us even further. We have clear evidence, that tumors are vastly different from normal tissue, and some of these differences lead to recognition by the immune system. Hence, we need potent tools to screen the immense putative epitope libraries resulting from genome-wide epitope mapping. Neo-epitope vaccination trials have reached the clinic; thus, we have entered the era of truly personalized cancer therapies. In this era, preclinical studies will continuously provide indispensable insights into immune recognition of cancer, why they are of key translational relevance.

6. BIBLIOGRAPHY

- [1] P. J. Delves and I. M. Roitt, “The Immune System - First of two parts,” *N. Engl. J. Med.*, vol. 343, no. 1, pp. 37–50, 2000.
- [2] D. Schenten and R. Medzhitov, “The Control of Adaptive Immune Responses by the Innate Immune System,” in *Advances in Immunology*, vol. 109, 2011, pp. 87–124.
- [3] J. Banchereau and R. M. Steinman, “Dendritic cells and the control of immunity,” *Nature*, vol. 392, no. March, pp. 245–252, 1998.
- [4] M. Hubo, B. Trinschek, F. Kryczanowsky, A. Tuetttenberg, K. Steinbrink, and H. Jonuleit, “Costimulatory molecules on immunogenic versus tolerogenic human dendritic cells,” *Front. Immunol.*, vol. 4, p. 82, Apr. 2013.
- [5] V. Schijns and D. O’Hagan, *Immunopotentiators in Modern Vaccines*. Elsevier, 2006.
- [6] C. J. Desmet and K. J. Ishii, “Nucleic acid sensing at the interface between innate and adaptive immunity in vaccination,” *Nat. Rev. Immunol.*, vol. 12, no. 7, pp. 479–491, Jun. 2012.
- [7] K. C. Garcia and I. A. Wilson, “Structural Basis of T cell Recognition,” *Annu. Rev. Immunol.*, vol. 17, pp. 369–397, 1999.
- [8] T. Trolle *et al.*, “The Length Distribution of Class I-Restricted T Cell Epitopes Is Determined by Both Peptide Supply and MHC Allele-Specific Binding Preference,” *J. Immunol.*, vol. 196, no. 4, pp. 1480–1487, Feb. 2016.
- [9] R. M. Chicz *et al.*, “Predominant naturally processed peptides bound to HLA-DR1 are derived from MHC-related molecules and are heterogeneous in size,” *Nature*, vol. 358, no. 6389, pp. 764–768, Aug. 1992.
- [10] M. Embgenbroich and S. Burgdorf, “Current Concepts of Antigen Cross-Presentation,” *Front. Immunol.*, vol. 9, p. 1643, Jul. 2018.
- [11] M. Kovacovics-Bankowski and K. L. Rock, “A phagosome-to-cytosol pathway for exogenous antigens presented on MHC class I molecules,” *Science (80-.)*, vol. 267, no. 5195, pp. 243 LP – 246, Jan. 1995.
- [12] O. P. Joffre, E. Segura, A. Savina, and S. Amigorena, “Cross-presentation by dendritic cells,” *Nat Rev Immunol*, vol. 12, no. 8, pp. 557–569, Aug. 2012.
- [13] K. S. Kobayashi and P. J. van den Elsen, “NLRC5: a key regulator of MHC class I-dependent immune responses,” *Nat Rev Immunol*, vol. 12, no. 12, pp. 813–820, Dec. 2012.
- [14] M. Fabbri, C. Smart, and R. Pardi, “T Lymphocytes,” *Int. J. Biochem. Cell Biol.*, vol. 35, no. 7, pp. 1004–1008, 2003.

- [15] B. O. Roep, M. J. Kracht, M. van Lummel, and A. Zaldumbide, “A roadmap of the generation of neoantigens as targets of the immune system in type 1 diabetes,” *Curr. Opin. Immunol.*, vol. 43, pp. 67–73, Dec. 2016.
- [16] M. Salou, B. Nicol, A. Garcia, and D.-A. Laplaud, “Involvement of CD8+ T Cells in Multiple Sclerosis,” *Front. Immunol.*, vol. 6, p. 604, Nov. 2015.
- [17] H. Lodish *et al.*, *Molecular Cell Biology*, vol. 4. 2008.
- [18] D. Hanahan and R. A. Weinberg, “The Hallmarks of cancer,” *Cell*, vol. 100, pp. 57–70, 2000.
- [19] D. S. Chen and I. Mellman, “Oncology Meets Immunology: The Cancer-Immunity Cycle,” *Immunity*, vol. 39, no. 1, pp. 1–10, Jul. 2013.
- [20] D. Hanahan and R. A. Weinberg, “Hallmarks of cancer: The Next Generation,” *Cell*, vol. 144, no. 5, pp. 646–674, 2011.
- [21] J. Galon, “Type, Density, and Location of Immune Cells Within Human Colorectal Tumors Predict Clinical Outcome,” *Science (80-.)*, vol. 313, no. 5795, pp. 1960–1964, Sep. 2006.
- [22] J. Galon *et al.*, “Cancer classification using the Immunoscore: a worldwide task force,” *J. Transl. Med.*, vol. 10, p. 205, Oct. 2012.
- [23] J. Galon and D. Bruni, “Approaches to treat immune hot, altered and cold tumours with combination immunotherapies,” *Nat. Rev. Drug Discov.*, p. 1, Jan. 2019.
- [24] G. P. Dunn, L. J. Old, and R. D. Schreiber, “The Three Es of Cancer Immunoediting,” *Annu. Rev. Immunol.*, vol. 22, no. 1, pp. 329–360, Mar. 2004.
- [25] S. H. van der Burg, R. Arens, F. Ossendorp, T. van Hall, and C. J. M. Melief, “Vaccines for established cancer: overcoming the challenges posed by immune evasion,” *Nat Rev Cancer*, vol. 16, no. 4, pp. 219–233, 2016.
- [26] S. Hadrup, M. Donia, and P. thor Straten, “Effector CD4 and CD8 T Cells and Their Role in the Tumor Microenvironment,” *Cancer Microenviron.*, vol. 6, no. 2, pp. 123–133, Aug. 2013.
- [27] L. von Boehmer *et al.*, “NY-ESO-1-specific immunological pressure and escape in a patient with metastatic melanoma,” *Cancer Immun.*, vol. 13, p. 12, 2013.
- [28] T. Nicholaou *et al.*, “Immunoediting and persistence of antigen-specific immunity in patients who have previously been vaccinated with NY-ESO-1 protein formulated in ISCOMATRIX,” *Cancer Immunol. Immunother.*, vol. 60, no. 11, pp. 1625–1637, Nov. 2011.
- [29] P. G. Coulie, B. J. Van Den Eynde, P. Van Der Bruggen, and T. Boon, “Tumour antigens recognized by T lymphocytes: At the core of cancer immunotherapy,” *Nat. Rev. Cancer*, vol. 14, no. 2, pp. 135–146, 2014.
- [30] E.-K. Yim and J.-S. Park, “The Role of HPV E6 and E7 Oncoproteins in HPV-associated Cervical Carcinogenesis,” *Cancer Res. Treat.*, vol. 37, no. 6, pp. 319–324, Dec. 2005.
- [31] C. C. Smith *et al.*, “Machine-learning prediction of tumor antigen immunogenicity in the selection of therapeutic epitopes,” *Cancer Immunol. Res.*, vol. 7, no. 10, pp. 1591–1604, 2019.

- [32] C. M. Laumont *et al.*, “Noncoding regions are the main source of targetable tumor-specific antigens,” *Sci. Transl. Med.*, vol. 10, no. 470, p. eaau5516, Dec. 2018.
- [33] C. Chong *et al.*, “Integrated Proteogenomic Deep Sequencing and Analytics Accurately Identify Non-Canonical Peptides in Tumor Immuno-peptidomes,” *bioRxiv*, p. 758680, 2019.
- [34] S. M. Schmidt *et al.*, “Survivin is a shared tumor-associated antigen expressed in a broad variety of malignancies and recognized by specific cytotoxic T cells,” *Blood*, vol. 102, no. 2, pp. 571–576, Jul. 2003.
- [35] I. Kawashima *et al.*, “The Multi-epitope Approach for Immunotherapy for Cancer: Identification of Several CTL Epitopes from Various Tumor-Associated Antigens Expressed on Solid Epithelial Tumors,” *Hum. Immunol.*, vol. 59, no. 1, pp. 1–14, Jan. 1998.
- [36] X. Kang *et al.*, “Identification of a tyrosinase epitope recognized by HLA-A24-restricted, tumor-infiltrating lymphocytes,” *J. Immunol.*, vol. 155, no. 3, pp. 1343–1348, Aug. 1995.
- [37] E. Jager *et al.*, “Simultaneous humoral and cellular immune response against cancer-testis antigen NY-ESO-1: definition of human histocompatibility leukocyte antigen (HLA)-A2-binding peptide epitopes,” *J. Exp. Med.*, vol. 187, no. 2, pp. 265–270, Jan. 1998.
- [38] S. A. Rosenberg, J. C. Yang, and N. P. Restifo, “Cancer immunotherapy: moving beyond current vaccines,” *Nat. Med.*, vol. 10, no. 9, pp. 909–915, Sep. 2004.
- [39] J. L. Gulley *et al.*, “Phase III Trial of PROSTVAC in Asymptomatic or Minimally Symptomatic Metastatic Castration-Resistant Prostate Cancer,” *J. Clin. Oncol.*, vol. 37, no. 13, pp. 1051–1061, May 2019.
- [40] L. A. Johnson *et al.*, “Gene therapy with human and mouse T-cell receptors mediates cancer regression and targets normal tissues expressing cognate antigen,” *Blood*, vol. 114, no. 3, pp. 535–546, Jul. 2009.
- [41] J. H. Kessler and C. J. M. Melief, “Identification of T-cell epitopes for cancer immunotherapy,” *Leuk. Off. J. Leuk. Soc. Am. Leuk. Res. Fund, U.K.*, vol. 21, pp. 1859–1874, 2007.
- [42] M. S. Rooney, S. A. Shukla, C. J. Wu, G. Getz, and N. Hacohen, “Molecular and Genetic Properties of Tumors Associated with Local Immune Cytolytic Activity,” *Cell*, vol. 160, no. 1–2, pp. 48–61, Jan. 2015.
- [43] S. D. Brown *et al.*, “Neo-antigens predicted by tumor genome meta-analysis correlate with increased patient survival,” *Genome Res.*, vol. 24, no. 5, pp. 743–750, May 2014.
- [44] R. M. Samstein *et al.*, “Tumor mutational load predicts survival after immunotherapy across multiple cancer types,” *Nat. Genet.*, Jan. 2019.
- [45] A. Snyder *et al.*, “Genetic basis for clinical response to CTLA-4 blockade in melanoma,” *N. Engl. J. Med.*, vol. 371, no. 23, pp. 2189–2199, 2014.
- [46] N. A. Rizvi *et al.*, “Cancer immunology. Mutational landscape determines sensitivity to PD-1

- blockade in non-small cell lung cancer.,” *Science*, vol. 348, no. 6230, pp. 124–8, Apr. 2015.
- [47] M. Lauss *et al.*, “Mutational and putative neoantigen load predict clinical benefit of adoptive T cell therapy in melanoma,” *Nat. Commun.*, vol. 8, no. 1, pp. 1–10, 2017.
- [48] N. Zacharakis *et al.*, “Immune recognition of somatic mutations leading to complete durable regression in metastatic breast cancer,” *Nat. Med.*, vol. 24, no. 6, pp. 724–730, 2018.
- [49] E. Tran, P. F. Robbins, and S. A. Rosenberg, “‘Final common pathway’ of human cancer immunotherapy: Targeting random somatic mutations,” *Nat. Immunol.*, vol. 18, no. 3, pp. 255–262, 2017.
- [50] E. F. Fritsch, M. Rajasagi, P. A. Ott, V. Brusic, N. Hacohen, and C. J. Wu, “HLA-binding properties of tumor neoepitopes in humans,” *Cancer Immunol. Res.*, vol. 2, no. 6, pp. 522–529, 2014.
- [51] A. M. Bjerregaard *et al.*, “An analysis of natural T cell responses to predicted tumor neoepitopes,” *Front. Immunol.*, vol. 8, no. NOV, pp. 1–9, 2017.
- [52] K. R. Loeb and L. a Loeb, “Significance of multiple mutations in cancer,” *Carcinogenesis*, vol. 21, no. 3, pp. 379–385, 2000.
- [53] F. Castro-Giner, P. Ratcliffe, and I. Tomlinson, “The mini-driver model of polygenic cancer evolution,” *Nat. Rev. Cancer*, vol. 15, no. 11, pp. 680–685, 2015.
- [54] B. Heemskerk, P. Kvistborg, and T. N. M. Schumacher, “The cancer antigenome,” *EMBO J.*, vol. 32, no. 2, pp. 194–203, 2013.
- [55] C. A. Klebanoff and J. D. Wolchok, “Shared cancer neoantigens: Making private matters public,” *J. Exp. Med.*, vol. 215, no. 1, pp. 5–7, Jan. 2018.
- [56] M. Gerlinger *et al.*, “Intratumor heterogeneity and branched evolution revealed by multiregion sequencing,” *N. Engl. J. Med.*, vol. 366, no. 10, pp. 883–892, Mar. 2012.
- [57] N. McGranahan *et al.*, “Clonal neoantigens elicit T cell immunoreactivity and sensitivity to immune checkpoint blockade,” *Science*, vol. 351, no. 6280, pp. 1463–9, Mar. 2016.
- [58] H. Hackl, P. Charoentong, F. Finotello, and Z. Trajanoski, “Computational genomics tools for dissecting tumour-immune cell interactions,” *Nat. Rev. Genet.*, vol. 17, no. 8, pp. 441–458, 2016.
- [59] C. Linnemann *et al.*, “High-throughput epitope discovery reveals frequent recognition of neoantigens by CD4+T cells in human melanoma,” *Nat. Med.*, vol. 21, no. 1, pp. 81–85, 2015.
- [60] M. Bassani-Sternberg *et al.*, “Direct identification of clinically relevant neoepitopes presented on native human melanoma tissue by mass spectrometry,” *Nat. Commun.*, vol. 7, no. May, 2016.
- [61] B. Bulik-Sullivan *et al.*, “Deep learning using tumor HLA peptide mass spectrometry datasets improves neoantigen identification.,” *Nat. Biotechnol.*, vol. 37, no. 1, Dec. 2018.
- [62] J. G. Abelin *et al.*, “Defining HLA-II Ligand Processing and Binding Rules with Mass

- Spectrometry Enhances Cancer Epitope Prediction,” *Immunity*, vol. 51, no. 4, pp. 766-779.e17, 2019.
- [63] V. Jurtz, S. Paul, M. Andreatta, P. Marcatili, B. Peters, and M. Nielsen, “NetMHCpan-4.0: Improved Peptide–MHC Class I Interaction Predictions Integrating Eluted Ligand and Peptide Binding Affinity Data,” *J. Immunol.*, vol. 199, no. 9, pp. 3360 LP – 3368, Nov. 2017.
- [64] A. M. Bjerregaard, M. Nielsen, S. R. Hadrup, Z. Szallasi, and A. C. Eklund, “MuPeXI: prediction of neo-epitopes from tumor sequencing data,” *Cancer Immunol. Immunother.*, vol. 66, no. 9, pp. 1123–1130, 2017.
- [65] L. B. Alexandrov *et al.*, “Signatures of mutational processes in human cancer,” *Nature*, vol. 500, no. 7463, pp. 415–421, Aug. 2013.
- [66] E. Strønen *et al.*, “Targeting of cancer neoantigens with donor-derived T cell receptor repertoires,” *Science (80-.)*, vol. 352, no. 6291, pp. 1337–1341, 2016.
- [67] H. Besser, S. Yunger, E. Merhavi-Shoham, C. J. Cohen, and Y. Louzoun, “Level of neo-epitope predecessor and mutation type determine T cell activation of MHC binding peptides,” *J. Immunother. Cancer*, vol. 7, no. 1, pp. 1–9, 2019.
- [68] P. A. Ott *et al.*, “An Immunogenic Personal Neoantigen Vaccine for Melanoma Patients,” *Nature*, vol. 547, no. 7662, pp. 217–221, Jul. 2017.
- [69] M. Corr *et al.*, “T cell receptor-MHC class I peptide interactions: affinity, kinetics, and specificity,” *Science (80-.)*, vol. 265, no. 5174, 1994.
- [70] J. D. Altman *et al.*, “Phenotypic Analysis of Antigen-Specific T Lymphocytes,” vol. 274, no. 5284, pp. 94–96, 1996.
- [71] M. Toebes *et al.*, “Design and use of conditional MHC class I ligands,” *Nat. Med.*, vol. 12, no. 2, pp. 246–251, Feb. 2006.
- [72] A. H. Bakker *et al.*, “Conditional MHC class I ligands and peptide exchange technology for the human MHC gene products HLA-A1, -A3, -A11, and -B7,” *PNAS*, vol. 105, pp. 3825–3830, 2008.
- [73] G. M. Grotenbreg *et al.*, “Discovery of CD8+ T cell epitopes in *Chlamydia trachomatis* infection through use of caged class I MHC tetramers,” *Proc. Natl. Acad. Sci. U. S. A.*, vol. 105, no. 10, pp. 3831–3836, 2008.
- [74] E. Frickel *et al.*, “Parasite Stage-Specific Recognition of Endogenous *Toxoplasma gondii* – Derived CD8 + T Cell Epitopes,” *J. Infect. Dis.*, vol. 198, no. 11, pp. 1625–1633, Dec. 2008.
- [75] T. M. Frøsig *et al.*, “Design and validation of conditional ligands for HLA-B*08:01, HLA-B*15:01, HLA-B*35:01, and HLA-B*44:05,” *Cytom. Part A*, vol. 87, no. 10, pp. 967–975, Oct. 2015.
- [76] M. M. Davis, J. D. Altman, and E. W. Newell, “Interrogating the repertoire: broadening the scope of peptide-MHC multimer analysis,” *Nat. Rev. Immunol.*, vol. 11, no. 8, pp. 551–8, 2011.

- [77] R. S. Andersen *et al.*, “Parallel detection of antigen-specific T cell responses by combinatorial encoding of MHC multimers,” *Nat. Protoc.*, vol. 7, no. 5, pp. 891–902, May 2012.
- [78] E. W. Newell, N. Sigal, N. Nair, B. A. Kidd, H. B. Greenberg, and M. M. Davis, “Combinatorial tetramer staining and mass cytometry analysis facilitate T-cell epitope mapping and characterization,” *Nat. Biotechnol.*, vol. 31, no. 7, pp. 623–629, Jul. 2013.
- [79] A. K. Bentzen *et al.*, “Large-scale detection of antigen-specific T cells using peptide-MHC-I multimers labeled with DNA barcodes,” *Nat. Biotechnol.*, vol. 34, no. 10, pp. 1037–1045, 2016.
- [80] S. K. Saini *et al.*, “Empty peptide-receptive MHC class I molecules for efficient detection of antigen-specific T cells,” *Sci. Immunol.*, vol. 4, no. 37, p. eaau9039, Jul. 2019.
- [81] P. Braendstrup *et al.*, “MHC Class II Tetramers Made from Isolated Recombinant α and β Chains Refolded with Affinity-Tagged Peptides,” *PLoS One*, vol. 8, no. 9, p. e73648, Sep. 2013.
- [82] S. R. Hadrup and E. W. Newell, “Determining T-cell specificity to understand and treat disease,” *Nat. Biomed. Eng.*, vol. 1, no. 10, pp. 784–795, 2017.
- [83] S. Farkona, E. P. Diamandis, and I. M. Blasutig, “Cancer immunotherapy: the beginning of the end of cancer?,” *BMC Med.*, vol. 14, no. 1, p. 73, Dec. 2016.
- [84] P. Sharma and J. P. Allison, “The future of immune checkpoint therapy,” *Science (80-.)*, vol. 348, no. 6230, pp. 56–61, Apr. 2015.
- [85] T. R. Simpson *et al.*, “Fc-dependent depletion of tumor-infiltrating regulatory T cells co-defines the efficacy of anti-CTLA-4 therapy against melanoma,” *J. Exp. Med.*, vol. 210, no. 9, pp. 1695–1710, Aug. 2013.
- [86] M. J. Selby *et al.*, “Anti-CTLA-4 antibodies of IgG2a isotype enhance antitumor activity through reduction of intratumoral regulatory T cells,” *Cancer Immunol. Res.*, vol. 1, no. 1, pp. 32–42, Jul. 2013.
- [87] A. O. Kamphorst *et al.*, “Proliferation of PD-1+ CD8 T cells in peripheral blood after PD-1-targeted therapy in lung cancer patients,” *Proc. Natl. Acad. Sci. U. S. A.*, vol. 114, no. 19, pp. 4993–4998, May 2017.
- [88] A. C. Huang *et al.*, “T-cell invigoration to tumour burden ratio associated with anti-PD-1 response,” *Nature*, vol. 545, no. 7652, pp. 60–65, May 2017.
- [89] A. Gros *et al.*, “Prospective identification of neoantigen-specific lymphocytes in the peripheral blood of melanoma patients,” *Nat. Med.*, vol. 22, no. 4, pp. 433–438, 2016.
- [90] K. E. Yost *et al.*, “Clonal replacement of tumor-specific T cells following PD-1 blockade,” *Nat. Med.*, vol. 25, no. 8, pp. 1251–1259, Aug. 2019.
- [91] T. Duhon *et al.*, “Co-expression of CD39 and CD103 identifies tumor-reactive CD8 T cells in human solid tumors,” *Nat. Commun.*, vol. 9, no. 1, p. 2724, Dec. 2018.
- [92] Y. Simoni *et al.*, “Bystander CD8 + T cells are abundant and phenotypically distinct in human

- tumour infiltrates,” *Nature*, vol. 557, no. 7706, pp. 575–579, 2018.
- [93] S. Das and D. B. Johnson, “Immune-related adverse events and anti-tumor efficacy of immune checkpoint inhibitors,” *J. Immunother. Cancer*, vol. 7, no. 1, p. 306, 2019.
- [94] S. A. Rosenberg and N. P. Restifo, “Adoptive cell transfer as personalized immunotherapy for human cancer,” *Science (80-.)*, vol. 348, no. 6230, pp. 62–68, Apr. 2015.
- [95] C. H. June, R. S. O’Connor, O. U. Kawalekar, S. Ghassemi, and M. C. Milone, “CAR T cell immunotherapy for human cancer,” *Science (80-.)*, vol. 359, no. 6382, pp. 1361–1365, Mar. 2018.
- [96] P. Sharma, S. Hu-Lieskovan, J. A. Wargo, and A. Ribas, “Primary, Adaptive, and Acquired Resistance to Cancer Immunotherapy,” *Cell*, vol. 168, no. 4, pp. 707–723, Feb. 2017.
- [97] Z. Hu, P. A. Ott, and C. J. Wu, “Towards personalized, tumour-specific, therapeutic vaccines for cancer,” *Nat. Rev. Immunol.*, vol. 18, no. 3, pp. 168–182, Mar. 2018.
- [98] T. N. Schumacher and R. D. Schreiber, “Neoantigens in cancer immunotherapy,” *Science (80-.)*, vol. 348, no. 6230, pp. 69–74, 2015.
- [99] B. Temizoz, E. Kuroda, and K. J. Ishii, “Vaccine adjuvants as potential cancer immunotherapeutics,” *Int. Immunol.*, vol. 28, no. 7, pp. 329–338, Jul. 2016.
- [100] K. Vermaelen, “Vaccine Strategies to Improve Anti-cancer Cellular Immune Responses,” *Front. Immunol.*, vol. 10, no. JAN, pp. 1–17, Jan. 2019.
- [101] C. Gouttefangeas and H.-G. Rammensee, “Personalized cancer vaccines: adjuvants are important, too,” *Cancer Immunol. Immunother.*, vol. 67, no. 12, pp. 1911–1918, Dec. 2018.
- [102] E. N. Vinageras *et al.*, “Phase II randomized controlled trial of an epidermal growth factor vaccine in advanced non-small-cell lung cancer,” *J. Clin. Oncol.*, vol. 26, no. 9, pp. 1452–1458, 2008.
- [103] S. S. Neelapu *et al.*, “Human Autologous Tumor-Specific T-Cell Responses Induced by Liposomal Delivery of a Lymphoma Antigen,” *Clin. Cancer Res.*, vol. 10, no. 24, pp. 8309 LP – 8317, Dec. 2004.
- [104] D. Wang, Y. Sun, Y. Liu, F. Meng, and R. J. Lee, “Clinical translation of immunoliposomes for cancer therapy: recent perspectives,” *Expert Opin. Drug Deliv.*, vol. 15, no. 9, pp. 893–903, Sep. 2018.
- [105] K. S. Korsholm *et al.*, “Induction of CD8+ T-cell responses against subunit antigens by the novel cationic liposomal CAF09 adjuvant,” *Vaccine*, vol. 32, no. 31, pp. 3927–3935, 2014.
- [106] J. Gao, L. Ochyl, E. Yang, and J. Moon, “Cationic liposomes promote antigen cross-presentation in dendritic cells by alkalizing the lysosomal pH and limiting the degradation of antigens,” *Int. J. Nanomedicine*, vol. Volume 12, pp. 1251–1264, Feb. 2017.
- [107] D. B. Keskin *et al.*, “Neoantigen vaccine generates intratumoral T cell responses in phase Ib glioblastoma trial,” *Nature*, vol. 565, no. 7738, pp. 234–239, Jan. 2019.

- [108] P. Sabbatini *et al.*, “Phase I Trial of Overlapping Long Peptides from a Tumor Self-Antigen and Poly-ICLC Shows Rapid Induction of Integrated Immune Response in Ovarian Cancer Patients,” *Clin. Cancer Res.*, vol. 18, no. 23, pp. 6497–6508, Dec. 2012.
- [109] M. L. Salem, S. A. El-Naggar, A. Kadima, W. E. Gillanders, and D. J. Cole, “The adjuvant effects of the toll-like receptor 3 ligand polyinosinic-cytidylic acid poly (I:C) on antigen-specific CD8+ T cell responses are partially dependent on NK cells with the induction of a beneficial cytokine milieu,” *Vaccine*, vol. 24, no. 24, pp. 5119–5132, Jun. 2006.
- [110] M. L. Salem, A. N. Kadima, D. J. Cole, and W. E. Gillanders, “Defining the antigen-specific T-cell response to vaccination and poly(I:C)/TLR3 signaling: evidence of enhanced primary and memory CD8 T-cell responses and antitumor immunity,” *J. Immunother.*, vol. 28, no. 3, pp. 220–228, 2005.
- [111] H. Ishikawa, Z. Ma, and G. N. Barber, “STING regulates intracellular DNA-mediated, type I interferon-dependent innate immunity,” *Nature*, vol. 461, no. 7265, pp. 788–792, 2009.
- [112] M. Motwani, S. Pesiridis, and K. A. Fitzgerald, “DNA sensing by the cGAS–STING pathway in health and disease,” *Nat. Rev. Genet.*, vol. 20, no. November, 2019.
- [113] K. J. Ishii *et al.*, “TANK-binding kinase-1 delineates innate and adaptive immune responses to DNA vaccines,” *Nature*, vol. 451, no. 7179, pp. 725–729, 2008.
- [114] Y. M. Murad and T. M. Clay, “CpG oligodeoxynucleotides as TLR9 agonists: therapeutic applications in cancer,” *BioDrugs*, vol. 23, no. 6, pp. 361–375, 2009.
- [115] L. M. Kranz *et al.*, “Systemic RNA delivery to dendritic cells exploits antiviral defence for cancer immunotherapy,” *Nature*, vol. 534, no. 7607, pp. 396–401, 2016.
- [116] U. Sahin *et al.*, “Personalized RNA mutanome vaccines mobilize poly-specific therapeutic immunity against cancer,” *Nature*, vol. 547, no. 7662, pp. 222–226, 2017.
- [117] N. Hilf *et al.*, “Actively personalized vaccination trial for newly diagnosed glioblastoma,” *Nature*, vol. 565, no. 7738, pp. 240–245, Jan. 2019.
- [118] B. J. Laidlaw, J. E. Craft, and S. M. Kaech, “The multifaceted role of CD4+ T cells in CD8+ T cell memory,” *Nat. Rev. Immunol.*, vol. 16, no. 2, pp. 102–111, Feb. 2016.
- [119] L. H. Butterfield, “Cancer vaccines,” *BMJ*, vol. 350, pp. 1–14, 2015.
- [120] U. Sahin and Ö. Türeci, “Personalized vaccines for cancer immunotherapy,” *Science (80-.)*, vol. 359, no. 6382, pp. 1355–1360, Mar. 2018.
- [121] G. P. Dunn, L. J. Old, and R. D. Schreiber, “The immunobiology of cancer immunosurveillance and immunoediting,” *Immunity*, vol. 21, no. 2, pp. 137–148, 2004.
- [122] S. I. S. Mosely *et al.*, “Rational selection of syngeneic preclinical tumor models for immunotherapeutic drug discovery,” *Cancer Immunol. Res.*, vol. 5, no. 1, pp. 29–41, 2017.
- [123] H. Jespersen *et al.*, “Clinical responses to adoptive T-cell transfer can be modeled in an autologous immune-humanized mouse model,” *Nat. Commun.*, vol. 8, no. 1, 2017.

- [124] O. L. Gammelgaard, M. G. Terp, B. Preiss, and H. J. Ditzel, “Human cancer evolution in the context of a human immune system in mice,” *Mol. Oncol.*, vol. 12, no. 10, pp. 1797–1810, Oct. 2018.
- [125] J. C. Castle *et al.*, “Immunomic, genomic and transcriptomic characterization of CT26 colorectal carcinoma,” *BMC Genomics*, vol. 15, no. 1, 2014.
- [126] S. Kreiter *et al.*, “Mutant MHC class II epitopes drive therapeutic immune responses to cancer,” *Nature*, vol. 520, no. 7549, pp. 692–696, 2015.
- [127] M. Yadav *et al.*, “Predicting immunogenic tumour mutations by combining mass spectrometry and exome sequencing,” *Nature*, vol. 515, no. 7528, pp. 572–576, 2014.
- [128] B. J. Hos *et al.*, “Identification of a neo-epitope dominating endogenous CD8 T cell responses to MC-38 colorectal cancer,” *Oncoimmunology*, vol. 00, no. 00, p. 1673125, Oct. 2019.
- [129] J. C. Castle *et al.*, “Exploiting the mutanome for tumor vaccination,” *Cancer Res.*, vol. 72, no. 5, pp. 1081–1091, 2012.
- [130] H. Matsushita *et al.*, “Cancer exome analysis reveals a T-cell-dependent mechanism of cancer immunoediting,” *Nature*, vol. 482, no. 7385, pp. 400–404, Feb. 2012.
- [131] M. M. Gubin *et al.*, “Checkpoint blockade cancer immunotherapy targets tumour-specific mutant antigens,” *Nature*, vol. 515, no. 7528, pp. 577–581, Nov. 2014.
- [132] M. Fehlings *et al.*, “Checkpoint blockade immunotherapy reshapes the high-dimensional phenotypic heterogeneity of murine intratumoural neoantigen-specific CD8⁺T cells,” *Nat. Commun.*, vol. 8, no. 1, 2017.
- [133] M. M. Gubin *et al.*, “High-Dimensional Analysis Delineates Myeloid and Lymphoid Compartment Remodeling during Successful Immune-Checkpoint Cancer Therapy,” *Cell*, vol. 175, no. 4, pp. 1014-1030.e19, Nov. 2018.
- [134] E. K. Duperret *et al.*, “A Synthetic DNA, Multi-Neoantigen Vaccine Drives Predominately MHC Class I CD8 + T-cell Responses, Impacting Tumor Challenge,” *Cancer Immunol. Res.*, vol. 7, no. 2, pp. 174–182, Feb. 2019.
- [135] E. Alspach *et al.*, “MHC-II neoantigens shape tumour immunity and response to immunotherapy,” *Nature*, no. February, 2019.
- [136] J. Borst, T. Ahrends, N. Bąbala, C. J. M. Melief, and W. Kastenmüller, “CD4⁺ T cell help in cancer immunology and immunotherapy,” *Nat. Rev. Immunol.*, vol. 18, no. 10, pp. 635–647, 2018.
- [137] M. A. Taylor *et al.*, “Longitudinal immune characterization of syngeneic tumor models to enable model selection for immune oncology drug discovery,” *J. Immunother. Cancer*, vol. 7, no. 1, p. 328, 2019.
- [138] I. W. Mak, N. Evaniew, and M. Ghert, “Lost in translation: animal models and clinical trials in cancer treatment,” *Am. J. Transl. Res.*, vol. 6, no. 2, pp. 114–118, Jan. 2014.

- [139] A. L. Ackerman and P. Cresswell, “Cellular mechanisms governing cross-presentation of exogenous antigens,” *Nat. Immunol.*, vol. 5, no. 7, pp. 678–684, Jul. 2004.
- [140] F. Spadaro *et al.*, “IFN- α enhances cross-presentation in human dendritic cells by modulating antigen survival, endocytic routing, and processing,” *Blood*, vol. 119, no. 6, pp. 1407–1417, Feb. 2012.
- [141] A. J. Currie, R. G. van der Most, S. A. Broomfield, A. C. Prosser, M. G. Tovey, and B. W. S. Robinson, “Targeting the effector site with IFN- α -inducing TLR ligands reactivates tumor-resident CD8 T cell responses to eradicate established solid tumors,” *J. Immunol.*, vol. 180, no. 3, pp. 1535–1544, Feb. 2008.
- [142] A. M. D’Alise *et al.*, “Adenoviral vaccine targeting multiple neoantigens as strategy to eradicate large tumors combined with checkpoint blockade,” *Nat. Commun.*, vol. 10, no. 1, pp. 1–12, 2019.
- [143] L. Aurisicchio *et al.*, “Poly-specific neoantigen-targeted cancer vaccines delay patient derived tumor growth,” *J. Exp. Clin. Cancer Res.*, vol. 38, no. 1, pp. 1–13, 2019.
- [144] E. Tondini *et al.*, “A poly-neoantigen DNA vaccine synergizes with PD-1 blockade to induce T cell-mediated tumor control,” *Oncoimmunology*, vol. 8, no. 11, p. 1652539, 2019.
- [145] H. R. Ali *et al.*, “Association between CD8+ T-cell infiltration and breast cancer survival in 12,439 patients,” *Ann. Oncol. Off. J. Eur. Soc. Med. Oncol.*, vol. 25, no. 8, pp. 1536–1543, Aug. 2014.
- [146] P. Savas *et al.*, “Clinical relevance of host immunity in breast cancer: from TILs to the clinic,” *Nat. Rev. Clin. Oncol.*, 2015.
- [147] P. Savas *et al.*, “Single-cell profiling of breast cancer T cells reveals a tissue-resident memory subset associated with improved prognosis,” *Nat. Med.*, vol. 24, no. 7, pp. 986–993, 2018.
- [148] P. Schmid *et al.*, “Atezolizumab and Nab-Paclitaxel in Advanced Triple-Negative Breast Cancer,” *N. Engl. J. Med.*, p. NEJMoa1809615, 2018.
- [149] M. P. Pinho, T. A. Patente, E. A. Flatow, F. Sallusto, and J. A. M. Barbuto, “Frequency determination of breast tumor-reactive CD4 and CD8 T cells in humans: unveiling the antitumor immune response,” *Oncoimmunology*, vol. 8, no. 8, p. 1607674, Aug. 2019.
- [150] L. B. Alexandrov *et al.*, “Signatures of mutational processes in human cancer,” *Nature*, vol. 500, no. 7463, pp. 415–421, 2013.
- [151] N. W. Pedersen *et al.*, “CD8+ T cells from patients with narcolepsy and healthy controls recognize hypocretin neuron-specific antigens,” *Nat. Commun.*, vol. 10, no. 1, p. 837, Dec. 2019.
- [152] V. I. Jurtz *et al.*, “NetTCR: sequence-based prediction of TCR binding to peptide-MHC complexes using convolutional neural networks,” *bioRxiv*, p. 433706, Jan. 2018.
- [153] B. Routy *et al.*, “Gut microbiome influences efficacy of PD-1–based immunotherapy against

epithelial tumors,” *Science (80-.)*, vol. 359, no. 6371, pp. 91–97, Jan. 2018.

- [154] V. Matson *et al.*, “The commensal microbiome is associated with anti-PD-1 efficacy in metastatic melanoma patients,” *Science (80-.)*, vol. 359, no. 6371, pp. 104 LP – 108, Jan. 2018.

